INFORMATION TO USERS

This manuscript has been reproduced from the microfilm master. UMI films the text directly from the original or copy submitted. Thus, some thesis and dissertation copies are in typewriter face, while others may be from any type of computer printer.

The quality of this reproduction is dependent upon the quality of the copy submitted. Broken or indistinct print, colored or poor quality illustrations and photographs, print bleedthrough, substandard margins, and improper alignment can adversely affect reproduction.

In the unlikely event that the author did not send UMI a complete manuscript and there are missing pages, these will be noted. Also, if unauthorized copyright material had to be removed, a note will indicate the deletion.

Oversize materials (e.g., maps, drawings, charts) are reproduced by sectioning the original, beginning at the upper left-hand corner and continuing from left to right in equal sections with small overlaps.

Photographs included in the original manuscript have been reproduced xerographically in this copy. Higher quality 6" x 9" black and white photographic prints are available for any photographs or illustrations appearing in this copy for an additional charge. Contact UMI directly to order.

ProQuest Information and Learning
300 North Zeeb Road, Ann Arbor, MI 48106-1346 USA
800-521-0600

SYNTHESIS OF NOVEL ORGANOFUNCTIONAL SILICONES AND SILANES FOR INTERFACE CONTROL

By

RODICA SÎNZIANA STAN, Dipl. Eng.

A Thesis

Submitted to the School of Graduate Studies

In Partial Fulfillment of the Requirements

For the Degree

Doctor of Philosophy

McMaster University

SYNTHESIS OF NOVEL ORGANOFUNCTIONAL SILICONES AND SILANES FOR INTERFACE CONTROL

DOCTOR OF PHILOSOPHY (1999) McMaster University

(Chemistry) Hamilton Ontario

TITLE: Synthesis of Novel Organofunctional Silicones and Silanes for Interface Control

AUTHOR: Rodica Sînziana Stan, Dipl. Eng. (Bucharest Polytechnic Institute, Romania)

SUPERVISOR: Professor Michael A. Brook

NUMBER OF PAGES: xx, 179

ABSTRACT

The synthesis and characterization of new organo-functional silicones bearing nitrilotriacetic acid chelating moieties is described. Several synthetic pathways were explored towards this goal and the most promising synthesis was used in order to obtain five different chelating silicones. These compounds formed insoluble films on aqueous surfaces. An investigation of the surface pressure exerted by these films was performed by employing a Langmuir trough. For comparison, a series of five new carboxylic acid-functional silicones was also synthesized and studied. The effect of molecular weight, type and position of functional group, and metal cation presence in the subphase are discussed. Possible conformations adopted by these polysiloxane derivative polymers at the surface were also presented.

The design, synthesis, and characterization of small molecular weight organosilane linkers that can control hydrophobic – hydrophilic interfaces in wood – polyolefin composites by means of covalent bond formation is described. Several vinylallylsilane-based coupling agents were synthesized and their radical-initiated grafting onto polyethylene and squalane (a polyolefin mimic) was presented.

One such organosilane, dimethyl(γ-hydroxypropyl)-vinylsilane, combined with a low molecular weight polyethylene-*g*-maleic anhydride oligomer, was used in order to

reinforce wood - polyethylene composites and the mechanical properties of these materials were described.

ACKNOWLEDGEMENTS

I wish to express my sincere gratitude to my supervisor, Dr. Michael A. Brook, for offering me the opportunity to work in his group, and for the guidance and inspiration that he provided throughout the course of this work. When chemistry wasn't quite working out his continuous encouragement and support were much appreciated.

I would like to thank my supervisory committee, Dr. Robert H. Pelton and Dr. John Warkentin, for their time, helpful discussions, and for reading this thesis in a short period of time.

Special thanks go to Dr. Eckardt Wolf for mentoring me with endless patience at the beginning of my time at McMaster and for being a great friend. His advice on chemical synthetic problems and on experimental setups made my transition from a chemical engineer to a chemist so much easier.

I wish to express my sincere gratitude to the following people for their contribution to this work and for generously sharing their expertise:

Dr. Donald Hughes and Mr. Brian Sayer in the NMR facility, Dr. Richard Smith, Dr. James Francis, and Dr. Kirk Green in the mass spectrometry facility, and Mr. George Timmins.

A major debt of gratitude goes to Dr. Michael Owen and Dr. Randall Hill at Dow Corning Corporation, Midland (Michigan), who kindly allowed us to use their Langmuir trough for surface pressure measurements and offered much appreciated suggestions and scientific advice. Many thanks to Ms. Sue Perz from Dow Corning for performing many

of the surface pressure measurements presented in this work. Her outstanding technical skills and her enthusiasm for science were a source of inspiration.

I would like to extend thanks to Dr. John Balatinecz at the University of Toronto for helpful discussions and for allowing us to use the injection molding equipment and the Instron instruments, and to Mr. Shiang Law, and Dr. Laurent Matuana-Malanda for their assistance with the injection molding experiments.

Many thanks to my group colleagues Sonya, Vasso, Alex, Dave, Mustafa, Frank, Mark, Ralph, Gilles, J.J., and Gung for their friendship and chemical expertise and to Bryan for the exploratory work with EDTA- and NTAA-silicone chelators during the summer of 1998.

During my time at Mac I had the opportunity to make several very special friends. Darren, Mario, Ayumi, Craig, Andrew, Sabine, Heidi, and Marie have been my dear and loyal friends during these past years and brought inspiration, enjoyment, and encouragement in my life. They truly made me feel at home away from home. Thank you, my friends!

Finally, this work is dedicated to the three people in my life that helped me make my dreams come true. God bless my father Octavian and the memory of my mother Ana, who raised me with much love, encouraged me to learn and made sure that I had plenty of choices for personal fulfillment. Words are not enough to thank my husband Klaus, whose love and support made it all worthwhile. He kept me in touch with myself when I seemed to get lost in endless hours of work, offered great advice when I had questions about chemistry, and patiently typed this manuscript.

Table of Contents

List of Figures

List of Tables

List of Abbreviations and Symbols

γ	surface tension
π	surface pressure
Å	Angstrom
A	molecular area
A_C	area at collapse
ACE	acetamido
AcOH	acetic acid
Ar	aryl
Bn	benzyl
BnBr	benzylbromide
Boc	*tert*-butyloxycarbonyl
BuLi	*n*-butyllithium
$CHCl_3$	chloroform
CH_2Cl_2	methylene chloride
CH_3OH	methanol
CI	chemical ionization
COSY	correlation spectroscopy
DMF	dimethylformamide
DODA	dioctadecylamine

DPPE	1,2-dipalmitoyl-sn-glycero-3-phosphoethanolamine
EDCI	1-(3-dimethylaminopropyl)-3-ethylcarbodiimide
EDTA	ethylenediaminetetraacetic acid
EI	electron impact
eq.	equivalent
ES-MS	electrospray mass spectrometry
ESP	equilibrium spreading pressure
Et	ethyl
Et_2O	diethylether
EtOAc	ethyl acetate
F	area at collapse
FT-IR	Fourier transformed infrared mass spectroscopy
GC	gas chromatography
GPC	gel filtration chromatography
H	hydrogen
HMBC	heteronuclear single quantum correlation
IDA	iminodiacetic acid
k	Boltzmann's constant
K	Kelvin
LLDPE	linear low-density polyethylene
MA	maleic anhydride
Me	methyl

M_n	number average molecular weight
M_w	weight average molecular weight
MW	molecular weight
MWCO	molecular weight cutoff
m/z	mass to charge ratio
N	Newton
n	number of repeating monomer units
NEt_3	triethylamine
NHS	*N*-hydroxysuccinimide
NMR	nuclear magnetic resonance spectroscopy
NTA	N^{α},N^{α}-bis(carboxymethyl)-L-lysine
NTAA	nitrilotriacetic acid
P_C	collapse pressure
PD	polydispersity
PDMS	poly(dimethylsiloxane)
PE	polyethylene
PE-*g*-MA	polyethylene-graft-maleic anhydride
PEO	poly(ethyleneoxide)
PG	protecting group
Ph	phenyl
PNB	4-nitrobenzyl
PP	polypropylene

ppm	parts per million
RT	room temperature
SA	succinic anhydride
SSU	succinimidyl
St	stearate
SUCC	*N*-succinyl
R	alkyl
T	temperature
TFA	trifluoroacetic acid
THF	tetrahydrofuran
TLC	thin layer chromatography
TMS	trimethylsilyl
TMSCl	chlorotrimethylsilane
Vy	vinyl
Z	benzyloxycarbonyl

1 Introduction

1.1 General

1.1.1 Silicone Surfactants

Polydimethylsiloxanes, also known as silicones, were commercially introduced in the 1940's. The repeating unit of a polyorganosiloxane consists of alternating silicon-oxygen atoms with two organic radicals attached to each silicon atom. The best known siloxane polymer is poly(dimethylsiloxane) (PDMS), (R=Me in Figure 1-1).

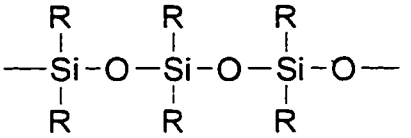

Figure 1-1: General structure of polyorganosiloxanes.

Silicones are specialty polymers that possess unique properties, such as low surface tension and surface energy, low glass temperatures, high water repellency, good wetting and spreading, good thermal stability, low chemical reactivity, and low toxicity.[1] Several reviews[1,2] have described in detail the relationship between the chemical features of these polymers and their properties, as well as how these properties, particularly surface activity, are responsible for a variety of practical applications.

Silicone surfactants are structural derivatives of poly(dimethylsiloxane) in which some of the methyl groups are substituted by lipophilic or hydrophilic (ionic or nonionic) moieties. The silicone backbone of these derivatives is the lyophilic component.

Depending on the structure of the substituents, PDMS derivatives are surface active not only in water but also in organic media. Their special properties, as well as the precision and reliability of routes to their synthesis, have led to the use of silicone surfactants as foam stabilizers, wetting agents, antistatic agents, defoamers, and emulsifiers.

Silicone surfactants were initially employed in polyurethane foam production and as mold release agents. For applications that require the lowering of surface energy in aqueous systems, some of the most efficient surfactants available are nonionic silicone polyether copolymers of various molecular weights and compositions[3] (Figure 1-2).

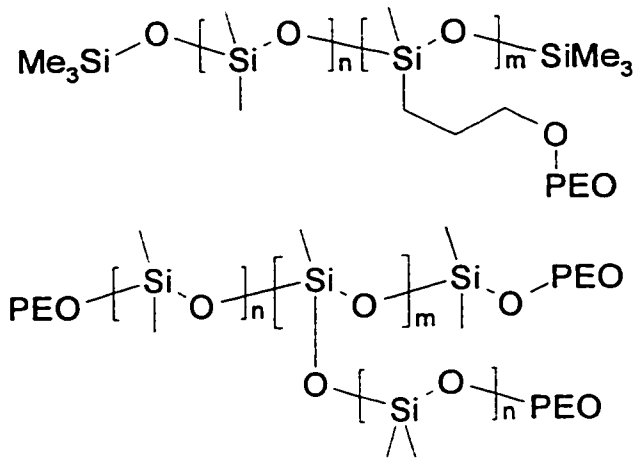

Figure 1-2: Comb-like surfactant type (top) and branched siloxane modified at the chain end (bottom); PEO = poly(ethylene oxide) oligomer.

Silicone polyethers are currently also used in water-based coatings and ink formulations[4,5] as defoamers and deaerators. In cosmetic formulations[6] these compounds improve the spreadability and distribution of pigments in lipstick, improve the combability and gloss of hair when added to shampoos and conditioners, and impart softness and smoothness to cleansed skin when added to shower gels. These compounds are known to depress the surface tension of aqueous layers to as little as 21 mN/m and to stabilize liquid-liquid interfaces (e.g. water-silicone). They are also excellent aqueous wetting agents for hydrocarbon surfaces.[1,2]

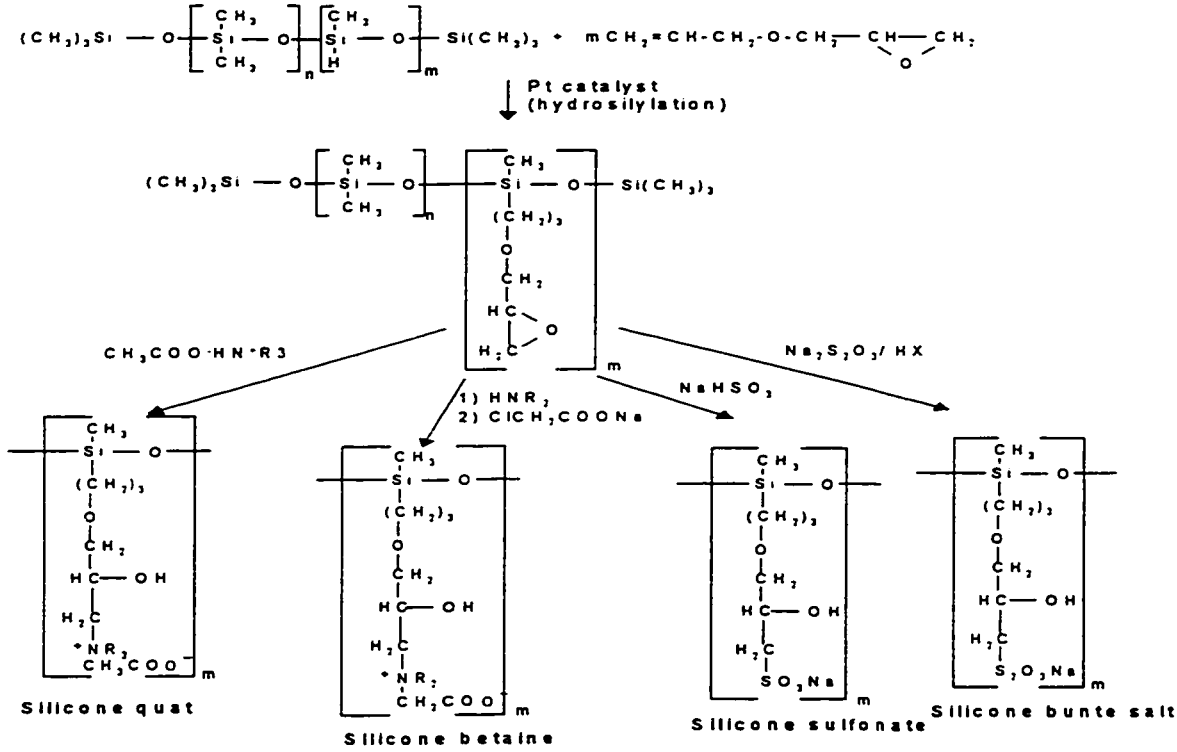

Figure 1-3: Ionic silicone surfactants and their syntheses (reprinted from *Tenside Surf. Det. 26* (1989) 5, with permission from Carl Hanser Verlag).

Silicone polymers bearing cationic or anionic groups are also of great interest for surface stabilization in aqueous systems, as proven by the multitude of existing patents describing the use of these materials. Figure 1-3 presents several classes of ionic silicone surfactants, such as silicone quaternary ammonium salts (quats), betaines, sulfonates, and bunte salts[3] and their syntheses, which involve the formation of an epoxide-functional silicone intermediate via hydrosilylation, followed by a nucleophilic attack on the epoxide reactants.

Cationic silicone surfactants $(Me_3SiO)_2Si(Me)(CH_2)_3{}^{+}NMe_2(CH_2)_2OR\ X^-$ (R = H, C(O)Me, C(O)NHPh; X = Cl, Br, I, NO_3, $MeOSO_3$) show fabric softening and antistatic effects when adsorbed onto cotton / polyester fibers.[7,8] Quaternary ammonium-functionalized silicones, prepared from reactions of carboxylic acid-functionalized quaternary ammonium compounds with γ-hydroxypropyl-functional silicones[9], can also impart antistatic properties to organic textile materials. Silicone surfactants of the formula $(Me_3Si)_2Si(Me)(CH_2)_3OCH_2CH(OH)\text{-}CH_2{}^{+}NMe_2R\ Cl^-$ (R = H, Me) were reported to protect metal surfaces against corrosion[10]. It was shown that the surface activity, surface tension reduction and adsorption at the air / water interface of such compounds can be changed by varying the counterion and by adding various salts to the solution.

Silicone betaines, which possess both anionic and cationic character (zwitterionic), originally patented by the researchers at Th. Goldschmidt AG[11,12], have been used in hair care products.

A number of silicone sulfonates[13], silicone ether sulfonates[14], and silicone sulfates[15] were patented as effective wetting agents, detergents, foaming and emulsifying

agents. Silicones containing carboxylic acids have been previously synthesized[16] and it was shown that varying the pH of the subphase could change their surface activity. The nature of the counterions (mono- or multivalent) of the carboxylate group can also alter the behavior of polymer layers containing such groups in solution and at air/ water interfaces.

1.1.2 Organofunctional Poly(dimethylsiloxane) Monolayers at Air-Water Interfaces

For many years there has been a great scientific and practical interest in the subject of insoluble monomolecular films (monolayers) on liquid surfaces. The liquid surface of choice has been water. These films are called Langmuir-Blodgett films.[17] There are two classes of materials that have the ability to form monolayers.[17] The first class consists of low molecular weight amphiphiles that contain a hydrophilic functional group (-COOH, –OH, -$CONH_2$, -CH_2COCH_3, -CH=NOH, -$NHCONH_2$, -$NHCOCH_3$, etc.) and a large hydrophobic chain (usually a hydrocarbon). The ability to form monolayers is a function of the balance between the effects that these two structural features will exert. The second class consists of polymers that have either both hydrophilic and hydrophobic components in the backbone, or a combination of hydrophilic groups pendant from the hydrophobic backbone, or *vice-versa*. It is considered that a polymer forms a true monolayer[17,18] if the surface film formed by a given amount occupies a maximum and reproducible area which is independent of the

concentration of the spreading solution, type of solvent used, and technical details. For a polymer monolayer to be stable it is necessary for the individual monomer units to have a finite free energy of adsorption from the bulk solution onto the subphase surface[17].

Silicone polymers with relatively low molecular weight, which are end-functionalized with hydrophilic groups, are a very interesting group of materials that can form Langmuir-Blodgett films. The molecular weight of these compounds must be high enough to ensure their insolubility in the subphase, yet low enough that chain separation and orientation can take place. It is also important that the interaction of the backbone with the subphase is weaker than that between polymer end groups and the subphase.

The behavior of PDMS and end-functionalized silicones at the air-water interface has been investigated by determining the surface pressure-area (π-A) isotherms with the help of Langmuir troughs (see Figure 1-4).

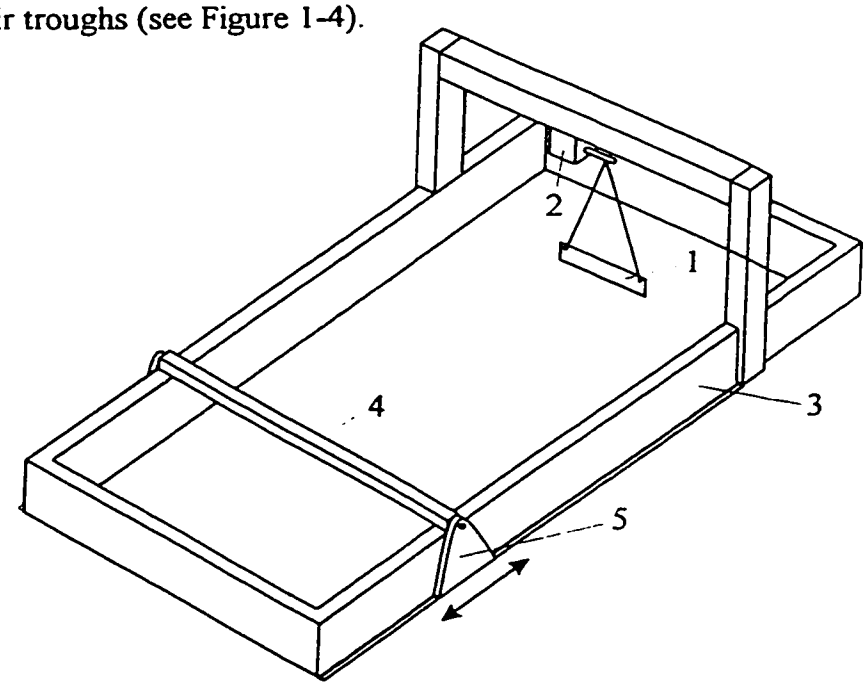

Figure 1-4: Langmuir trough. 1 – Wilhelmy port; 2 – force transducer; 3 – PTFE-trough; 4 – barrier of reinforced PTFE; 5 – barrier drive.

References 17 and 19 offer detailed descriptions of the experimental methods and the equipment used. Using this technique, Fox, Taylor, and Zisman[20] examined surface pressure-area isotherms for non-functionalized PDMS and phenyl-containing polysiloxanes of different viscosity and advanced the hypothesis that these polymers are able to form helices reversibly, consisting of about six monomers per turn, in the surface film.

Fox, Solomon, and Zisman[21] studied the influence of alkaline and acidic subphases on the surface behavior of PDMS. Rapid and significant layer degradation was noted when 0.1 N sulfuric acid, 0.1 N phosphoric acid, and 0.1 M potassium hydroxide subphases were used. The change in the shape of the isotherms was considerably slowed down when 10^{-3} N sulfuric acid was used. 10^{-2} M Acetic acid and distilled water did not seem to affect the shape of the isotherms. Granick, Clarson, and Semlyen[22] studied the surface pressure of linear PDMS and sharp fractions of cyclic PDMS and found that cyclic and linear PDMS with $n > 20$ collapse by a common mechanism.

Higher order effects arise with end-functional polysiloxanes. The surface behavior of hydroxy- and chloro-terminated silicones was investigated by Newing[23], who concluded that hydroxy groups anchored the molecules into the subphase. He also determined that the layer collapses at 8 - 10 dynes/cm. Koberstein and coworkers[24] provided an interesting account of the surface behavior of several poly(dimethylsiloxane) oligomers (MW 900 - 4000) end-terminated with methyl, epoxy, carboxy, amine, and hydroxy groups. They found that up to six transitions (A - F) were present in the π-A isotherms (Figure 1-5). The large areas leading to transition A were associated with the

polymer lying flat on the water. Region A to B, typical for high molecular weight functional (isotherms 2,3) and nonfunctional PDMS (isotherm 1), was attributed to a phase in which the polymer adopts a zigzag structure with every other oxygen or silicon at the surface. The region between B and C was characterized by an important decrease in the area occupied by each molecule without an appreciable increase in pressure. This is consistent with the formation of polydimethylsiloxane helices that lay flat on water and is typical for higher molecular weight oligomers (Figure 1 – 6). The transition between C and D (Figure 1 – 5, isotherms 1 and 2) corresponded to collapse, caused by the sliding of helices one past another.

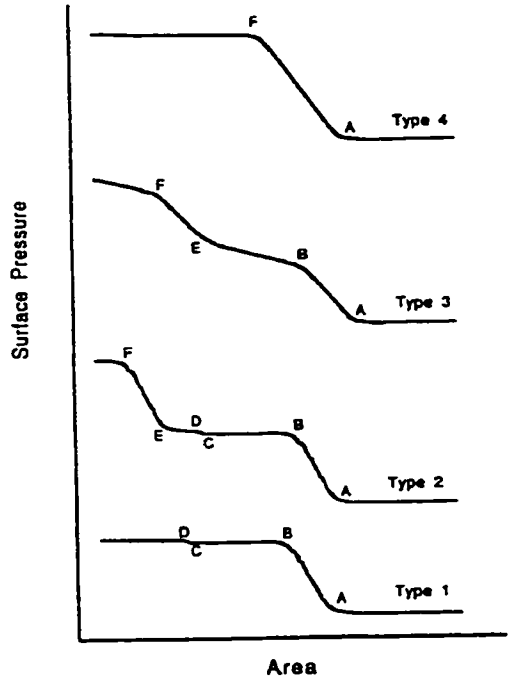

Figure 1-5: Four basic isotherm types observed for end-functionalized silicones; A – F = phase transitions (reprinted from *Langmuir 10* (1994) 1857, with permission from American Chemical Society).

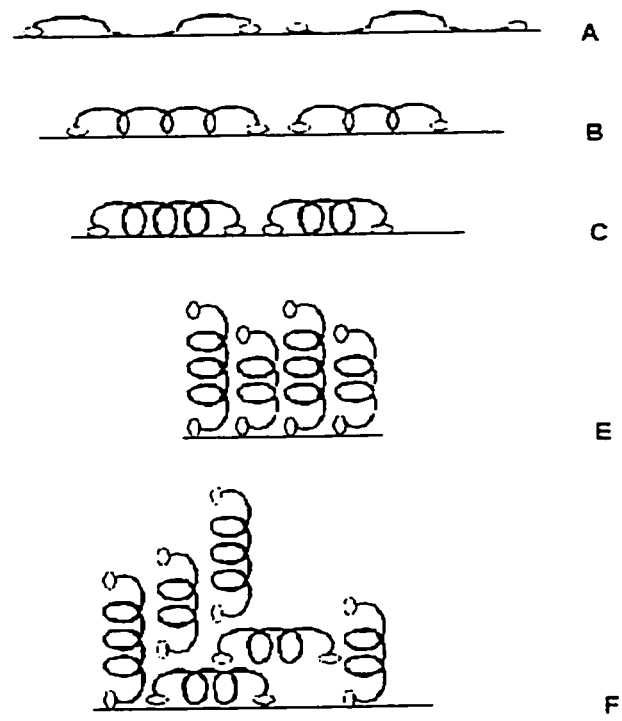

Figure 1-6: Possible conformations for end-functional polysiloxanes at the transitions A-F.

The region between E and F (Figure 1 – 5, isotherms 3 and 4, Figure 1 – 6) was observed for shorter chain-functionalized PDMS and was attributed to a transition to upright configurations (with one functional group anchored to the subphase), followed by collapse at point F.

As the molecular weight decreases, a transition from type 2 to type 4 isotherms was noted, due to the increasing overlap of molecular- and monomer-dependent transitions. The short chain, strongly anchored silicones had an area at collapse of 50 - 60 $Å^2$/molecule, consistent with closely packed chains having an extended *cis-trans*

structure. Longer chains that were weakly anchored presented cross-sectional areas at collapse of 100 $Å^2$/molecule which were consistent with partly extended helical structures.

The addition of cadmium ions to the subphase had a marked effect on the surface behavior of carboxylic acid-terminated silicones. The decrease in the cross-sectional area at collapse and the increase in the collapse pressure (by 3 - 5 mN/m) noted were due to the complexation of the carboxyl group by the metal cation, which led to an increase in the anchoring of the end-group to the surface.

We have seen above that the surface behavior of non-functional silicones can depend on the subphase. These effects are even more profound for end-functional silicones. We envisaged that the attachment of functional groups capable of forming stable complexes with metal ions to poly(dimethylsiloxane) oligomers could allow the construction of oriented films with useful and interesting properties at a variety of interfaces. Before outlining our synthetic objectives, an overview of the role of polyfunctional carboxylates as chelating agents will be presented.

1.1.3 N^{α},N^{α}-Bis(carboxymethyl)-L-Lysine-Based Metal Chelators

We have become interested in using different metal cations to control the surface activity of silicone-based surfactants at various interfaces. For this purpose we decided to

attach to a silicone a hydrophilic, multi-dentate ligand that binds a variety of metal cations to a silicone.

Some of the best-known and used metal-complexing ligands are nitrilotriacetic acid (NTAA), ethylenediaminetetraacetic acid (EDTA), iminodiacetic acid (IDA), and diethylenetriaminepentaacetic acid (DTPA) (Figure 1-7). These chelators and related compounds containing chelating moieties, such as N^{α},N^{α}-bis(carboxymethyl)-L-lysine (NTA) (Figure 1-7), have been attached to various types of polymers, such as oxirane-activated agarose, activated-crosslinked glycidyl methacrylate gel, maleic anhydride-crosslinked polystyrene, and chloromethylated styrene-10%-divinylbenzene copolymers (*vide infra*).

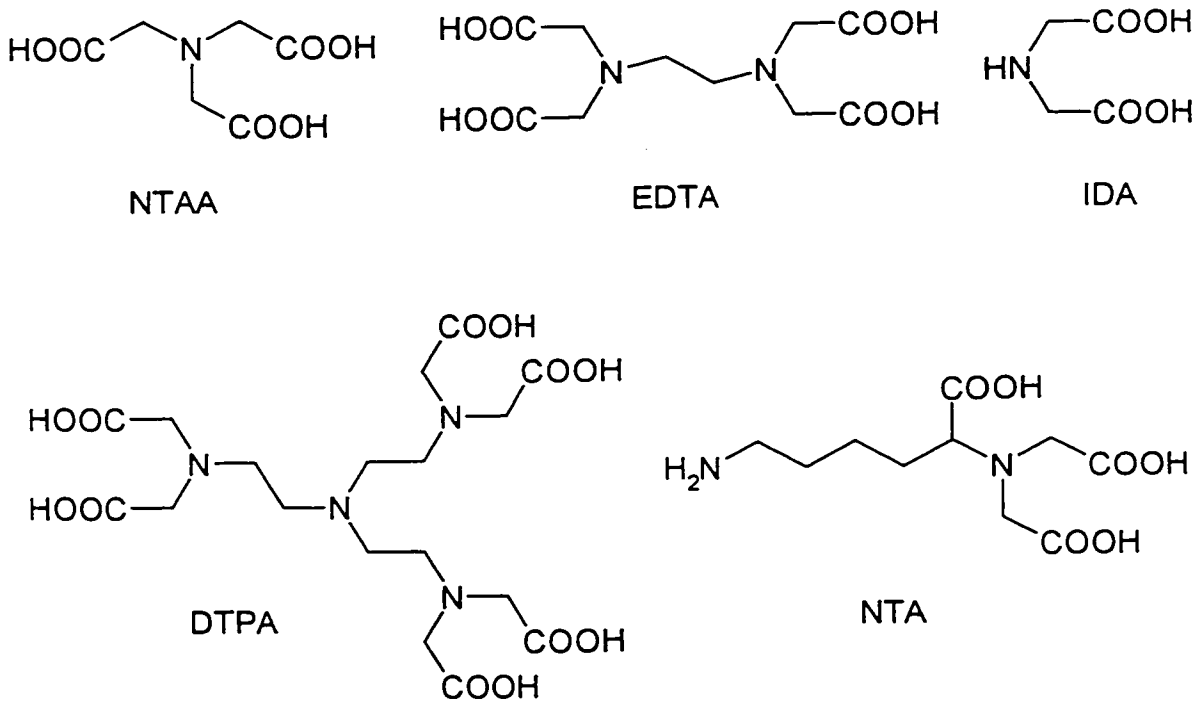

Figure 1-7: Structures of common chelating compounds.

Porath *et al.*[25] described a protein purification technique in which chelating ligands IDA and NTAA were bound covalently to oxirane-activated agarose and then charged with metal ions, such as Cu^{2+}, Zn^{2+}, and Ni^{2+}. The resulting chelated ions have coordination sites available for interactions with biopolymers such as histidine–tagged proteins. The proteins can be released by elution with EDTA or imidazole, which compete for the coordination sites on the resin bound ions. This purification technique was named immobilized metal ion affinity chromatography (IMAC).

When tridentate ligands such as IDA are used, chelated Ni^{2+} has 3 coordination sites available for protein interactions (Figure 1-8a), but often Ni^{2+} is not bound tightly enough and can be released from the absorbent. If a pentadentate ligand (such as EDTA) is employed, Ni^{2+} is strongly bound to the resin but has only one coordination site available to interact with the protein (Figure 1-8b).

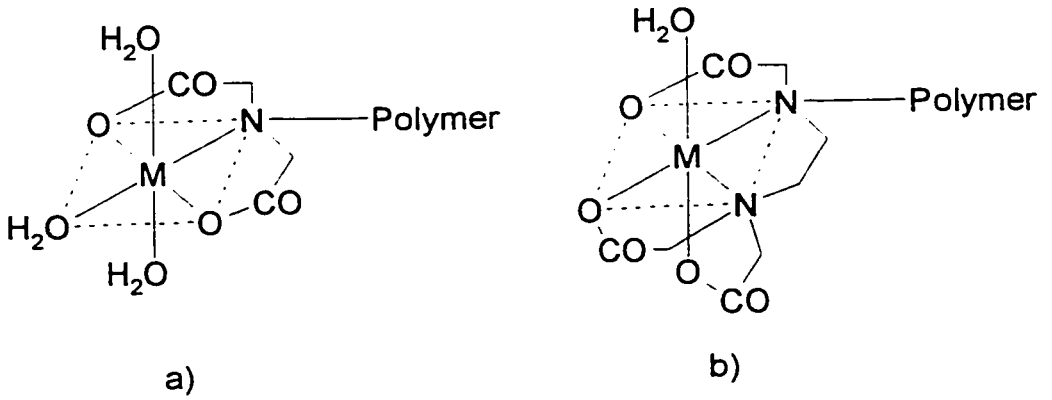

Figure 1-8: Chelation of metal ions with coordination number six by tridentate (IDA) and pentadentate (EDTA) chelate adsorbents (adapted form *J. Chromatogr. 411* (1987) 178, with permission from Elsevier Science).

Hochuli *et al.*[26] developed a new quadridentate chelating ligand, which binds Ni^{2+} well and leaves two coordination sites for biopolymer interaction. This new chelating agent, namely N^{α},N^{α}-bis(carboxymethyl)-L-lysine (NTA), presents a nitrilotriacetic acid moiety and an amino functional group that can facilitate binding onto various types of substrates. Its synthesis and attachment to an oxirane-activated resin, as well as the structure of the complex formed with a metal having a coordination number of 6 are presented in Figure 1-9.

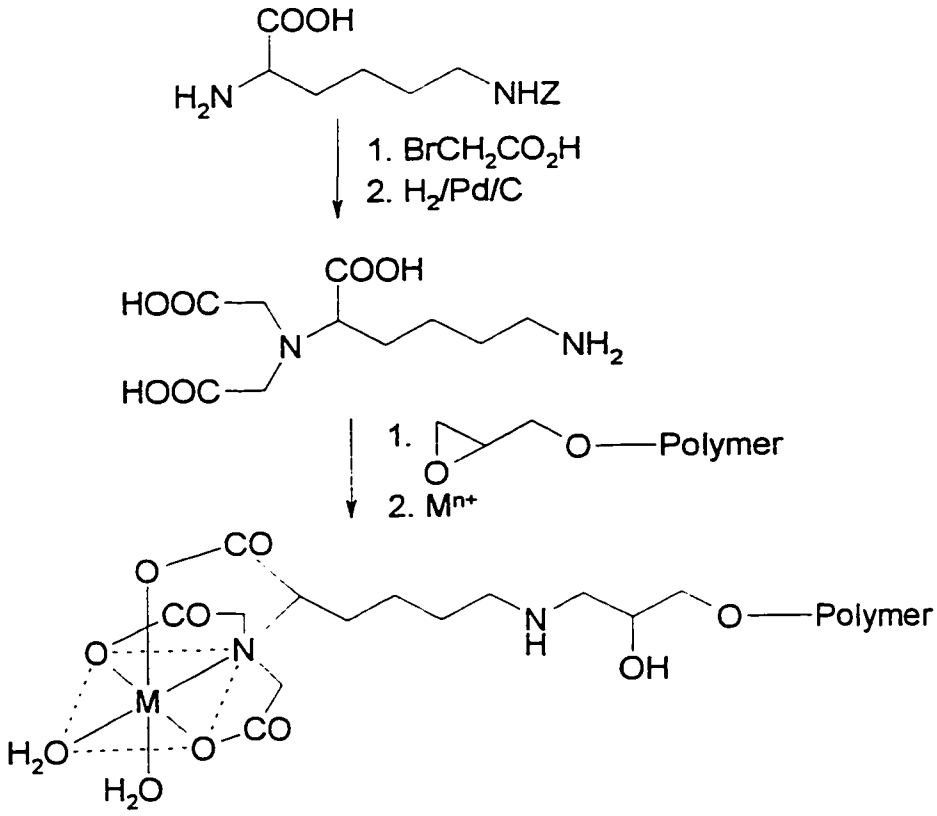

Figure 1-9: Preparation of an NTA functional resin and its complexation of an ion with a coordination number CO = 6 (adapted from *J. Chromatogr. 411* (1987) 178, with permission from Elsevier Science).

NTA has been extensively used in several different chromatographic applications. Yokoyama *et al.* attached NTA to crosslinked polystyrene[27, 28] and to crosslinked glycidyl methacrylate gel[29], and demonstrated that these supports can be successfully used to separate fifteen ions of rare-earth elements via ion chromatography. The adsorption of various types of metal ions from acidic aqueous solutions onto NTA and IDA chelating resins was studied. It was observed that the NTA ligands form 1:1 complexes with metal ions such as Ga^{3+}, In^{3+}, Cu^{2+}, Al^{3+}, Eu^{3+}, Ni^{2+}, Zn^{2+}, and Co^{2+}. The stability constants as well as the selectivity sequence of these complexes were found to be similar to the ones of complexes with nitrilotriacetic acid[28]. It was also noted that NTA resins retain metal ions more firmly than IDA resins[27].

Paborsky *et al.*[30] selectively immobilized histidine-tagged proteins onto maleic anhydride-activated polystyrene microtiter plates which had been derivatized with NTA and used these plates to develop an enzyme-linked immunoabsorbant assay that quantified protein concentrations and determined the affinity of protein-ligand interactions. O'Shannessy *et al.*[31] described a surface plasmon technique, which involved the use of a Ni^{2+}-NTA complex immobilized onto dextran, for the detection and quantification of hexahistidine-tagged recombinant proteins in solution. The same technique was used by Whitesides and coworkers[32] to study the interaction between histidine-tagged proteins which had been selectively bound to a self-assembled monolayer (SAM) and proteins in solution. The SAM was obtained by the adsorption of a mixture of two alkanethiols onto a gold surface. One of the alkanethiols contained a terminal NTA group, which was complexed with Ni^{2+} and bound the target proteins. The

other thiol had a terminal tri(ethyleneglycol) group that did not adsorb proteins. It was also shown that histidine-tagged proteins adsorbed by NTA-derivatized SAM had a better ability to interact with proteins in solution, when compared to proteins that had been covalently bound onto a thin dextran gel layer.

More recently, Tampé and coworkers attached NTA to a phospholipid (DPPE)[33], a synthetic lipid (DODA)[33], and to a fluorescence-labeled lipid[34]. In the first two examples a film balance technique was used to investigate the sensitivity of NTA-tagged lipid films to the presence of metal cations. It was noted that the area-pressure isotherms changed dramatically in the presence of Ni^{2+}. In the third example, fluorescence-tagged chelator lipids were used as spectroscopic probes in order to visualize directly the molecular recognition of fluorescence-labeled histidine-tagged peptides by using fluorescence resonance energy transfer.

We have seen that carboxylate-functional silicones are interesting surface-active compounds and that polycarboxylates also have special properties. Chapter 2 presents various synthetic routes explored towards the synthesis of novel NTA-tagged silicones. Surface properties of the resulting silicone chelators are described in Chapter 3.

1.1.4 Wood – Polyolefin Composites

Silicon-based compounds possess remarkable ability to stabilize liquid: liquid and liquid: gas interfaces, due to their unusual surface activity. However, silicones are not often used to stabilize solid: solid interfaces. For this purpose, small molecular weight

silanes that can act as coupling agents are more suitable and have been successfully used (i.e., stabilization of glass/polyester interfaces). Our particular challenge was to synthesize silanes that can stabilize the interface between hydrophobic polyethylene and hydrophilic wood.

The benefit of the use of wood-plastic composites, as a substitute for solid wood or pure polymers, has become increasingly obvious over the past few decades. These materials exhibit improved properties compared to virgin plastic including lighter weight, biodegradability, reduced creep, improved impact strength, acoustic properties and cost[35,36]. As importantly, if recycled plastic and wood are utilized, the materials can be used more than one time before the (until now) inevitable trip to the landfill.

Some of the most common thermoplastics that have found application in wood composites are polyethylene (PE), polypropylene (PP), polystyrene (PS), polyvinyl chloride (PVC), acrylics, nylons, and polyesters. Thermoset and thermoplastic polymers have been used to control wood-plastic adhesion in composites with varying degrees of success. Some of the most common thermoset resins used in composites are phenolic and epoxy resins, alkyds, melamines, polyurethanes, and urea-formaldehydes. The high surface energy at the wood/thermoplastic polymer interface, due to a large difference in hydrophilicity between the wood and polymer materials, often leads to low-performance composites. Frequently, the wood fibers have poor dispersion characteristics in the thermoplastic melt, limited compatibility with the plastic matrix and limited thermal stability[37] during processing, which generally involves intimate mixing of the polymer

with the wood fiber in conventional plastic mixing equipment, such as twin-screw extruders and turbine mixers[38].

Several strategies have been employed to improve the adhesion at the polymer/wood interface[39,40,41], which include: polymer and/or wood fiber modification by use of suitable solvent cleaning, mechanical abrasion, flame, plasma, thermal, corona, and chemical treatment, use of compatibilizing agents[42,43], and the combined use of adhesives and functionalized wood and/or plastic.[44] In these cases, covalent bonding is directed to the wood surface only: the stability of the interface then relies on physical adhesion between the coupling agent-modified wood surface and the plastic matrix. As a general rule, in the absence of coupling agents or other strategies, the maximum amount of wood incorporated in the wood-plastic composite is limited to about 50% (by weight) before the properties of the composite begin to suffer. Even with coupling agents, it is difficult to prepare composites with greater than 60% wood that perform well, although there are some exceptions[45]. A higher wood content is desirable because it leads to composites that are more easily composted, lighter, and more cost efficient than plastic-rich composites.

It is expected that improved adhesion between wood and plastic will permit higher wood content in composites without compromising the resulting properties. To address this hypothesis, we have chosen to examine the use of bifunctional compatibilization agents for wood/polyethylene composites that will function by forming covalent bonds to both the hydrophilic and hydrophobic substrates. Chapter 4 presents

the use of an *in situ* generated coupling agent in wood/polyethylene composites and the effect of the compatibilizing agent on the mechanical properties of these materials.

1.1.5 Radical Grafting of Vinylsilanes onto Hydrocarbon Substrates

The radical grafting of compounds containing vinyl groups has been used extensively to functionalize polyolefins. This process is initiated by peroxides at temperatures between 180 - 240°C, and generates functional polyolefins with improved adhesion properties. The use of such reactive polymers in blend compatibilization has been reviewed by Baker[46] and Naqvi[47].

A particularly attractive process is the peroxide-initiated grafting of vinyltriethoxysilane onto PE, a well-known industrial process[48,49,50,51,52,53,54] that, when followed by moisture curing (Figure. 1-10), leads to crosslinked polyethylene that shows better thermal performance, enhanced impact strength, and good chemical resistance, and improved creep and wear behavior, than the unmodified material. The process succeeds because the competing homopolymerization process of vinylsilanes is inefficient[55,56,57,58,59,60]. Sen and coworkers reported on the kinetics of peroxide initiated grafting of vinyltrimethoxysilane and vinyltriethoxysilane onto polyethylene and

ethylene-propylene rubber and the moisture-catalyzed crosslinking of the silane-grafted copolymers[61].

Liptak and Mlejnik[62] performed a kinetic study of dicumyl peroxide decomposition reaction in *n*-heptane (used as a model hydrocarbon for PE) in the presence of vinyltri(2-methoxyethoxy)silane, in order to understand the mechanism of the vinyltrialkoxysilane grafting onto PE in the peroxide crosslinked reaction. The process was followed by measuring the cumyl alcohol / acetophenone ratio. Possible reactions in this process are presented in Figure 1-11 (Eq. 1-1 to 1-5).

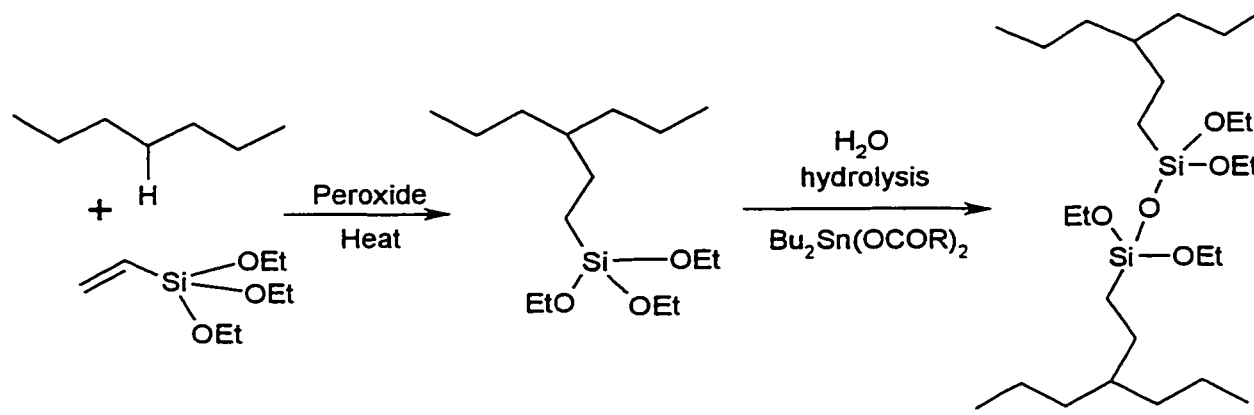

Figure 1-10: Peroxide-initiated grafting of vinyltriethoxysilane onto PE.

It was found that at 145°C the cumyl alcohol/ acetophenone ratio has a linear dependence on the amount of silane added. Reaction (1-4) is 150 times faster than reaction (1-2) and 270 times faster than reaction (1-3).[62] Therefore, it was deduced that the grafting onto PE chains occurs mainly by the addition of the vinylsilane to macroradicals. The macroradicals are generated in one of the following ways: H

abstraction from PE by the cumyloxy radicals; H abstraction from PE by PE macroradicals, and H abstraction from PE by the polyvinylsilane radicals. The recombination of macroradicals will also contribute to crosslinking. The total consumption of vinyl monomer, even when the latter was used in excess relative to dicumyl peroxide (DCP) suggests that a radical chain reaction of silane take place, initiated by peroxide or alkyl radicals.

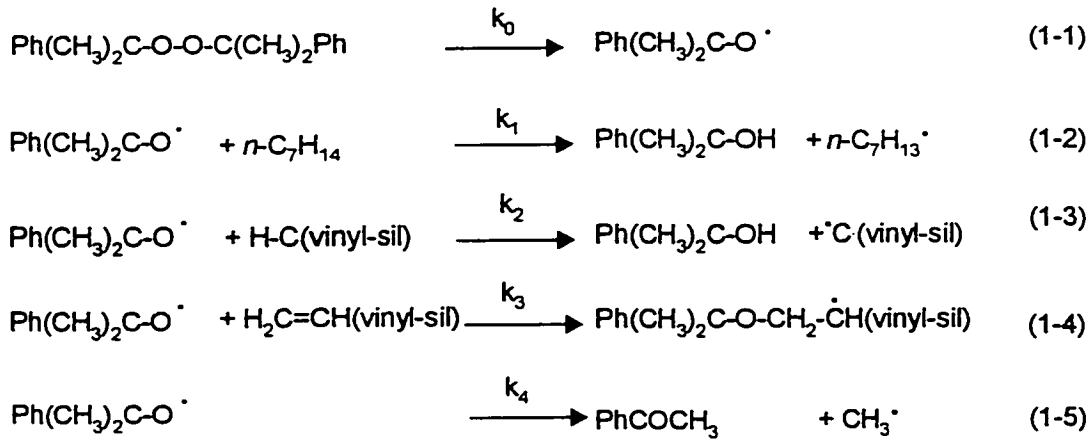

Figure 1-11: Possible mechanism for the vinyltrialkoxysilane grafting onto PE.

More recently Whitney *et al.* used dodecane as a model hydrocarbon in a structural study of the peroxide initiated grafting of vinyltrimethoxysilane in order to elucidate the nature of the grafts[63]. This study concluded that the use of small amounts of vinylsilane (2% v/v) and initiator (0.08% v/v) at 160°C leads to multiple single grafts (an average of 2.37 per mol dodecane) generated on alternate carbon atoms via an intramolecular 1,5-H-atom transfer[64] and to the extensive isomerization of dodecane and grafted products.

We have been actively involved in the development of reactive coupling agents containing vinylsilane moieties that could improve the adhesion between wood and polyethylene or polypropylene in composite materials.

While vinyltrialkoxysilanes readily graft to polyethylene, they are not suitable as coupling agents for wood/plastic composites due to their propensity to hydrolyze, which would result in the cleavage of the coupling agent from the components in composite materials, leading to little or no improvement in mechanical properties[65,66,67,68]. Therefore, we chose to use related vinylalkylsilanes for radical grafting to PE, an area that, to our knowledge, has not been explored. Unlike the trialkoxysilanes, vinylalkylsilanes are generally stable to moisture and a wide variety of other reagents, except strong acids[69] and fluoride ions[70]. Chapter 4 summarizes our investigations of the free-radical grafting of several vinylalkylsilanes (Figure 1-12) onto the model hydrocarbon squalane (Figure 1-12), a polyolefin (PP, LLDPE) mimic, using gel permeation chromatography and NMR techniques.

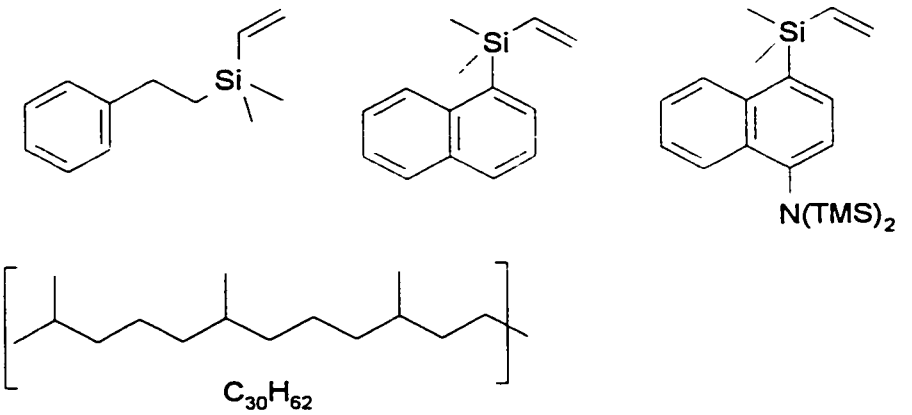

Figure 1-12: Structures of model vinylalkyl silanes and a model hydrocarbon (squalane) used for free radical grafting.

1.2 Research Objectives

The research presented in this thesis had two major objectives. The first was to design and synthesize new organo-functional silicones bearing chelating moieties and to evaluate their surface activity. These new materials are expected to combine the high surface activity conferred by the silicone-based backbone with the hydrophilicity and metal binding properties of the nitrilotriacetic acid and related derivatives, and lead to good performance for several applications involving hydrophilic-hydrophobic interface stabilization. Some of the interfaces targeted include but are not limited to, air-water, inorganic minerals-silicone rubber, inorganic minerals-dodecane (and related hydrophobic organic media), inorganic minerals-air, silicone-water. Chapter 2 presents several synthetic routes towards silicone chelators. Full synthetic details and characterization of the silicone chelators are presented. The surface activity of the novel silicone chelators is described in Chapter 3. Surface pressure isotherms (π-A) were measured in the presence and absence of metal cations such as Ca^{2+} and Ni^{2+} and at different pH values for the subphase. Some insight into possible conformations adopted by the silicone chelators at the surface is presented.

The second objective of this work has been to design and synthesize small molecular weight organosilane linkers that can control hydrophobic-hydrophilic interfaces in wood-polyolefin composites by means of covalent bond formation. Chapter 4 presents the synthesis of several vinyl/alkyl- and arylsilanes used as model compounds for the study of vinylsilane grafting onto squalane, initiated by several peroxide based

radicals. A coupling agent, namely (γ-hydroxypropyl)vinyldimethylsilane was used in order to improve adhesion in wood-polyethylene composites. Mechanical tests were performed in order to compare the properties of such composites with similar materials containing polyethylene-*g*-maleic anhydride and / or peroxides as adhesion promoters. A summary of the work is presented and a brief account of future projects deriving from this research is given in Chapter 5.

Chapter 6 presents details of the general experimental procedures including sources of reagents, solvents and solvent purification and analytical and instrumental techniques used for characterization purposes, as well as full experimental procedures and characterization for the compounds synthesized.

2 Silicone Chelators

2.1 Synthetic Targets: Silicone Chelators

Poly(dimethylsiloxane) oligomers functionalized with EDTA, NTA, and NTAA chelating groups have not been previously synthesized, to the best of our knowledge. The metal ion binding moieties can be attached either at the ends or along the backbone of the silicone. We anticipate that these new materials could find possible applications as dispersing agents, as surfactants (e.g., in the polymerization of octamethyl-cyclotetrasiloxane, D_4, in aqueous media), as heavy metal sequestrants, and flocculation agents. We predict that the presence of metal cations such as Ni^{2+}, Ca^{2+}, Fe^{3+}, etc., in an aqueous subphase will have a marked influence over the surface behavior of the silicone chelators. It is also expected that such materials will have a strong affinity towards metal ions in solid salts.

Our approach to chelating silicones, which will be presented in detail in Chapter 2.2, uses commercially available amino-functional silicones (see Chapter 6) as starting materials. Figure 2-1 presents NTA-based silicone chelators as well as EDTA and NTAA related structures that could be equally interesting as synthetic targets.

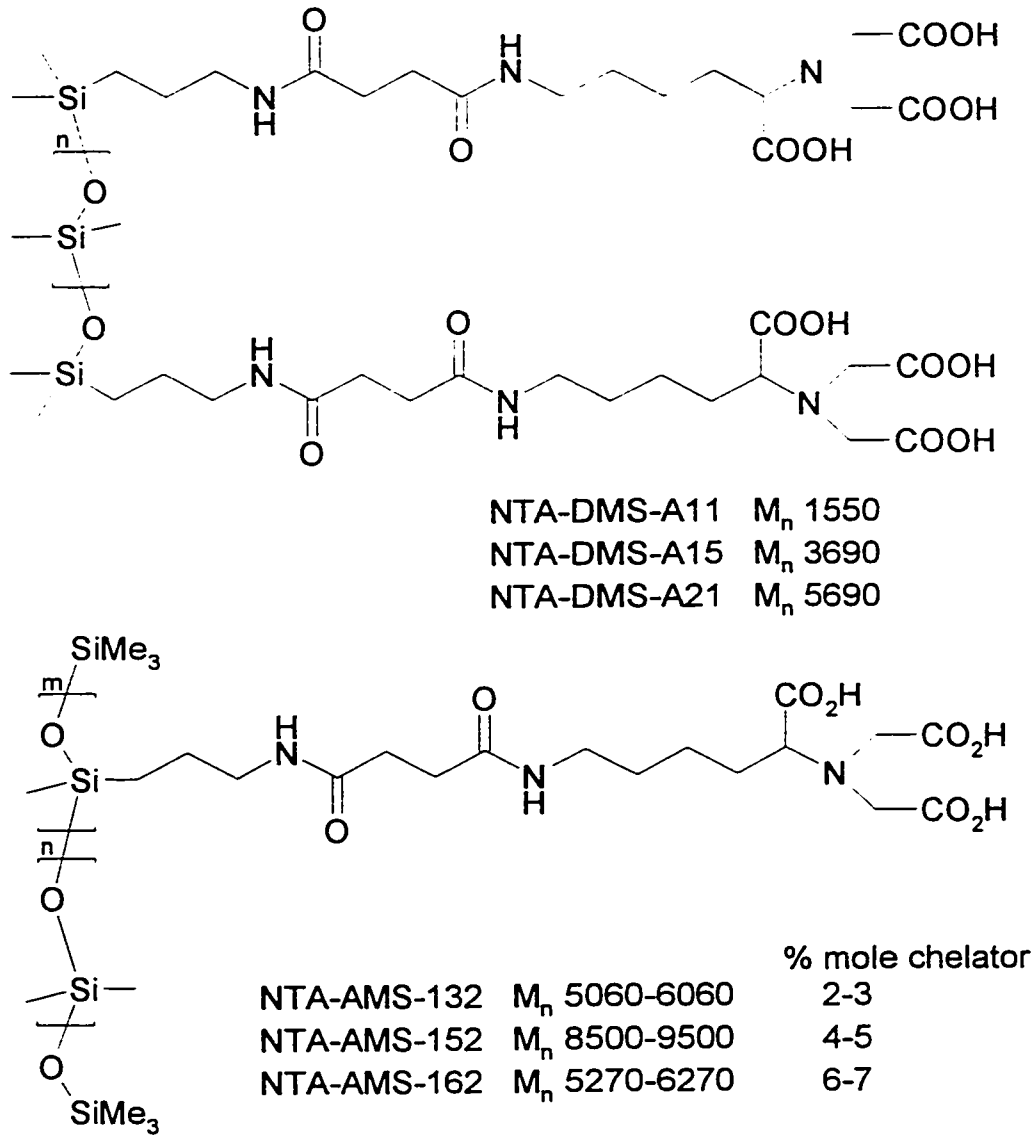

Figure 2-1: NTA-silicone chelators.

In order to be able to compare the surface properties of NTA-silicone chelators with those of silicones functionalized with simple carboxylic acid moieties, the same amino-functional silicone starting materials were used to synthesize a series of succinyl

silicones of comparable molecular weights. Figure 2-2 presents the structures of the succinyl silicones.

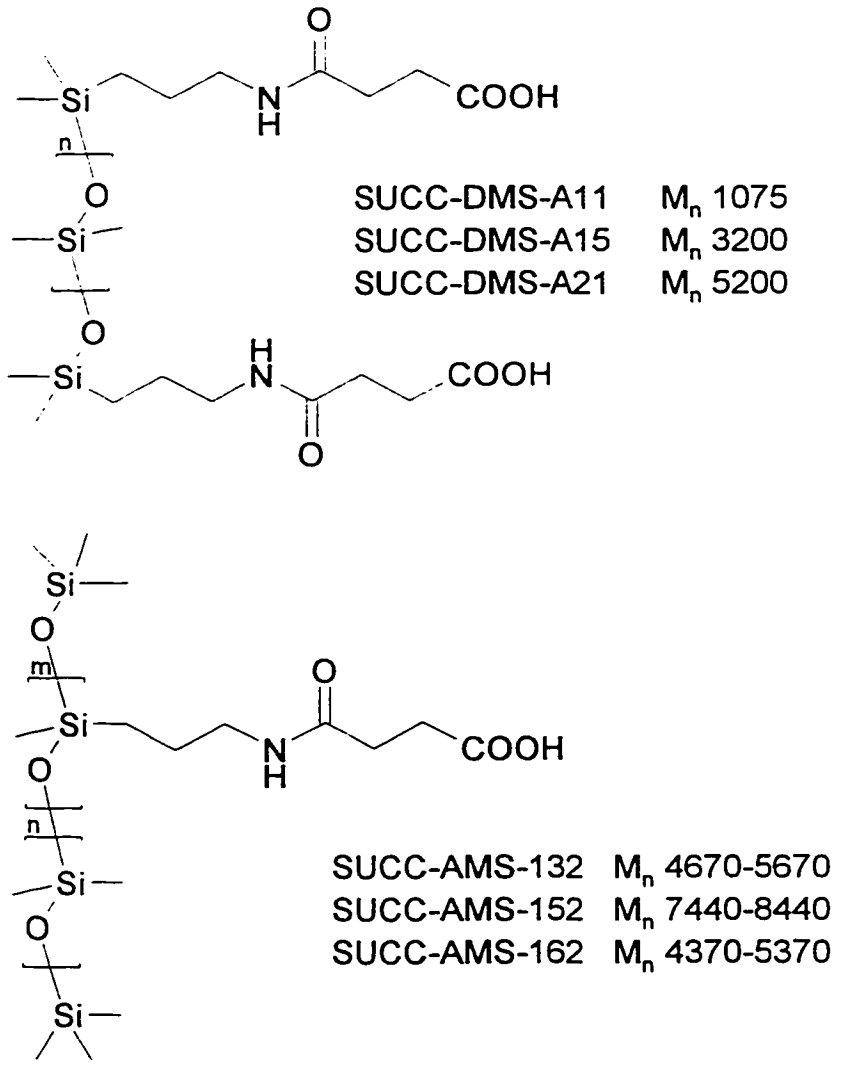

Figure 2-2: Succinyl silicone structures.

The acetamide derivatives of the starting materials were also synthesized, in order to determine the molecular weight and the polydispersity of the starting materials by gel

permeation chromatography (GPC). The structures of these derivatives are presented in Figure 2-3.

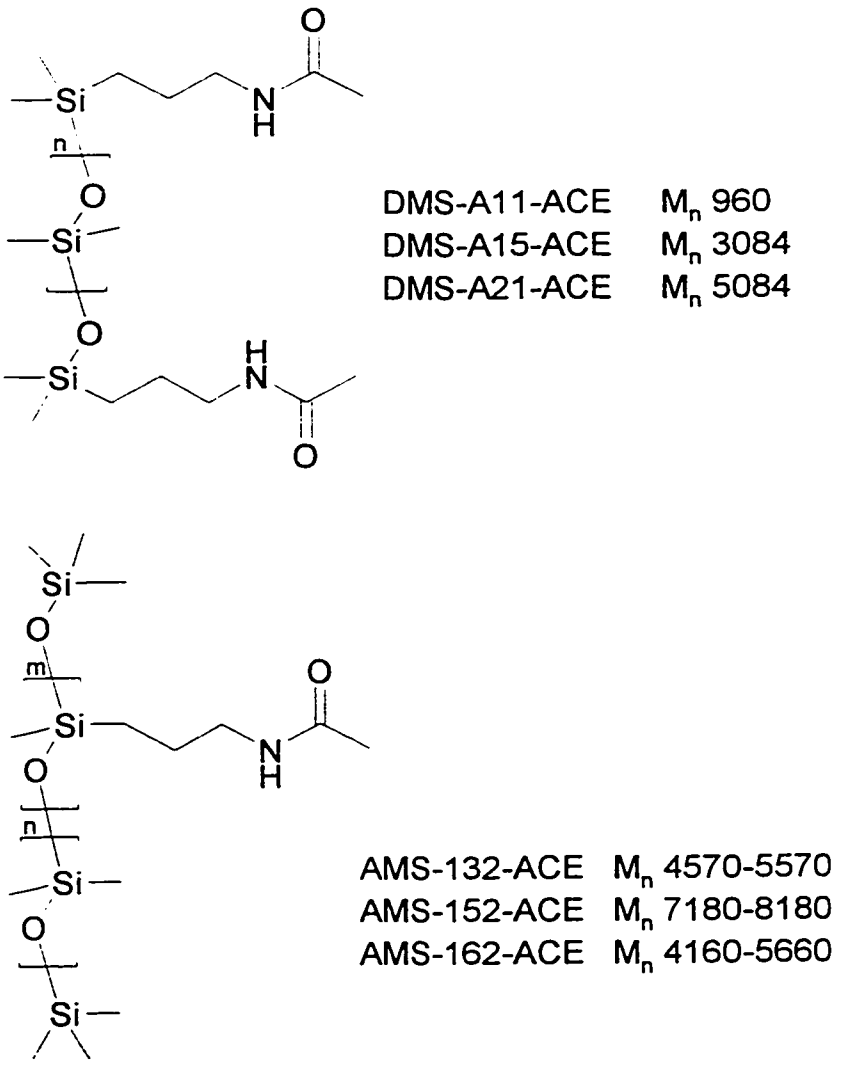

Figure 2-3: Acetamido-functional silicone structures

This chapter presents the synthesis and characterization of the following compounds: NTA-silicones, succinyl silicones, and acetamido-silicones. The polymers obtained were characterized by ^{1}H- and ^{13}C-NMR, gel permeation chromatography (GPC), electrospray-mass spectroscopy (ES-MS), and Fourier transformation infrared spectroscopy (FT-IR).

2.2 Synthetic Routes to Silicone Chelators

The primary amine group in NTA can serve as the attachment of the chelating moiety onto suitably functionalized silicones. Some of the most promising silicone starting materials are epoxy- and amino-functionalized silicones, due to their commercial availability in several structural types and molecular weights (Figure 2-4). The amino-functional silicones must first be converted to carboxylic acid derivatives in order to make the attachment of NTA via the amine group possible.

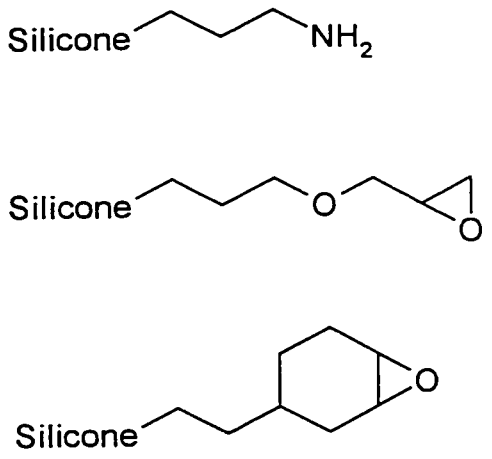

Figure 2-4: Commercially available end-functional silicones.

There are two possible convenient routes to NTA functional silicones, starting from the polymers shown in Figure 2-4. One route involves the nucleophilic attack of the amine functionality onto the epoxide resulting in the formation of an amino-hydroxy-silicone chelator (Figure 2-5). For reasons that will be explained in Chapter 2.3, this pathway was abandoned.

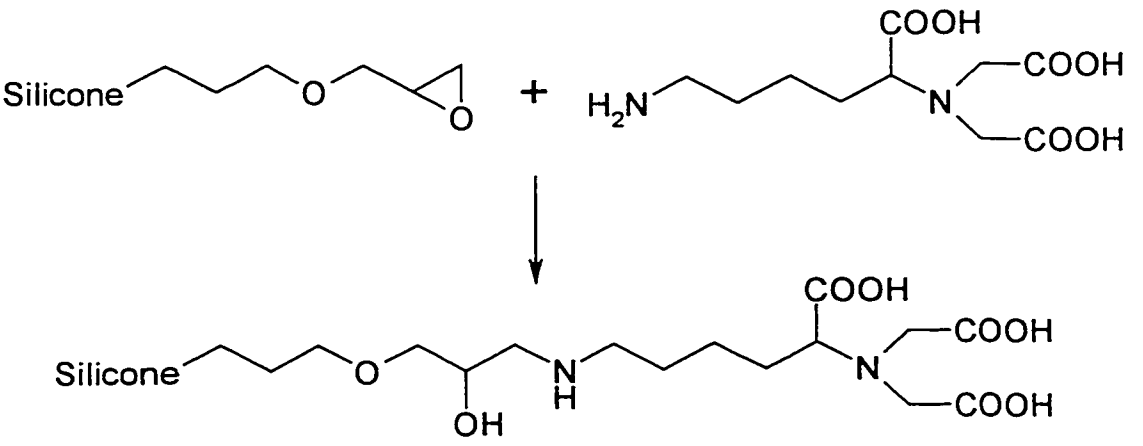

Figure 2-5: Synthesis of NTA-silicones from epoxide-functional silicones.

A second route involves the synthesis of a carboxylic acid-functional silicone from an amino-functional silicone by treatment with succinic anhydride (SA), followed by the attachment of the chelator via amide bond formation (Figure 2-6). The carboxylic acid-functional silicone intermediates are also of interest since the presence of the hydrophilic succinyl group can impart surface activity to these compounds. It is useful to measure their surface pressure-area isotherms using the same experimental conditions as for silicone chelators and compare the results.

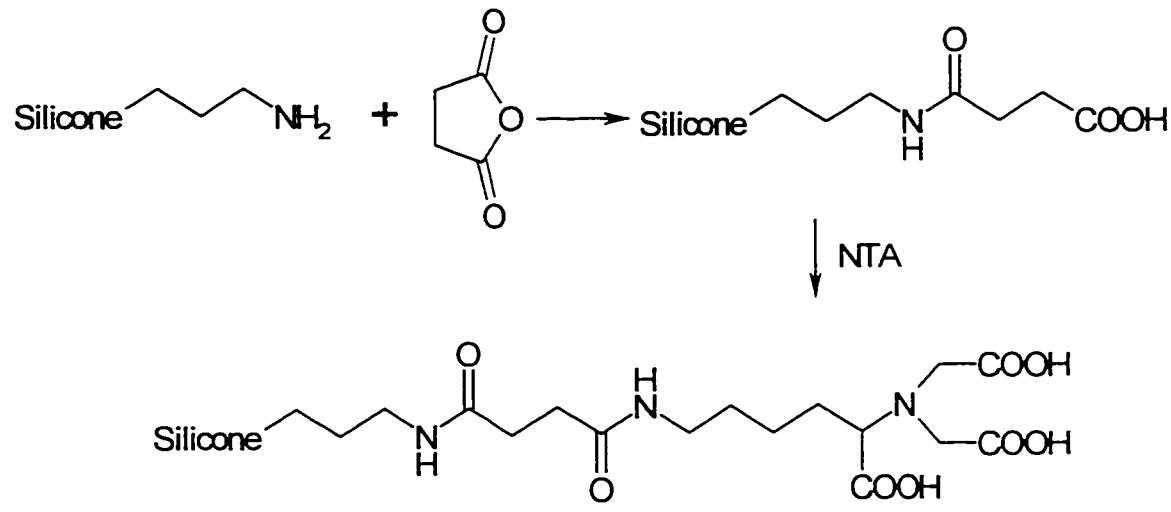

Figure 2-6: Synthesis of NTA-silicones via amide bond formation.

An alternative to this synthesis involves the attachment and activation of the succinyl group to a suitably protected NTA, followed by coupling with the amino functional silicone via amide bond formation, and protecting group removal (Figure 2-7).

Synthetic procedures and purification methods typical for peptides and lipids[71,72,73] can be adapted and employed for these syntheses. There are several types of amino-functional silicones commercially available, and each type comes in several molecular ranges. Two such classes of materials were used throughout this work: aminopropyl-terminated polydimethylsiloxanes and aminopropyl-methylsiloxane-dimethylsiloxane copolymers (see Chapter 6 for technical specifications).

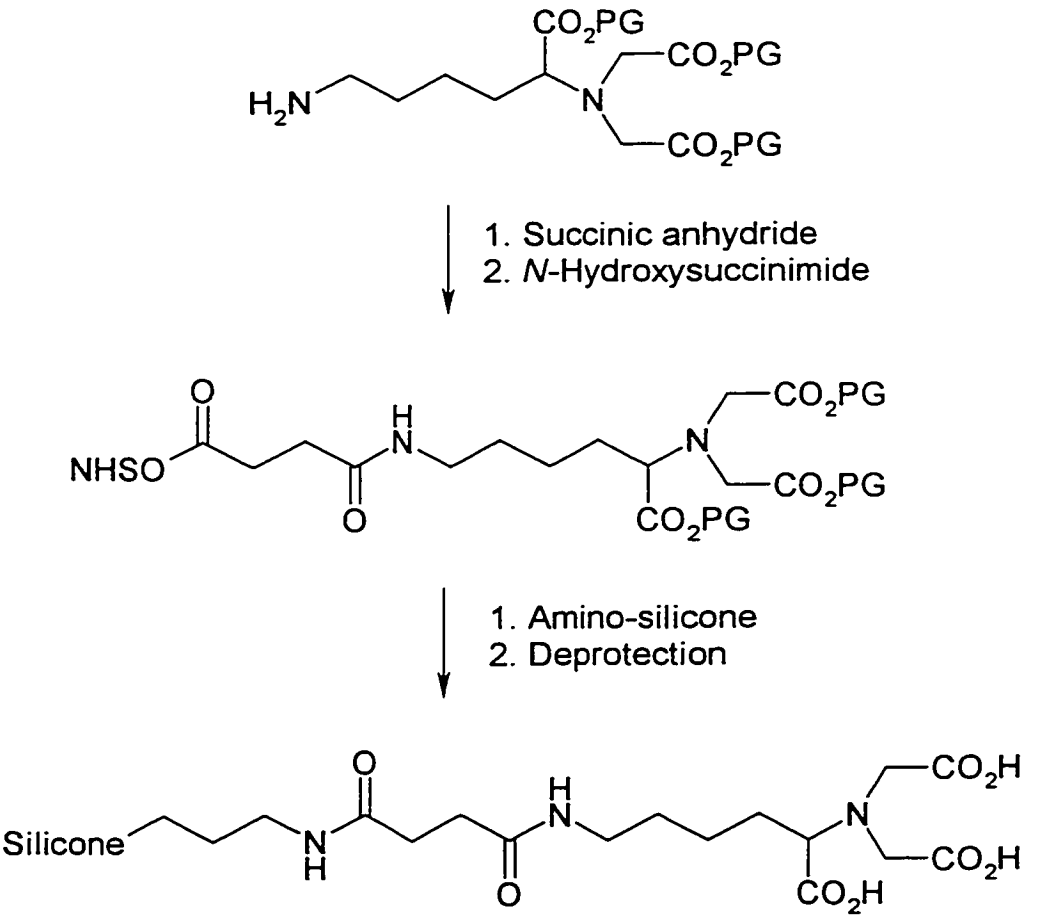

Figure 2-7: Alternative synthesis of NTA-silicones.

2.3 Results and Discussion

2.3.1 Synthesis of NTA

The chelating agent used, namely N^{α},N^{α}-bis(carboxymethyl)-L-lysine (NTA) was synthesized according to the procedure presented by Hochuli *et al.*[26] (Figure 2-8).

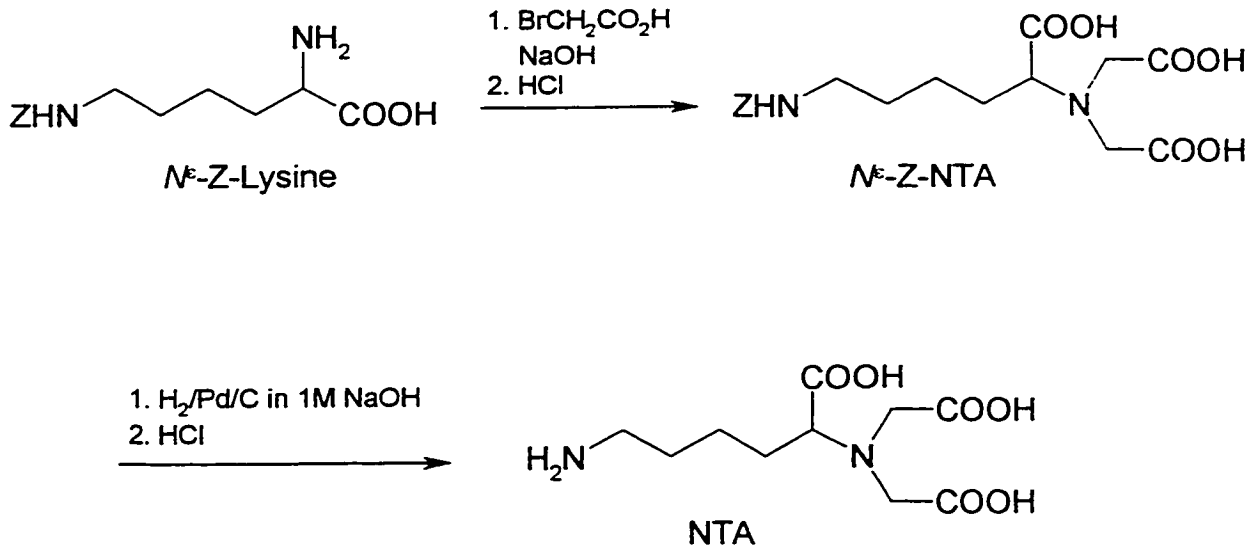

Figure 2-8: Synthesis of NTA.

The final product (NTA) was purified by trituration with hot methanol, followed by partial removal of the solvent. The product crystallized from the solution after two days. An alternative procedure for the purification of NTA involved desalting on a column filled with Sephadex-G10 size exclusion gel (MW cutoff < 700), followed by lyophilization.

2.3.2 Attempts Towards the Synthesis of Silicone Chelators via Epoxide Ring Opening

As mentioned previously (Chapter 2.2, Figure 2-5), one possible route to silicone chelators involved the nucleophilic attack of the amino group of NTA at the epoxide ring

of a suitably functionalized silicone. In order for the reaction to occur, the amino group must not be protonated, and for this purpose a minimum pH value of 8–8.5 was necessary. In order to optimize this reaction several model epoxide functional siloxanes and silicones were used (Figure 2-9).

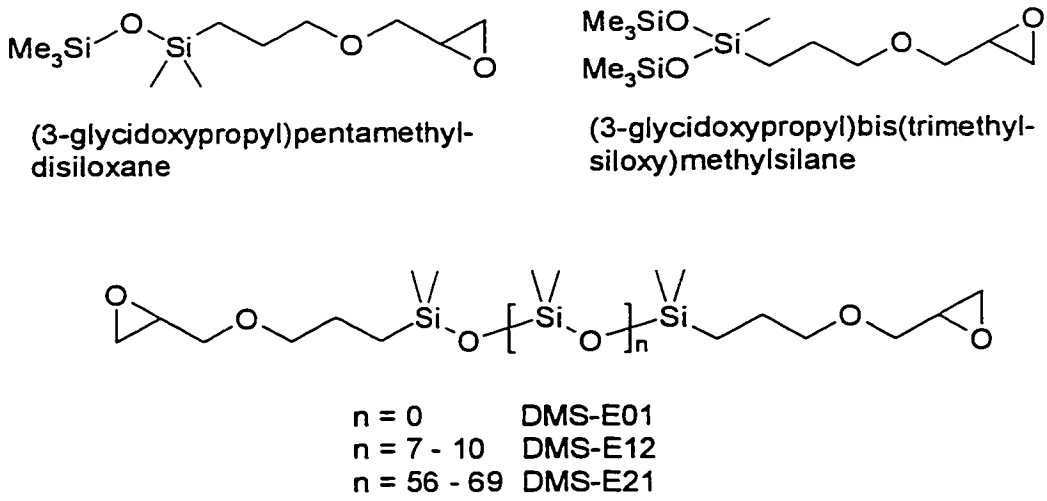

Figure 2-9: Epoxy-functional siloxane structures.

(3-Glycidoxypropyl)pentamethyldisiloxane and (3-glycidoxypropyl)bis(trimethyl-siloxy)methylsilane were synthesized via the hydrosilylation of pentamethyldisiloxane and bis(trimethylsiloxy)methylsilane, respectively, with allyl glycidyl ether catalyzed by Karstedt's catalyst (Figure 2-10).

Two problems were raised by this approach. The first problem was the insolubility of NTA in organic solvents such as methylene chloride, THF, and 2-propanol, in which the silicone substrate was soluble. As a consequence, all reactions were performed in mixtures of aqueous and organic solvents, under vigorous stirring at temperatures between 20 and 60°C, for duration of between four hours and three days.

The basic environment needed for the reaction to occur created the second problem. Different aqueous solutions of NTA, containing $NaHCO_3$, Na_2CO_3, or phosphate buffers (pH 6.8–7.8), were tested. In all cases GC and GPC analysis of aliquots taken from the reaction mixtures evidenced extensive degradation of the siloxane or silicone substrate.

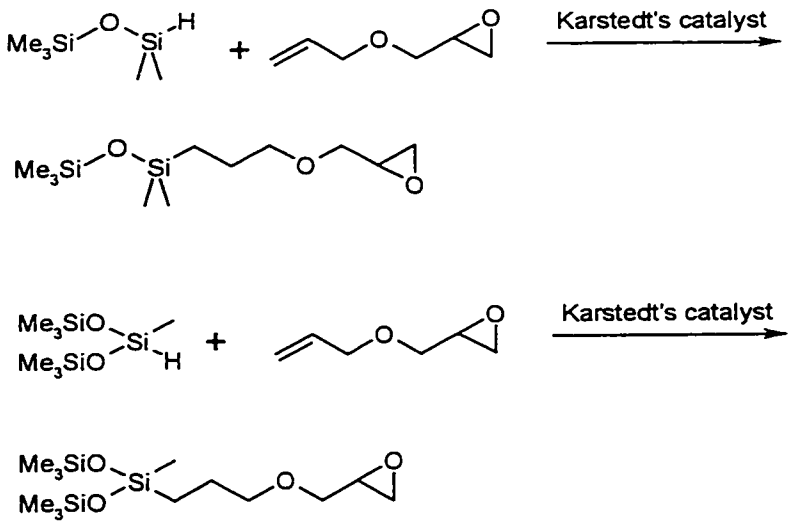

Figure 2-10: Synthesis of model epoxy-functional siloxanes.

An alternative route, involving the attachment of allylglycidyl ether to NTA, followed by hydrosilylation onto pentamethylsiloxane or bis(trimethylsiloxy)silane using a variety of palladium and platinum based catalysts, also failed (Figure 2-11), due to the fact that non of the catalysts used led to hydrosilated product.

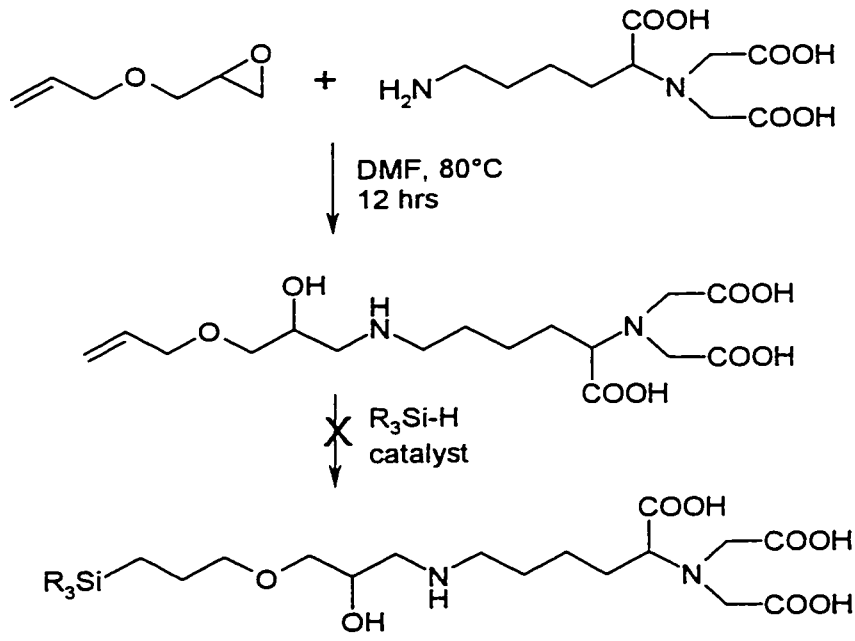

Figure 2-11: A second approach towards silicone chelator synthesis via epoxide ring opening and hydrosilylation.

Yet another approach involved first the solubilization of NTA by derivatization as TMS-ester, followed by treatment with epoxy-functional siloxanes in methylene chloride at 60°C (Figure 2-12). This approach also failed, leading only to the recovery of the starting materials. As a consequence these routes were abandoned and new synthetic strategies, involving aminopropyl-functional silicones as starting materials, were explored.

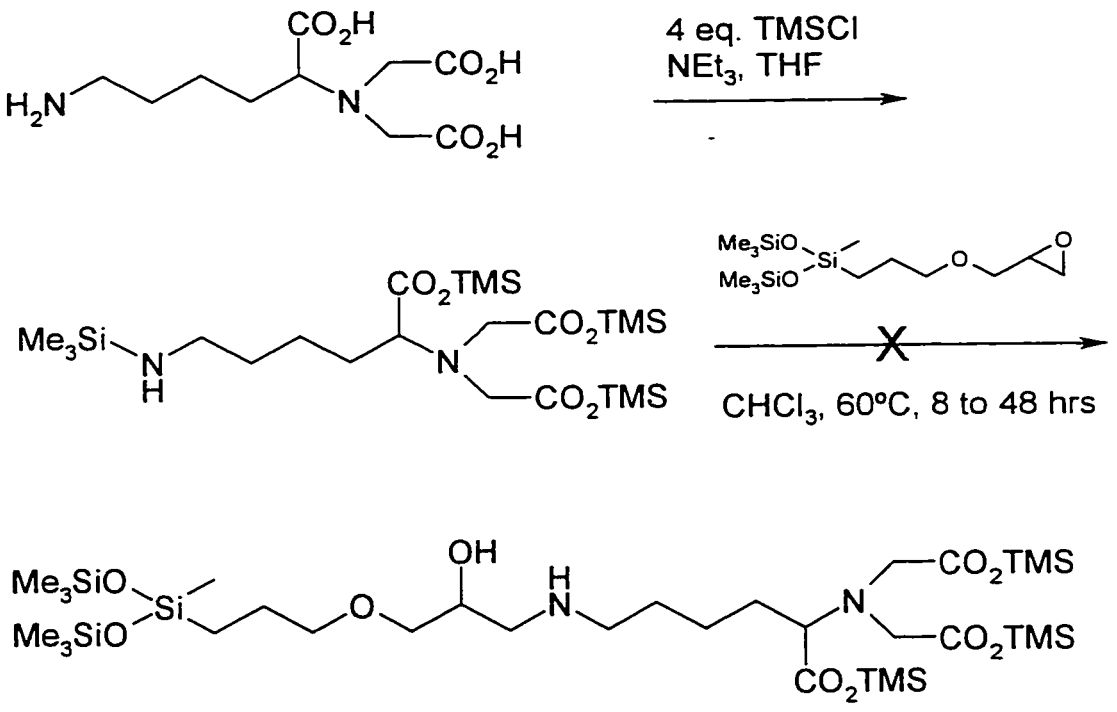

Figure 2-12: Third approach towards silicone chelator synthesis via silylation and epoxide ring opening.

2.3.3 Synthesis and Characterization of (3-Acetamidopropyl) Silicones

Two classes of aminopropyl-functional silicone starting materials were readily available commercially: aminopropyl-terminated polydimethylsiloxanes, and (aminopropyl)-methyl-siloxane-dimethylsiloxane copolymers (Chapter 6). For the purpose of determining their molecular weight using gel filtration chromatography (GPC), these compounds were derivatized using acetic anhydride and triethylamine in methylene chloride (Figure 2-13).

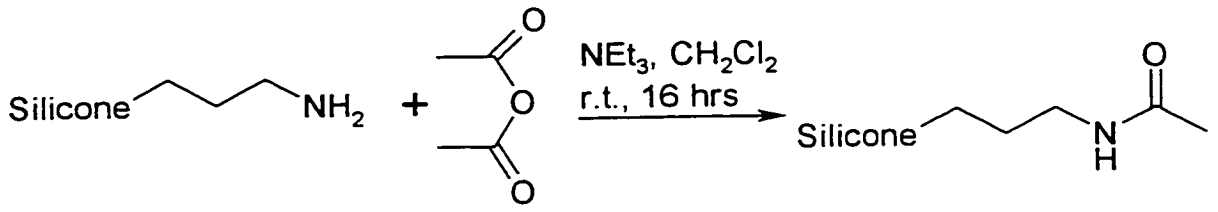

Figure 2-13: Synthesis of 3-acetamidopropyl-silicones.

The number average molecular weight (M_n), weight average molecular weight (M_w), and polydispersity (PD) obtained experimentally are presented in Table 2-1.

Table 2-1: Molecular weights for amino-functional silicones and their acetylated derivatives from ^{1}H-NMR and GPC measurements.

Silicones	Theory	Experimental Results				
		^{1}H-NMR		GPC		
	M_n	M_n	Degree of polymeriz.	M_n	M_w	PD
DMS-A11	850 – 900[a]	850 – 900	8 – 9	-	-	-
DMS-A11-ACE	934 – 984[b]	990	8	447	920	2.06
DMS-A15	3000[a]	3000 – 3100	37 – 38	-	-	-
DMS-A15-ACE	3084[b]	3100	37	1817	3727	2.05
DMS-A21	5000[a]	6500 – 6600	84 – 85	-	-	-
DMS-A21-ACE	5084[b]	5200	66	3465	8527	2.46
AMS-132	4500 – 5500[a]	-	-	-	-	-
AMS-132-ACE	4570 – 5570[b]	-	-	3925	6864	2.09
AMS-152	7000 – 8000[a]	-	-	-	-	-
AMS-152-ACE	7180 – 8180[b]	-	-	3583	7774	2.17
AMS-162	4000 – 5000[a]	-	-	-	-	-
AMS-162-ACE	4160 – 5160[b]	-	-	1583	2801	1.77

[a] – Manufacturer specification, determined by using polystyrene standards

[b] – Values calculated using the manufacturer specifications given for amino-functional silicones

The molecular weight of the starting materials and of the derivatized silicones could also be determined from ^{1}H-NMR spectra for the end-functional compounds (Table 2-1). The M_n values for (3-acetamidopropyl) silicones, as determined from GPC, were significantly lower than the M_n values determined from ^{1}H-NMR and given by the manufacturers specifications, in the case of DMS-A15-ACE and DMS-A21-ACE. It is possible that some errors in the integration of the $SiCH_3$ peaks at ~0.3 ppm could account potentially for this difference. A better explanation could be our choice of PDMS standards used for the calibration curve for the GPC runs, while the manufacturer used polystyrene standards. The M_n values for pendant functionalized silicones AMS-132-ACE, AMS-152-ACE, and AMS-162-ACE were also found to be higher than the ones specified by the manufacturer.

2.3.4 Synthesis of Silicone Chelators. Route 1.

2.3.4.1 Synthesis of Silicone Chelators via Amide Bond Formation. Route 1.

Two synthetic routes starting with amino-functional silicones were explored. The first route (Figure 2-14) had the advantage of being concise. In the first step, the amino-functional silicones were converted to the carboxylic acid functional derivatives by treatment with succinic anhydride at room temperature in the presence of triethylamine. A brief extraction with 1M HCl and extensive washing with deionized water purified the products. The yields for end-functional succinyl silicones SUCC-DMS-A11, -A15, and

-A21 were very high (95%) and the functional group deprotection was quantitative, as determined by ^{1}H-NMR. The pendant succinyl silicones SUCC-AMS-132, -152, and-162 were obtained in lower yields (66–86%), due to poor phase separation during the extraction (emulsions were formed).

The second step of the synthesis involved activation of the carboxylic acid group with *N*-hydroxysuccinimide (NHS) mediated by a carbodiimide. Dicyclohexyl-carbodiimide was used for the initial experiments. The precipitated dicyclohexylurea by-product was very difficult to remove. The formation of significant amounts of the unwanted *N*-acylurea derivative of the succinyl silicones, as well as the difficulty of its removal during purification using silica gel chromatography, led to the use of an alternative reagent, the water soluble carbodiimide (EDCI). The urea byproducts as well as unreacted NHS were easily removed by brief aqueous extraction in this case. Succinimidyl-terminated succinyl-polydimethylsiloxane DMS-A11 was obtained in 94% yield.

The final step of the synthesis involved the coupling of the NHS-activated silicone with NTA followed by extensive dialysis to remove small molecular weight by-products and unreacted starting materials. This step met with several difficulties. The first major problem was the difference in polarities between the functional silicone (soluble in solvents such as THF, 1,2-dimethoxyethane, methylene chloride, chloroform) and NTA (soluble only in water or large amounts of methanol). A mixture of methylene chloride/methanol (1:3) was used successfully to maintain all reagents in solution for the synthesis of NTA-DMS-A11. Larger molecular weight silicones, however, separated

from methylene chloride / methanol solutions of various compositions and did not react with NTA.

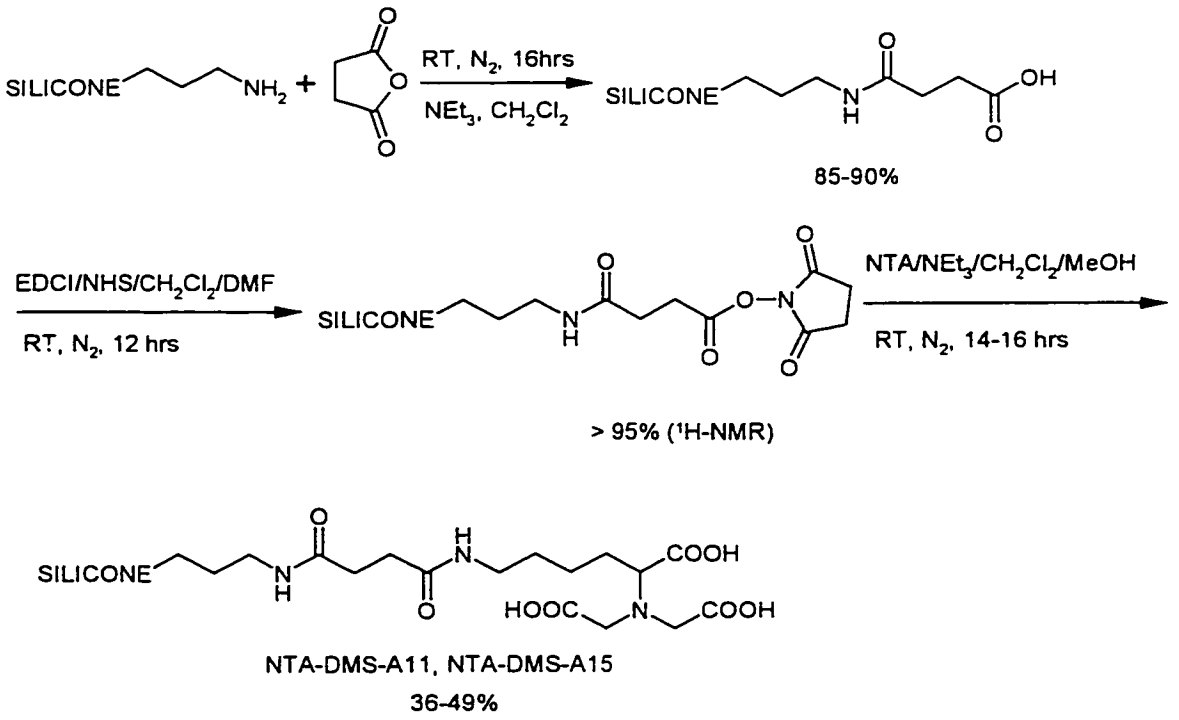

Figure 2-14: Route 1 to silicone chelators via amide bond formation.

A base had to be employed in order to deprotonate NTA. Both 4-*N*-ethylmorpholine and triethylamine were used with success. Extensive dialysis in methanol/methylene chloride (1:1) solution using a Spectrapor membrane with a MWCO (molecular weight cutoff) of 1000 led to small amounts of NTA-DMS-A11 (10–30 mg). Due to the high cost of the membranes, as well as the large amounts of solvents used, this purification method is not feasible when larger amounts (1–2 g) of product are desired. Attempts to remove unreacted NTA as well as triethylamine by employing ion-exchange

chromatography on various cation exchange resins failed. The use of strongly acidic Dowex-50W (H^+-form) led to significant decomposition of the silicone via equilibration within 30–40 minutes. The use of strongly acidic Dowex 88 (sodium-form) and weakly acidic Dowex CCR-3-hydrogen did not lead to any improvement. Purification by gel filtration chromatography on Toyopearl gel using methylene chloride/methanol (3:7) led to small amounts of pure NTA-DMS-A11.

A second solvent combination used to conduct the final step was 1,2-dimethoxyethane: water. NTA was dissolved in water, $NaHCO_3$ (3 mmol/mmol NTA) was added and the silicone solution in 1,2-dimethoxyethane was added with vigorous stirring. NTA-DMS-A11 (sodium salt) formed an emulsion with water and could be dialyzed using a Spectrapor CE membrane with a MWCO of 500. Some equilibration took place during purification. Larger molecular weight silicones could not be successfully obtained using water/1,2-dimethoxyethane solvent mixtures due to phase-separation problems.

2.3.4.2 ES-MS of Metal Complexes of NTA-DMS-A11

In order to test the ability of NTA-DMS-A11 to form complexes with metal cations, the chelating silicone was dissolved in deionized water (5×10^{-4} M) and treated with 10^{-3} M solutions of $CuCl_2$, $FeCl_3$, and $CoCl_2$, respectively. The solutions obtained were analyzed by electrospray-mass-spectroscopy (ES-MS). Ammonium hydroxide (1 drop of 0.1% NH_4OH solution) was added and the data were recorded in negative ion

mode. It is known that Fe^{3+}, Co^{2+}, and Cu^{2+} form stable complexes with iminodiacetic acid type chelators[27] (tridentate ligands) and EDTA[74,75] (a pentadentate ligand for Cu^{2+} and Co^{2+}, and a hexadentate ligand for Fe^{3+}) at pH values larger than 5. It is also known[27] that NTA forms stable complexes with Cu^{2+} and Co^{2+} at pH > 4. It was therefore expected that all the above metal ions would form stable chelates with NTA derivatized silicone NTA-DMS-A11 under the experimental conditions used for the ES-MS analysis (pH 8–10). The nuclidic masses and isotopic abundance[76] for Co, Cu, and Fe are presented in Table 2-2.

Table 2-2: Nuclidic masses and isotopic abundances for Co, Cu, and Fe.

Mass	Element	Isotope, % Abundance
55.9349393	Fe	^{54}Fe, 6.3: ^{57}Fe, 2.4; ^{58}Fe, 0.31
58.9331976	Co	
62.9295989	Cu	^{65}Cu, 44.6

Ionic species having the molecular weights of 529, 533, and 536 were positively identified as a specific organic residue containing Fe^{3+}, Co^{2+}, and Cu^{2+}, respectively and the same organic residue (Figure 2-15). This fact demonstrated the presence of the metal ion-NTA complexes attached to dimethylsiloxane units. The isotopic pattern modeling confirmed the identity of these complexes (Figure 2-16). No other larger molecular weight species could be detected. This could be a consequence of the equilibration of the siloxane backbone either during dialysis, or during the ES - MS experiment while the sample was exposed to ammonium hydroxide.

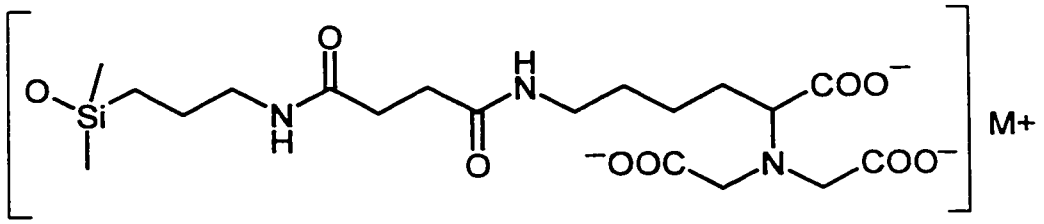

Fe **Cu** **Co**

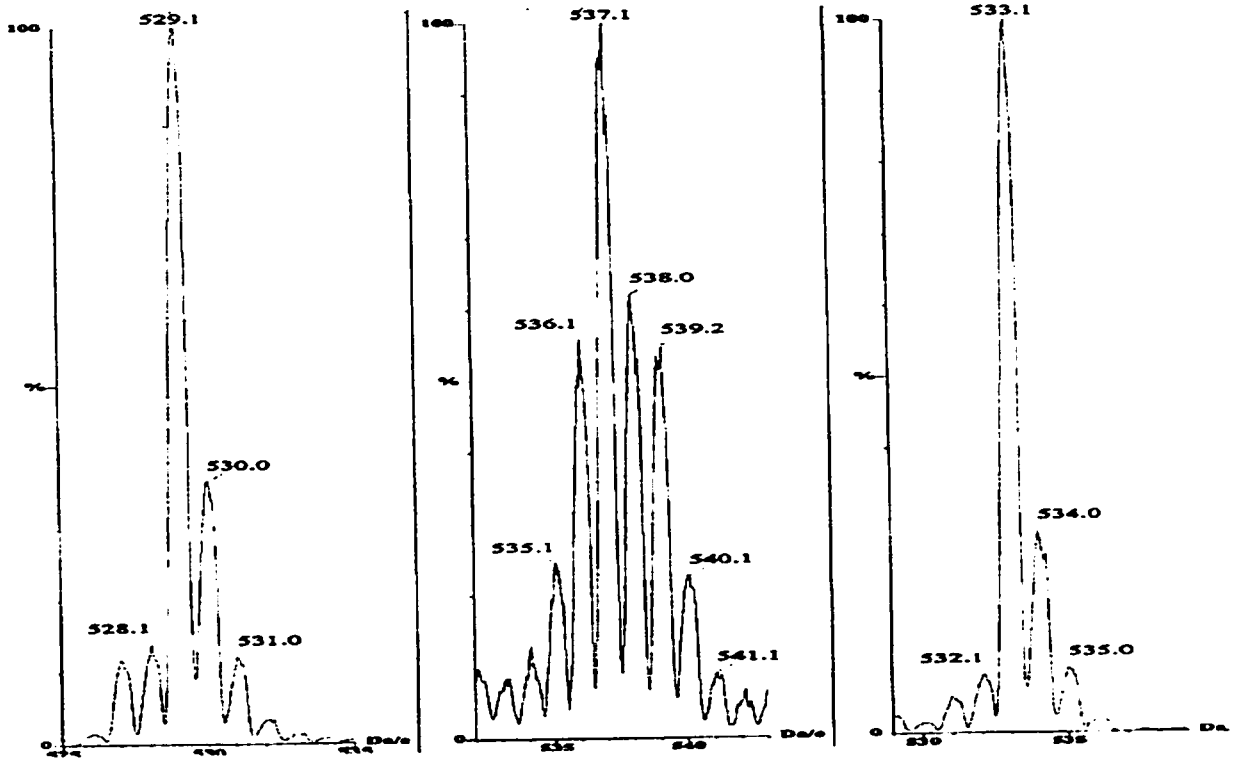

Figure 2-15: Transition metal cation complexes identified by ES-MS.

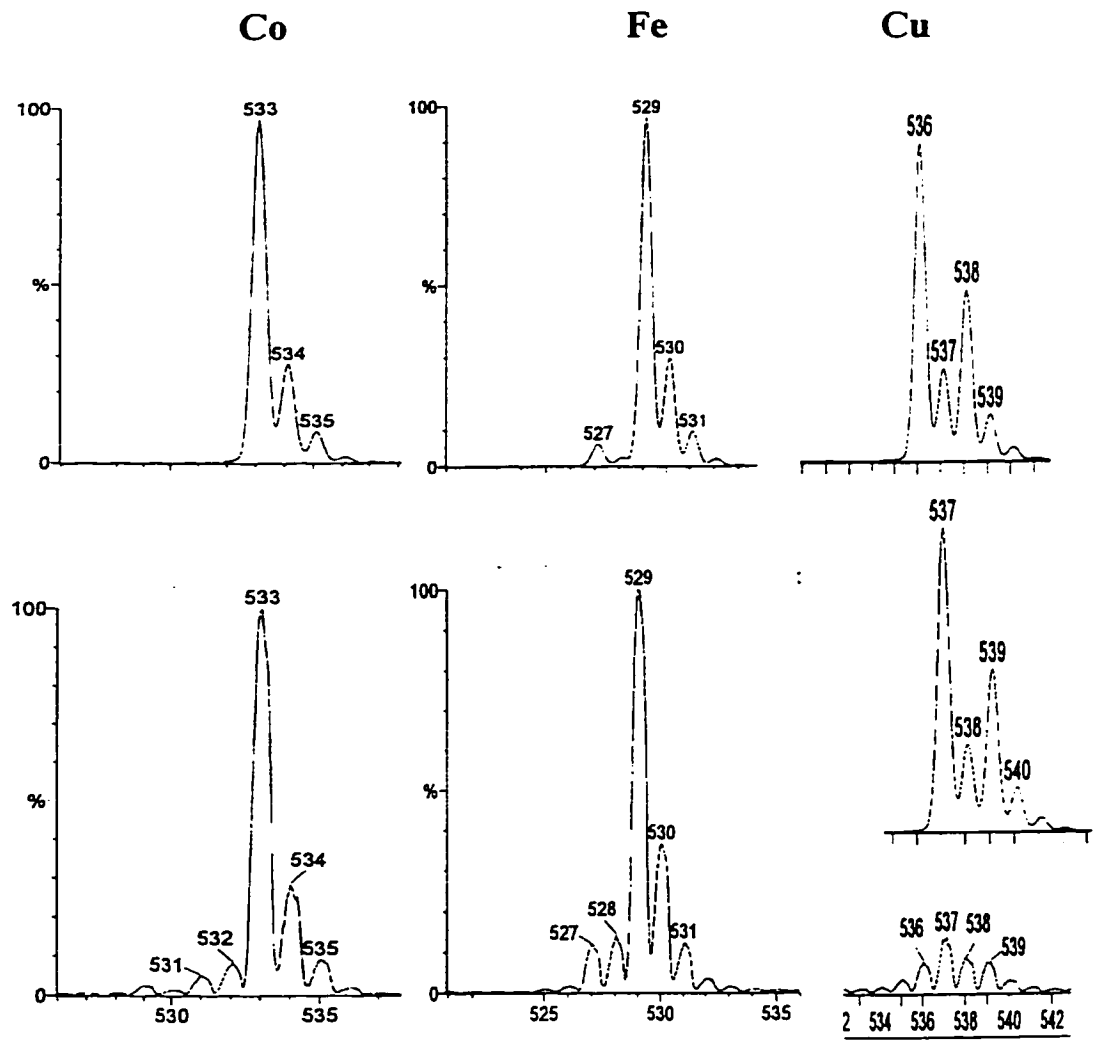

Figure 2-16: Isotopic modeling of metal-chelated fragments. Top: isotopic modeling. Bottom: experimental results.

2.3.4.3 *Synthesis and Characterization of Succinyl Functional Silicones*

The first step of the synthetic route presented in section 2.3.4.1 yielded a series of succinyl functional silicones, which could also present surface activity (Figure 2-17).

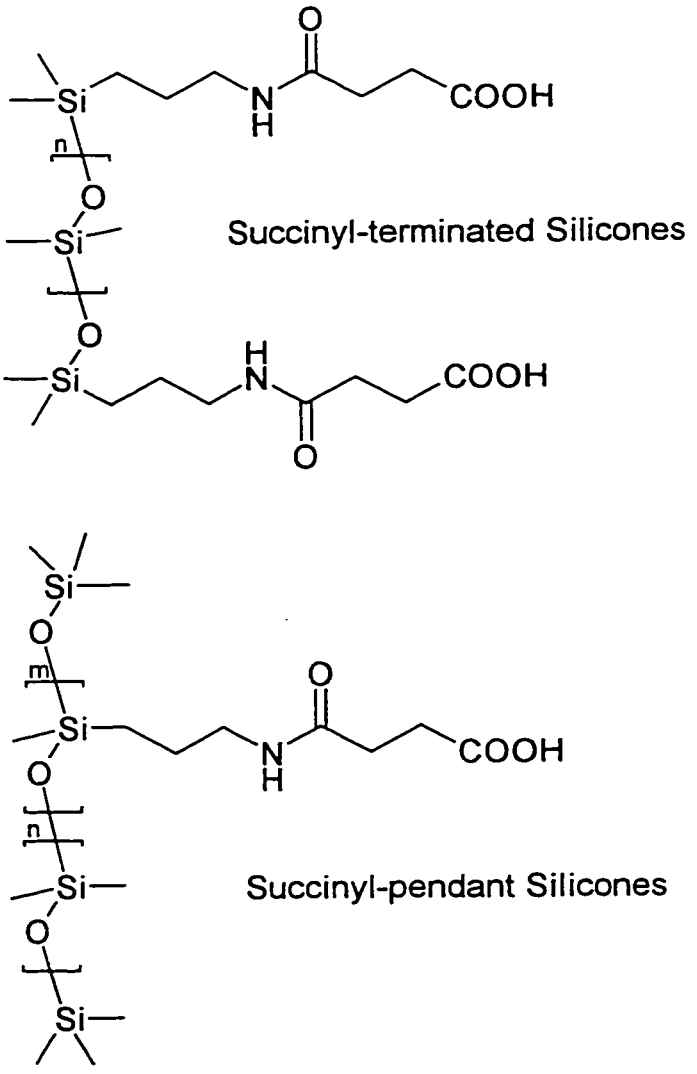

Figure 2-17: Succinyl functional silicone structures.

The molecular weights of all the succinyl silicones (except for SUCC-DMS-A11) were determined by gel permeation chromatography. For the end-terminated silicones the molecular weight could also be determined from ^{1}H-NMR. Table 2-3 presents the values obtained experimentally, as well as the values calculated using the data provided by the manufacturer for the amino-functional silicones.

Table 2-3: Molecular weight determination using ^{1}H-NMR and GPC for succinyl-functional silicones.

Silicones	Theoretical[a] M_n	Experimental Results				
		^{1}H-NMR		GPC		
		Mn_w	Degree of polymeriz.	M_n	M_w	PD
SUCC-DMS-A11	1050 - 1150	1050 – 1150	8 - 9	-	-	-
SUCC-DMS-A15	3200	3400	40 - 41	1185	3552	3.0
SUCC-DMS-A21	5200	5500	68 - 69	1369	5746	4.19
SUCC-AMS-132	4660 - 5660	-	-	1348	3162	1.62
SUCC-AMS-152	7435 - 8435	-	-	1200	3162	2.63
SUCC-AMS-162	4370 - 5370	-	-	785	1709	2.18

[a] – Values calculated using the manufacturer specifications given for aminofunctional silicones

No values for M_n, M_w, or polydispersity could be obtained for SUCC-DMS-A11, due to severe distortions of the detected refractive index signal. The experimental values determined by ^{1}H-NMR and GPC were reasonably close to each other and to the calculated values for the end-functional silicones. No molecular weight estimates could be obtained from the ^{1}H-NMR data for the succinyl-pendant silicones.

The molecular weight values determined experimentally by gel permeation chromatography for these compounds were significantly lower in the case of SUCC-

AMS-152 and SUCC-AMS-162, when compared to the calculated values. This could be due to reasons discussed in Chapter 2.3.3. It is also possible that during chromatography, the compounds, which have polar groups along the backbone, were separated not only by size exclusion, but also by some adsorption onto the solid support, which would explain the apparent lower molecular weight values measured. The fact that the polydispersities of all the silicones had greater values than the ones determined for the (3-acetamidopropyl)-functional polydimethyldiloxanes suggested that some adsorption on the column may have taken place. Since the GPC measurements were performed after the products had been stored for several months, it was possible that degradation of the silicone backbone might have occurred to some extent during this period of time.

The presence of succinyl groups at the ends or pending from the backbone of polysiloxanes imparts amphiphilic character to these inherently hydrophobic materials. In addition, the carboxylic acid groups can form carboxylates with a multitude of metal cations. The formation of such salts could lead to aggregation (e.g., with Ni^{2+}) and possibly flocculation (e.g., if Ca^{2+} is used). The surface behavior of succinyl functional silicones will be presented in Chapter 3.

2.3.5 Synthesis of silicone chelators. Route 2

2.3.5.1 Synthesis of Silicone Chelators via Amide Bond Formation. Route 2

A second synthetic route towards silicone chelators, consisting of seven steps, was devised in order to avoid the problems presented in Chapter 2.3.4.1. An NHS-activated succinyl-functional NTA bearing benzyl protective groups (N^{ε}-SSU-NTA-Bn ester) was obtained using adaptations of synthetic procedures and purification methods typical for peptides[71,72,73] (Figure 2-18).

N^{ε}-*tert*-Butyloxycarbonyl-NTA (cesium salt) was synthesized from NTA and di-*tert*-butyldicarbonate and used for the next step without further purification. The introduction of the benzyl groups met with some difficulties and the low yield (45% after silica gel chromatography) was due to the fact that significant amounts of mono and di-benzyl esters were obtained along with the desired tribenzyl ester.

The *tert*-butyloxycarbonyl group was removed by treatment with trifluoroacetic acid and the product (as a TFA salt) was used for the next step without further purification. The free amino group of the NTA-benzyl ester was reacted with succinic anhydride (96% yield), and the free carboxylic acid group of the succinyl-NTA-benzyl ester was esterified with *N*-hydroxysuccinimide. The final product was purified by silica gel chromatography and stored in the refrigerator for two weeks without detectable decomposition.

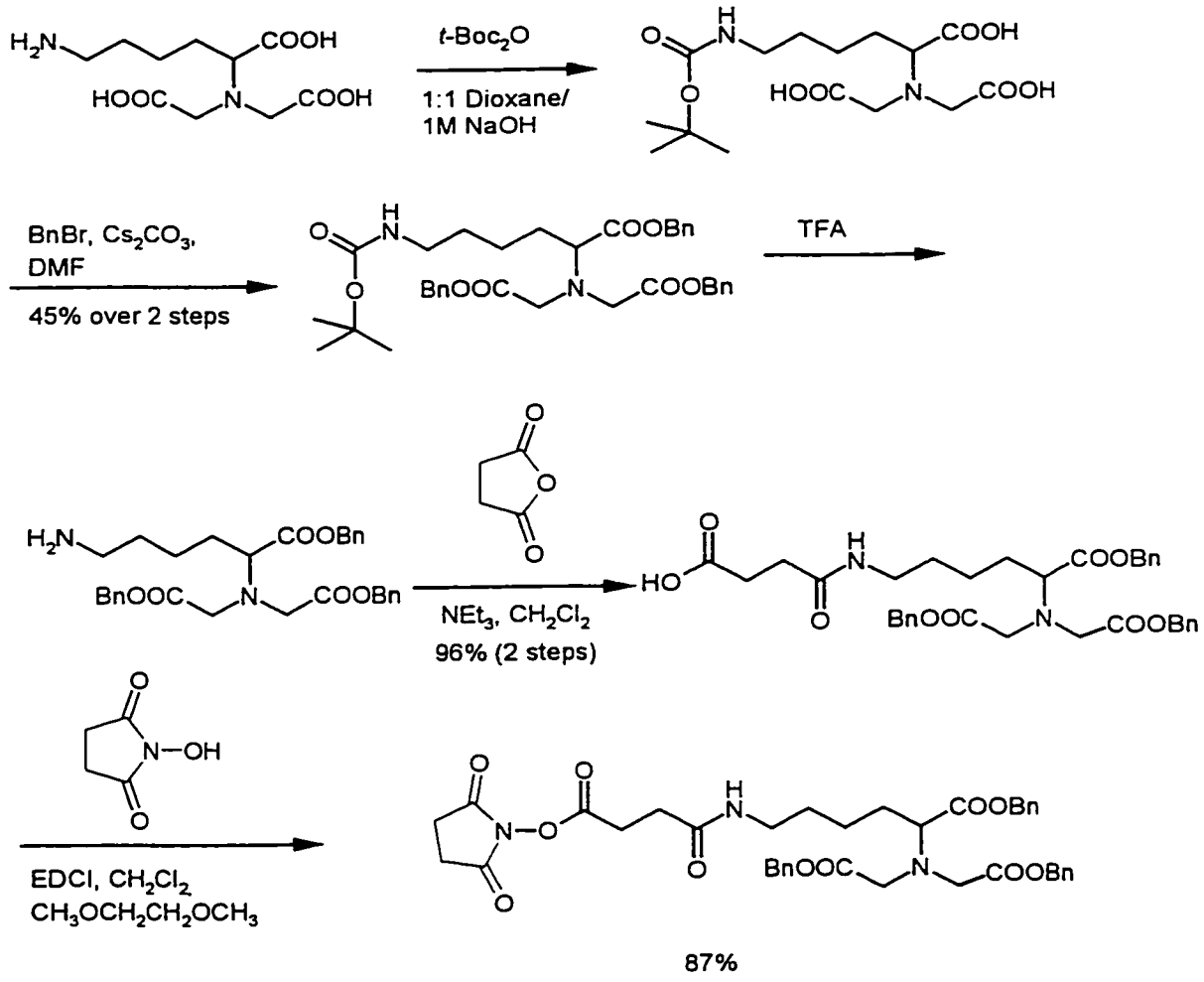

Figure 2-18: Synthesis of N^{ε}-SSU-NTA-Bn ester.

This suitably functionalized and protected NTA derivative presented advantages that offset the drawbacks of introducing several additional steps in the synthesis. Not only did the benzyl groups offer the desired protection for the carboxylic acid group of NTA and imparted excellent solubility in solvents such as dichloromethane and 1,2-

dimethoxyethane, but they also could be easily removed (with one exception, *vide infra*) in the final step of the synthesis.

The succinyl moiety attached to NTA and activated as a succinimidyl ester could be easily reacted with the amino group of the silicone starting materials, to generate a stable amide bond. This conversion was quantitative according to ^{1}H-NMR results, since no residual unreacted aminopropyl groups were detected. This route (Figure 2-19) provided a generic two step synthesis for a variety of silicone chelators, with the chelating moiety attached either to the ends or pendant from the polysiloxane backbone.

In the final step, the aminopropyl-functional silicone was reacted with a 10–15% molar excess of N^{ε}-SSU-NTA-Bn ester. The excess reactant was consumed by small amounts of AMS-162, an aminopropyl-methylsiloxane-dimethylsiloxane having 7–8% mol amino groups and M_n 4000–5000, forming a product that contained both free amino groups, as well as protected chelating groups along the backbone. These compounds were completely retained by silica gel during the column chromatography purification step.

It was noted that end-functional-protected silicone chelators were obtained in higher yields (95, 55, and 70% for DMS-A11, DMS-A15, and DMS-A21 derivatives, respectively) than the pendant ones (54, 37, and 74% for AMS-132, AMS-152, and AMS-162, respectively) and no residual aminopropyl groups were detected by ^{1}H-NMR. Since the latter products are synthesized from less well-defined starting materials, it is possible that the amounts of activated protected chelator used did not allow for the complete derivatization of all the amino groups, and that the loss of these partly derivatized compounds occurred during chromatography.

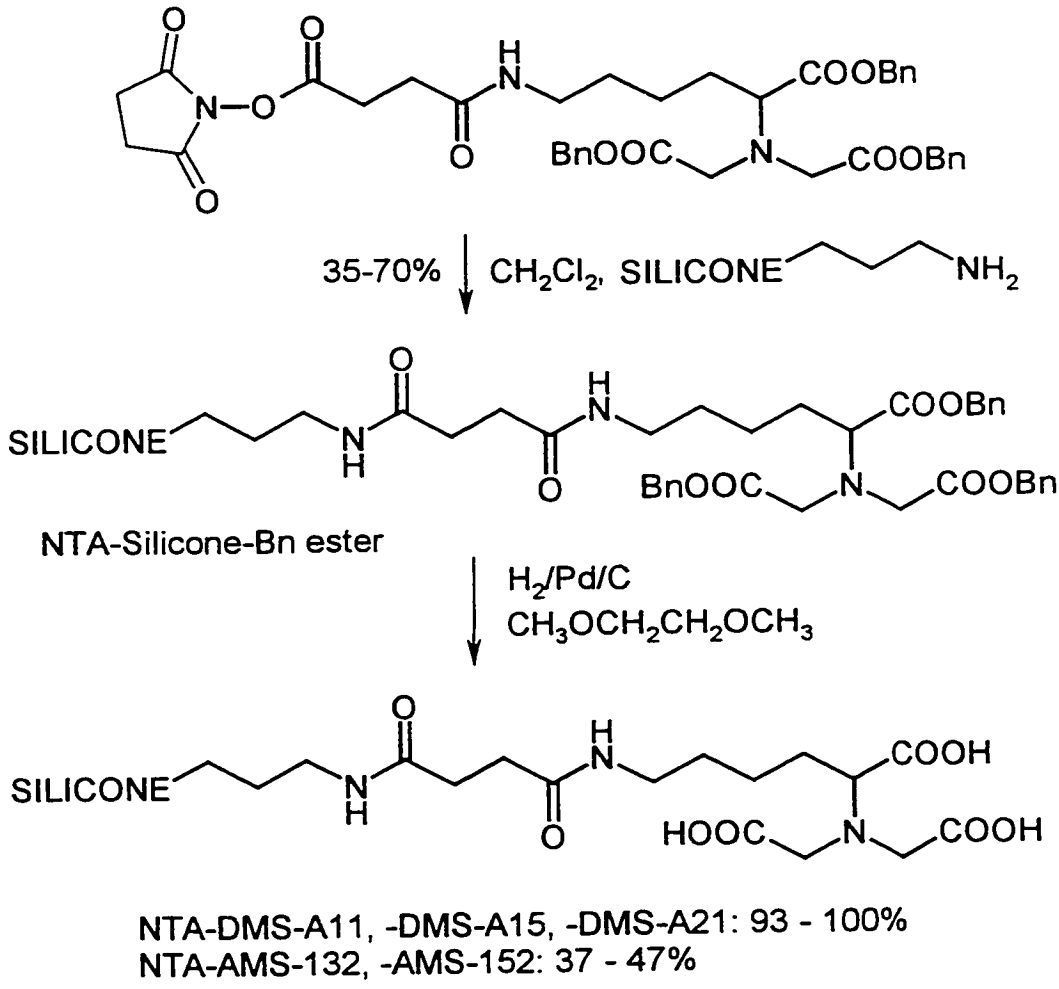

Figure 2-19: Synthesis of silicone chelators.

The second and final step of the synthesis involved the removal of the benzyl protective groups by hydrogenation in the presence of palladium on charcoal. Again the end functional silicone chelators were obtained in higher yields (93–100%) after catalyst and solvent removal, than the pendant silicone chelators: NTA-AMS-132 and NTA-AMS-152 were obtained in 47% and 33% yield, respectively. The removal of the catalyst was quite difficult for these two cases, due to the formation of very finely dispersed

colloidal suspensions, which were not retained on 0.45 μm Millipore filters.

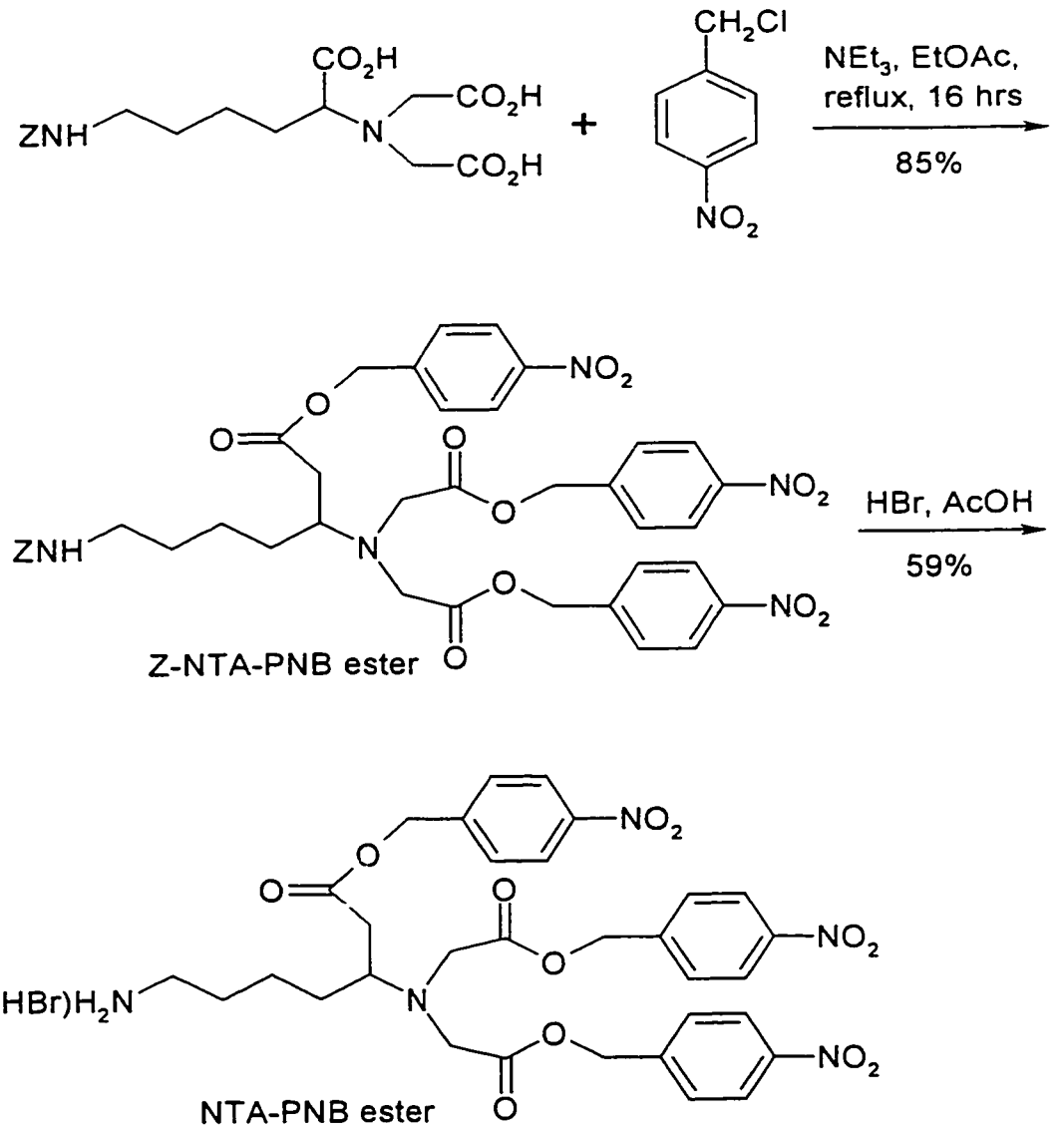

Figure 2-20: Synthesis of 4-nitrobenzyl ester of NTA.

The formation of a viscous mixture of silicone chelator and 1,2-dimethoxyethane in the remaining solution was noted during solvent evaporation. The silicone chelators

separated as thick gels on the walls of the flask and could be purified by successive dissolution in methylene chloride and precipitation with water. NTA-AMS-162 could not be obtained due to the fact that it formed a stable colloidal suspension with the catalyst, which could not be separated by passing it through a 0.45 μm Millipore filter.

In conclusion this synthetic route offered the possibility to obtain chelator silicones in a reproducible manner and was also amenable to scaling-up.

One further attempt was made to simplify the synthesis of NTA-functional silicones, by replacing the benzyl protective group with 4-nitrobenzyl moieties. Schwarz[77] and Bodanszky[78] had synthesized 4-nitrobenzyl esters of carbobenzyloxy (Z) aminoacids and peptides and showed that both protecting groups (4-nitrobenzyl and Z) could be removed simultaneously by hydrogenation at room temperature. The selective cleavage of the Z-group was achieved by employing 2.5 M HBr in glacial acetic acid. We took advantage of this selectivity and synthesized 4-nitrobenzyl protected NTA from Z-NTA, without the need to employ the Boc-protecting group (Figure 2-20).

The Z-NTA-PNB ester was purified by silica gel chromatography. 2.5 M HBr in acetic acid effected the complete and selective cleavage of the Z-group in less than 45 minutes. The 4-nitrobenzyl ester of NTA (as hydrobromide salt) was obtained after precipitating it with diethyl ether from an acetone solution in 59% yield. This compound was attached to the succinimidyl-activated succinyl-terminated silicone SSU-DMS-A11 via an amide bond formation to yield the 4-nitrobenzyl ester of NTA-DMS-A11 (Figure 2-21).

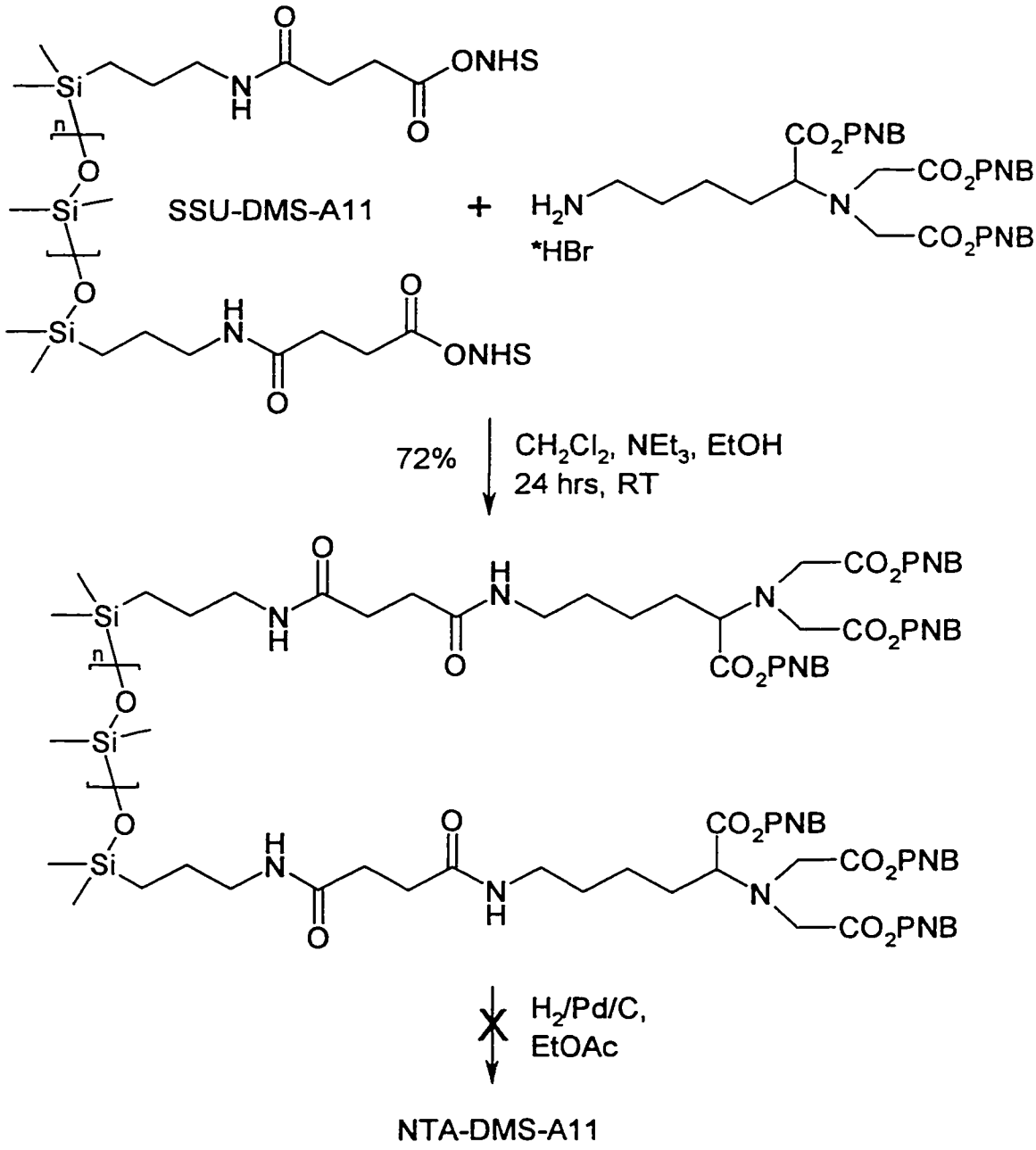

Figure 2-21: Attempted synthesis of NTA-DMS-A11 via 4-nitrobenzyl esters.

Unfortunately, the last step of the synthesis, namely the removal of the ester protecting groups by hydrogenation in the presence of palladium on charcoal, led only to

partly deprotected compounds. Repeated attempts to optimize the reaction, as well as to separate and identify the components of the crude product by employing gel filtration chromatography on Toyopearl gel (water/ethanol, 85:15) or Bio-beads (chloroform) did not succeed.

2.3.5.2 *Characterization of the Benzyl Esters of Silicone Chelators*

Chapter 2.3.5.1 (Figure 2-19) presented a successful synthetic route towards NTA-functional silicones, which comprised two steps. In the first step the NHS-activated succinyl-functional NTA was attached to the aminopropyl polysiloxane starting material via amide bond formation leading to benzyl protected NTA-silicones, which were purified by silica gel chromatography as described earlier. ^{1}H-NMR, ^{13}C-NMR, FT-IR, GPC, and electrospray-mass spectroscopy were used to characterize the products obtained.

The presence of the ester (~1745 cm^{-1}) and amide (~1642 and 1550 cm^{-1}) groups was evidenced by FT-IR. ^{1}H- and ^{13}C-NMR spectra confirmed the identity of the desired products. Approximate values for the molecular weights of the end-functional silicones could be calculated from ^{1}H-NMR data, using the integration values for the Si-CH_2 and Si-CH_3 groups (Table 2-4).

Table 2-4: Molecular weights of benzyl protected NTA functional silicones.

NTA-silicone Bn ester	Theory	Experimental Results								
		^{1}H-NMR		GPC			ES-MS			
	M_n	M_n	n[c]	M_n	M_w	PD	Series	m/z	M_w	n[c]
DMS-A11[a]	2080-2130	1995	7	-	-	-	M^+	1478-2364	1476-2362	0-11
							M^{2+}	739-1407	1476-2812	0-18
DMS-A15[b]	4230	5400	53	2137	2398	1.12	M^{2+}	1407-2291	2812-4580	18-41
							M^{3+}	1260-1851	3778-5550	31-55
DMS-A21	6230	7400	80	1922	2813	1.46	M^{2+}	776-2766	1550-5530	1-55
							M^{3+}	912-2245	2734-6732	17-71
AMS-132	5500-6500	-	-	3311	5566	1.68	M^+	1263-2962	1262-2962	-
							M^{2+}	1161-2223	2330-4444	
AMS-152	9680-10680	-	-	3487	5082	1.45	-	-	-	-
AMS-162	6270-7270	-	-	2143	4178	1.95	-	-	-	-

[a] GPC signal very distorted
[b] GPC signal distorted; low molecular weight species were not included
[c] n = degree of polymerization

The molecular weight values obtained for DMS-A15 and DMS-A21 derivatives were significantly larger (by about 1100 units) than the values calculated by using the manufacturer specifications for the starting materials. The molecular weight determined from ^{1}H-NMR data for the NTA-DMS-A11 benzyl ester was quite close to the value calculated. The discrepancy noticed for the higher molecular weight silicones can be explained by the fact that as the size of the Si-CH_3 peak increases, it becomes more difficult to obtain accurate integration values for this peak. For pendant functional silicones the molecular weights cannot be calculated from ^{1}H-NMR data.

With one exception (NTA-DMS-A11-benzyl ester), it was possible to determine the number average molecular weight (M_n), weight average molecular weight (M_w), and the polydispersity (PD) by using gel permeation chromatography. Electrospray mass spectrometry offered additional information about the molecular weights of the end functional silicones, but was difficult to interpret in the case of the pendant functional polysiloxanes.

The ES-MS analysis of NTA-DMS-A11-benzyl ester revealed the presence of two series of ionic species, singly charged and doubly charged, respectively. The singly charged ion series comprised peaks separated by 74-mass units (corresponding to the repeating unit "$OSiMe_2$") starting at 1478 (n = 0) and ending at 2364 (n = 11). In the doubly charged ion series, the peaks were separated by 37-mass units (amu = average mass unit), starting at 739 (n = 0, MW ~1476) and ending at 1407 (n = 18, MW 2818). No values could be obtained from the GPC data acquired, due to severe signal distortion.

The M_n value determined from GPC for the NTA-DMS-A15-benzyl ester was considerably lower than both the values calculated from ^{1}H-NMR and manufacturer specifications, while the polydispersity was narrower than the corresponding value for the starting material. One reason for this discrepancy is the use of different polymer standards for molecular weight calibration curves (polystyrene used by the manufacturer, PDMS used in our experiments). It is possible that not all the product could be recovered during the purification via silica gel chromatography. The lower molecular weight compounds in the series could not be obtained free from residual impurities, while the highest molecular weight species could not be eluted completely. It is also quite possible

that these polar compounds were adsorbed on the solid support and were eluted late, leading to lower apparent molecular weights. Another plausible reason could be the fact that silicone-NTA-benzyl esters have very different hydrodynamic volumes compared to the non-functional PDMS used as standards.

The ES-MS results for NTA-DMS-A15-benzyl ester demonstrated the presence of a series of doubly charged ions with m/z values between 1407 and 2291, separated by 37 amu, corresponding to polymers with molecular weights between 2812 and 4580 (n = 18 to 41). A series of highly charged ions with peaks m/z values of 1260 to 1851 (separated by 26.7 amu) was also present, confirming the presence of polymer species having degrees of polymerization between 31 and 55 with molecular weights between 3778 and 5550 (Table 2-4). The NTA-DMS-A21-benzyl ester presented the same trends and discrepancies for the M_n determined by ^{1}H-NMR, GPC, and ES-MS (Table 2-4).

The M_n values determined by GPC for the benzyl esters of pendant silicones NTA-AMS-132, NTA-AMS-152, and NTA-AMS-162 were significantly lower than the theoretical values. The differences could be due to the modification of the molecular weight distribution of the products during the purification step and to adsorption on the column. It is also possible that the conformations and hydrodynamic volumes of these polymers in solution are significantly different from those of the PDMS standards used for calibration, hence the uncertainty of the values measured.

The ES-MS results for pendant functional silicones were of very limited use, due to their complexity, which led to severe difficulties in their interpretation. The least complex ES-MS results were obtained for NTA-AMS-132-benzyl ester. Two series of

ions corresponding to singly and doubly charged species, respectively, could be identified, which showed the presence of species with molecular weights between 1262 and 4444. These values were lower than the ones obtained from GPC data.

In conclusion, the ^{1}H-, ^{13}C-NMR and FT-IR spectra provided the information needed to unambiguously identify the structural features of the desired products, while the GPC and ES-MS data confirmed the presence of high molecular weight species. Several possible reasons that could account for discrepancies between molecular weight values obtained using different experimental techniques (^{1}H-NMR, GPC, ES-MS) were also presented.

2.3.5.3 Characterization of Silicone Chelators

NTA-functional silicones were obtained from the corresponding benzyl ester derivatives by hydrogenation at normal pressure catalyzed by palladium on charcoal. The removal of the solvent and the catalyst led to the pure NTA-end functional silicone chelators in very high yields. FT-IR, ^{1}H-NMR, and ^{13}C-NMR confirmed that all the desired structural features of the target compounds were present.

It is worthwhile mentioning that deuterated chloroform seemed to swell all silicone surfactants (clear "solutions" were obtained), but the ^{1}H-NMR spectra presented extremely poor resolution. When methanol-d_4 or methanol-d_4 / chloroform-d (1:1) were used, the resolution of all the signals increased dramatically, permitting the unambiguous

assignment and identification of all peaks. This is quite likely due to the breaking of hydrogen bonds between carboxylic acid groups by methanol.

Molecular weights calculated from ^{1}H-NMR spectra were consistent with the values obtained for the benzyl ester precursors. For NTA-DMS-A11 there was agreement between the molecular weights calculated using the manufacturer's specifications for the starting material and the value obtained from the ^{1}H-NMR spectrum. In the case of NTA-DMS-A15 and NTA-DMS-A21, the calculated molecular weights were significantly lower than the ones determined from ^{1}H-NMR (Table 2-5), quite likely due to errors in integrating the Si-CH_3 peaks. The ES-MS results confirmed the presence of species with the same degree of polymerization as the benzyl ester derivatives, leading to the conclusion that no polymer degradation occurred during the final synthetic step, as expected. No GPC results could be obtained for any of the silicone chelators due in part to their limited solubility in 1,1,1-trichloroethane (elution solvent used) and to the fact that these compounds were very strongly adsorbed onto the gel support.

No information about the molecular weights of NTA-pendant silicones could be obtained from ^{1}H-NMR spectra. The ES-MS results for NTA-AMS-132 (Table 2-5) demonstrated the presence of two singly charged ion series from 683 to 2017 and from 995 to 2997, respectively. The spacing between consecutive peaks in each series was 74 amu. The first series consisted of species having one NTA-pendant methylsiloxy group along with 3 to 21 dimethylsiloxy units. The second series had oligomers containing two NTA pendant methylsiloxy groups and between 1 and 28 dimethylsiloxy units. Very similar oligomers were identified for AMS-152-NTA (Table 2-5).

Table 2-5: Molecular weights of NTA-functional silicones.

NTA-silicone	Theory	Experimental Results					
		^{1}H-NMR		ES-MS			
	M_n	M_n	n	Ion-Series	m/z	M_w	n
DMS-A11	1564	1530	8	M^- M^{2-}	935-2119 467-1209	936-2120 936-2420	0-16 0-20
DMS-A15	3690	5230	58	M^{2-} M^{3-}	1096-2392 756.5-1545	21994-4786 2268-4632	17-52 18-51
DMS-A21	5690	6860	80	M^- M^{2-}	1084-3309 1096-2953	1086-3310 2194-5908	17-67 18-51
AMS-132	5060-6060	-	-	M^- M^-	683-2017 995-2997	684-2018 996-2998	-
AMS-152	8500-9500	-	-	M^- M^-	683-2389 1143-2557	684-2390 1144-2556	-
AMS-162	5270-6270	-	-	-	-	-	-

n – degree of polymerization

The results presented above, as well as the data shown in Chapter 2.3.5.3 confirmed the identity of the desired synthetic targets and their intermediates and offered some evaluation of the molecular weights of the oligomers synthesized. In Chapter 3 the surface behavior of NTA-functional silicones at air-water interfaces will be described. The results obtained for these compounds and for succinyl-functional silicones will be compared.

2.3.6 EDTA- and NTAA-Silicone Chelators

Previous sections in this chapter focused on several synthetic routes towards NTA-functional silicones by using aminopropyl-functional polysiloxanes as starting materials. Although only moderately successful, the synthesis presented in Chapter 2.3.4

seemed to be a promising starting point for the attachment of two other complexation agents (EDTA and NTAA) to amino-silicones, via amide bond formation. Figure 2-22 outlines a generic route for the attachment of EDTA to an amino-functional silicone.

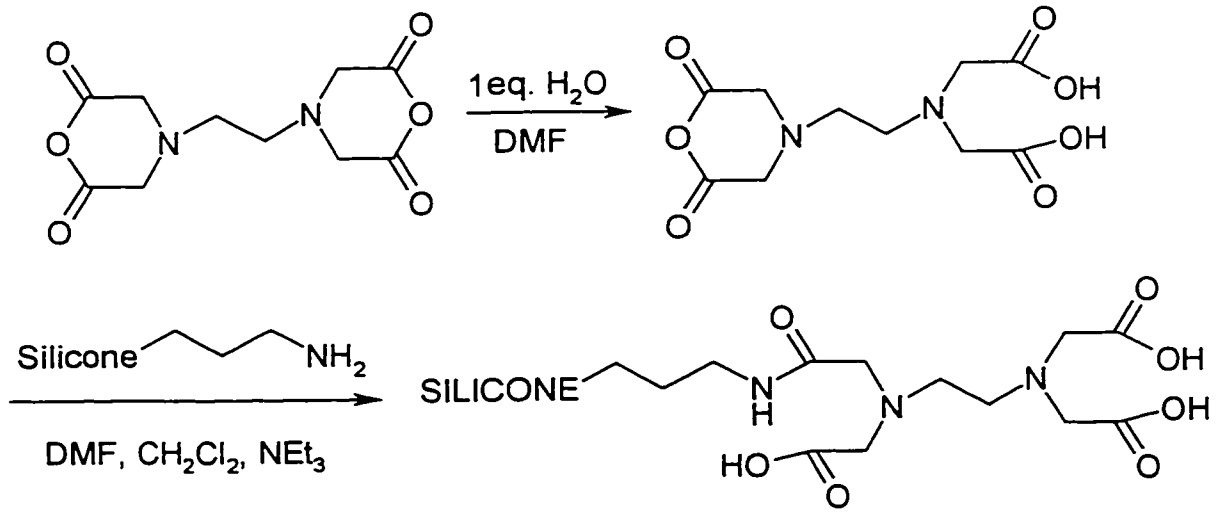

Figure 2-22: Synthesis of EDTA-functional silicones.

The first step involved partial hydrolysis of EDTA-dianhydride with one equivalent of water in DMF. The EDTA-monoanhydride obtained was attached to the amino-functional silicone via amide bond formation, in the presence of triethylamine in a mixture of dimethylformamide and methylene chloride. Several attempts to purify the product by aqueous extraction and ion exchange chromatography using strong and weak cation exchangers met with limited success. Partial equilibration of the silicone, as well as variable amounts of EDTA, which was not chemically bonded to the silicone were noted, along with the desired products.

Nitrilotriacetic acid (NTAA) can also be attached to amino-functional silicones via the synthetic route outlined in Figure 2-23.

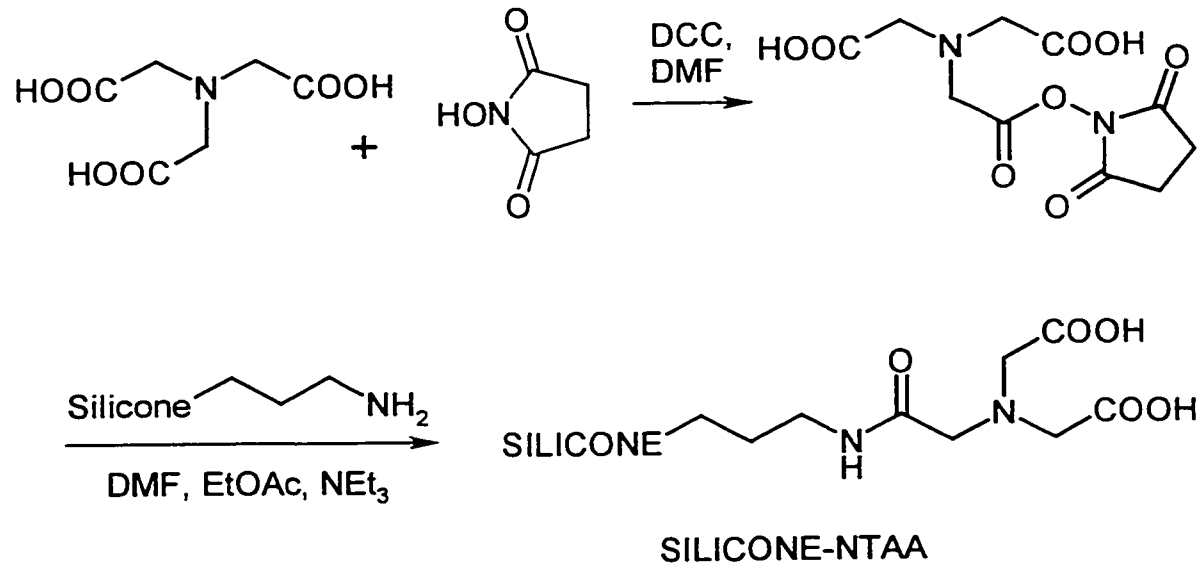

Figure 2-23: Synthesis of NTAA-functional silicones.

In the first step of the synthesis one of the carboxylic acid groups of NTAA was activated as an *N*-hydroxysuccinimide ester. Triethylamine (two equivalents) was added during the second step in order to neutralize the remaining carboxylic acid groups, followed by the addition of the aminopropyl-functional silicone dissolved in ethyl acetate. Purification methods similar to the ones used for EDTA silicones were applied, with the same limited success. Further work will have to involve the optimization of the final purification step for EDTA- and NTAA-silicones.

2.4 Summary

This chapter presented several synthetic routes towards silicone chelators. Attempts were made to attach N^{α},N^{α}-bis(carboxymethyl)-L-lysine (NTA) to epoxy-terminated silicones which led to silicone equilibration and decomposition. A second approach involved the attachment of a succinyl group to an amino functional silicone, followed by the activation of the carboxylic acid moiety with *N*-hydroxysuccinimide (NHS) and subsequent coupling to N^{α},N^{α}-bis(carboxymethyl)-L-lysine (NTA). This second approach met with limited success due to phase separation problems and final purification. These drawbacks were eliminated by a third approach. The synthesis involved the building of a NHS-activated fully protected NTA, followed by attachment to an amino functional silicone. The benzyl protective group was removed by hydrogenation in the final step, leading to five new silicone-chelators and a successful general synthetic methodology for this new class of silicone-based surfactants.

3 Silicone Chelator Insoluble Films at the Air-Water Interface

3.1 Insoluble Monolayer Films

3.1.1 Formation and Stability of Insoluble Monolayer Films

It is known that low molecular weight silicones with hydrophilic end-groups (-OH, -NH_2, COOH, epoxy) have the ability to form insoluble monolayers on aqueous subphases (see Chapter 1.1.2 and references cited therein). Therefore it is anticipated that the silicone – chelators NTA-DMS-A11, -A15, -A21, and NTA-AMS-132, -152 as well as the succinyl-functional silicones SUCC-DMS-A11, -A15, -A21, and SUCC-AMS-132, -152 also have the potential to form insoluble monolayer films on aqueous surfaces. The properties of these films were investigated by measuring the surface pressure-area (π-A) isotherms with the help of a Langmuir trough. The films are formed by spreading a very small amount of silicone chelator from a chloroform/methanol solution (9:1) onto the subphase liquid (i.e. deionized water, $NaHCO_3$ sol. pH 8, 10^{-4} M $NiCl_2$, and 10^{-4} M $CaCl_2/NaHCO_3$ sol. pH 8). As the solvent evaporates the monolayer is formed. This monolayer is generally not in a state of absolutely stable equilibrium, but if certain conditions are met, the film state can be approximated to the minimum free energy of the system (i.e. when film components are very insoluble and nonvolatile, a lower free energy state is achieved when these components are present at the interface rather than as

an additional bulk phase[17]). This situation is commonly encountered for films of polymeric materials. Meaningful experiments can be performed on such monolayers even if the monolayer is not in a state of absolute equilibrium. A mobile barrier compresses the monolayer formed and the surface pressure measured with a Wilhelmy plate is plotted against the area per mg film. The surface pressure π (equation 3.1.) is equal to the difference between the surface tension of the pure liquid surface and the one covered with a film:

$$\pi = \gamma_0 - \gamma, \tag{3.1}$$

where γ_0 is the surface tension of the pure liquid and γ is the tension of the film-covered surface.

Three pressures can characterize the stability of a monolayer with respect to its own bulk phase: the collapse pressure, the equilibrium spreading pressure, and the monolayer stability limit[17].

The collapse pressure (P_c) is the highest pressure to which a monolayer can be compressed without detectable expulsion of molecules to form a new layer. Very often the maximum pressure indicated by the sensing device at a given uniform compression rate has been used as a collapse criterion.

The equilibrium spreading pressure (ESP) is the pressure where the monolayer is in equilibrium with the stable bulk phase (liquid or solid) under the experimental conditions.

The monolayer stability limit is defined as the maximum pressure attainable in the film prior to collapse, or as the pressure at equilibrium between the film and the freshly collapsed material.

Many monolayers can be compressed to pressures higher than their ESP, but at some point it becomes impossible to increase the surface pressure further and it is found that the area of the film starts to decrease if the pressure is maintained constant. This point is referred to as the collapse point, and it corresponds to the formation of agglomerates of a new bulk phase[17] by molecules that are forced out of the monolayer.

The over-compression of large polymeric monolayers can lead to the displacement of some molecules or molecule segments from the surface. Two factors contribute to this situation: The molecular weight distribution of the polymer and the selective adsorption of certain segments of the polymer chains onto the surface.

Volatility and partial solubility of the film can also affect the stability of monolayers in the subphase. For the silicone chelators and succinyl-silicones used in this work volatility will not play a role, but partial solubility of the lowest molecular weight compounds in the water subphase could occur.

3.1.2 Monolayer States and Phase Transformations

Molecules in two-dimensional monolayers can exist in states analogous to three-dimensional liquids, solids and gases. The monolayer states are a reflection of the intermolecular forces between molecules in the film and between molecules in the film

and the subphase, which lead to various degrees of molecular freedom or order. The following three states are typical for non-polymeric materials: condensed (solid or liquid) films, expanded films (sometimes called "liquid"), and gaseous films[17]. In the gaseous state the molecules in the monolayer are widely separated due to thermal motion and they exert very little force on one another. The surface pressure in such films is typically less than 0.1 dynes/cm at room temperature. Such monolayers are difficult to investigate experimentally.

The molecules in condensed monolayers are arranged in a lightly packed structure similar to a two-dimensional crystal. Fatty acids, long chain alcohols, and glycerides form such insoluble films, with polar heads directed into the water subphase and closely packed chains almost perpendicular to the subphase surface. The cross-sectional area of stearic acid (a long chain fatty acid) is 20 $Å^2$/molecule in the film[79]. The pressure-area isotherms for such materials are very steep and nearly straight, reflecting the low compressibility of the monolayer, due to the strong chain-chain interactions that maintain the molecules in their closest packed arrangement[17]. Many condensed monolayers are extremely viscous and relatively incompressible.

The expanded monolayers (also called liquid-expanded or liquid) have molecular areas intermediate between gaseous and condensed films. The surface pressure-area isotherms of these films approach the $\pi = 0$ axis at a fairly steep angle and present a considerable curvature. The films formed are coherent down to low surface pressures with molecular areas two to three times larger than the molecular cross-section[17]. Long chain compounds with *cis*-double bonds or side chains, and some compounds such as

chlorophyll *a*, are known to form expanded monolayers. Some fatty acids on acid aqueous subphases form condensed monolayers at low temperature and expanded monolayers at temperatures above 25°C. The structure of expanded monolayers is thought to be similar to a very thin liquid phase, with the polar groups of the molecules in contact with the subphase and the hydrophobic chains in a random orientation[80].

Unlike the isotherms of many polymeric materials, the π-A diagrams for simple molecules can feature more than one state. Figure 3-1 presents a generalized π-A isotherm that includes the properties of many types of films stable over various pressures and molecular areas[17].

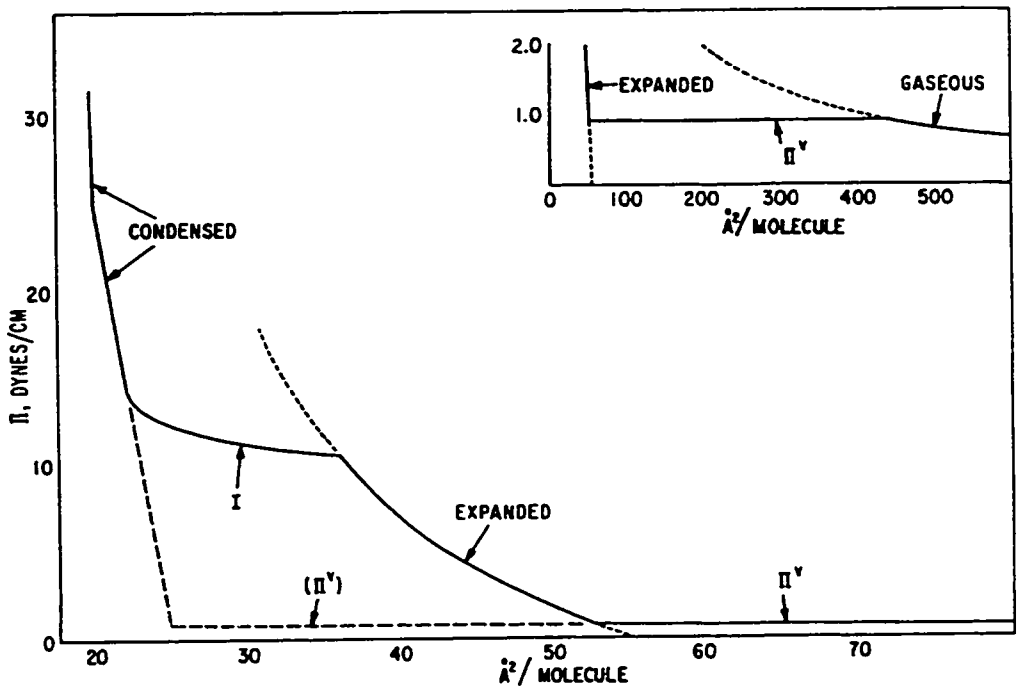

Figure 3-1: Generalized π-A diagram for a long-chain compound featuring various monolayer states and transitions that could occur upon compression at 25°C (Reprinted from reference 17, with permission).

The regions marked as "condensed" and the dashed extensions to low surface pressure in the low molecular area are typical for condensed films (e.g. of stearic acid) at room temperature. The curve marked "expanded" and its dotted extensions resemble closely the plots obtained for oleyl alcohol. The inset curve is typical for a gaseous film and can be obtained by plotting the ideal two-dimensional gas equation 3.2:

$$\pi A = kT, \tag{3.2}$$

where k is the Boltzmann constant and T is the temperature (in K), π is the surface pressure in dynes/cm and A is the molecular area in $Å^2$/molecule.

Numerous researchers have interpreted marked changes in the slope of π-A curves as reflecting a change in the structure or behavior of the film, and have reported the area and pressure values at various inflections or discontinuity points based on the assumption that these points are associated with monolayer phase transformations. Figure 3-2 presents the π-A isotherm of a stearic acid monolayer that was rapidly compressed at 25°C.

The following characteristic molecular areas are indicated: A_0 is the extrapolated "zero pressure" area, A_C is the area at collapse, A_T is the area corresponding to the phase transition from liquid-condensed (more compressible) to solid (incompressible). A_0 is easy to obtain experimentally, while A_T and A_C are subject to the uncertainties of establishing the transition and collapse points. A_C is especially difficult to estimate for condensed films since these films are almost incompressible close to the collapse point and small variations in molecular area are accompanied by fairly large changes in

observed collapse pressure. In all cases the interpretation of the characteristic area values should be done with caution.[17]

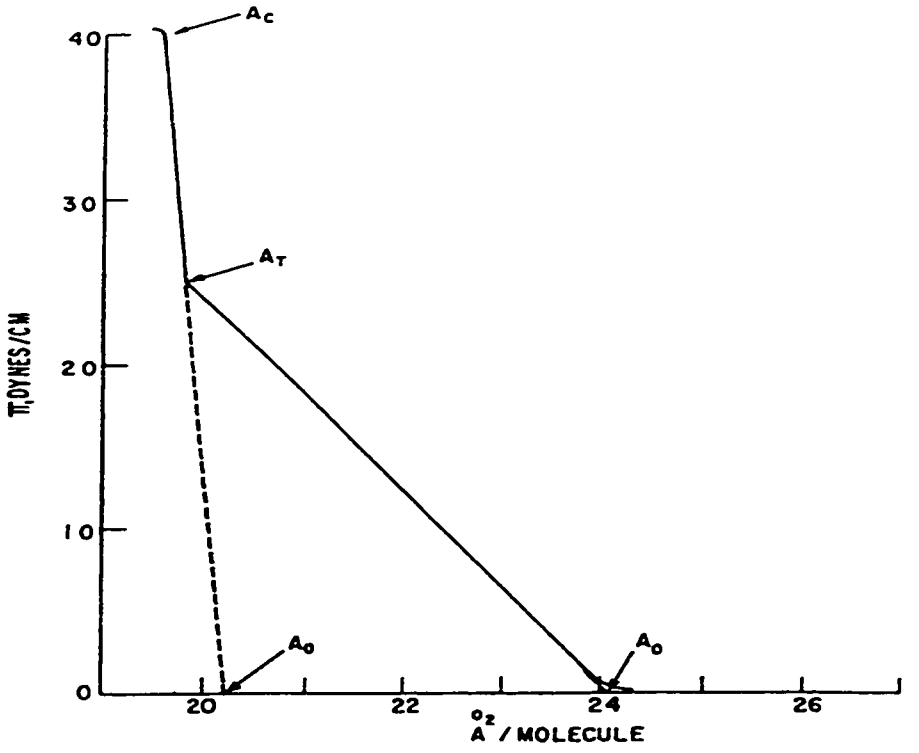

Figure 3-2: Various characteristic molecular areas for a rapidly compressed stearic acid monolayer at 25°C (Reprinted from reference 17, with permission).

3.1.3 Monolayers of Polymers

In Chapter 1.1.2 a true polymer monolayer was defined as having each segment of each molecule constrained to remain in the interface for the duration of the experiment.

This polymer configuration may not be in absolute thermodynamic equilibrium. The criterion used to decide that a polymer forms a monolayer is to demonstrate that the surface film formed by a given polymer sample occupies the maximum and reproducible area (which must be large enough to accommodate the polymer in a reasonable configuration) independent of solvent, solution concentration or details of the technique applied[17]. The main factors that govern the formation of polymer monolayers are solubility and the cohesive forces in the bulk phase. A polymer film may contain molecules arranged in coils, helices or other well-defined molecular arrangements. Collapse can occur when some molecular segments are forced out of the surface. Generally, it is difficult to define unambiguously the state of a given monolayer.

The surface pressure-area diagrams for well-spread polymers and protein films on aqueous subphases have fewer features when compared with curves obtained for small molecule monolayers. Usually the isotherms do not present evidence of phase transformations in the stable monolayer region, or marked discontinuities. In some cases (i.e. protein films) the hysteresis obtained during a compression-decompression cycle has been attributed (without full confirmation) to the expulsion of small chain segments from the surface. The study of surface pressure-area isotherms for several synthetic polymers (polydimethylsiloxanes, polyvinylethers, polyacrylates, and poly(vinyl acetates), and proteins revealed that at large specific areas the surface pressures are low, but upon compression a rapid increase in surface pressure is noted at areas of 0.7 – 5 m^2/mg (or 10- 40 $Å^2$ per monomer unit), to the point where the polymer molecules occupy most of the surface available. For synthetic polymers the areas occupied per monomer unit at

surface pressures larger than 1 dyne/cm are found to be independent of molecular weight. This is generally not true for polymers with low molecular weight and end groups that have high affinity for the subphase. According to Crisp[81], polymer monolayers can be of condensed or expanded type. Condensed polymer films have very steep π-A isotherms, high rigidity or viscosity, and have the macromolecules in contact with each other. The interpretation of π-A isotherms and the measurement of molecular areas for these films must be done with caution, due to the possible kinetic effects caused by high viscosity in the monolayer.

Expanded polymer monolayers exhibit less steep π-A isotherms, complete and well-defined collapse, and are fluid. Qualitative interpretations of the π-A diagrams for polymer monolayers rely on the hypothesis of polymer chain and side group rearrangement upon film compression and are supported by surface potential and viscosity measurements for several cases. The quantitative theoretical treatment of such monolayers has been impeded by some of the limitations of the theories available for the behavior of macromolecules in bulk phases.

3.1.4 Ionized Monolayers

Several studies have targeted the behavior of ionized polymer monolayers. The properties of ionized monolayers in general are influenced by the balance between the direct electrostatic repulsion or attraction, intermolecular forces between molecules in the film, and forces between the subphase and the film forming molecules. Small counterions

must be present in order to maintain the neutrality of the system. A major problem is caused by the increased solubility of the molecules that form the film. The solubility is due to increased polarity and to the reduction in free energy that is attained by removing charged species from the surface, where the electrical potential is high[17]. For weak electrolytes the solubility is pH and counterion dependent. In studies of ionized straight chain fatty acids it was noted that ionization and presence of counterions such as Ca^{2+}, Cu^{2+}, Al^{3+}, Fe^{3+}, and Ln^{2+} greatly influence the π-A isotherms[82,83,84,85,86,87]. The pH and ionic strength of the subphase were also found to influence the surface potentials of the ionized films. The counterion effects on ionized monolayers depend on a multitude of factors such as: ionization of films, structure of the ionic double layer, possibility of complexation, hydrolysis or incomplete dissociation of counterions in solution, possibility of true specific chemical bonding, and ion effects on water microstructure. Studies on fatty acids (e.g. stearic acid) monolayers revealed that at low pH (pH < 6) very little (if any) ionization occurs, and the presence of positive counterions does not affect the π-A isotherms. When the acids are completely ionized (at high pH) the monolayers expand, presumably due to repulsive electrostatic forces between the ionized carboxyl groups. The behavior of fatty acids at intermediate pH values is not clear. Small contractions in the areas occupied by molecules in the film are attributed to favorable interactions between ionized and non-ionized molecules (i.e. dipole-ion interactions) that increase the cohesion of the film[82,84]. In the case of stearic acid the adhesion between polar groups is found to be maximized when about 50% of the groups are ionized[84]. Some authors noted[82,85] that the pH at the interface is generally 0.5 to 2 units lower than

in the bulk for fatty acid films. As mentioned above, numerous studies found that the presence of metal cations in the subphase has a dramatic effect on the π-A isotherms of films containing carboxylic acid functional molecules. The condensation of fatty acid monolayer films initiated by bulky cations (Ca^{2+}, Ba^{2+}) was explained by some researchers[87] as being due to the penetration of the cation into the monolayer. Matsubara and coworkers[82] noted that at higher pH values calcium stearate condenses more than stearic acid in monolayers, suggesting that the cohesive forces between Ca-stearate are stronger than between stearic acid molecules (the energy of mixing of stearic acid and calcium stearate $\neq 0$ at higher pH values). Spink and Sanders[83] measured force-area isotherms for monolayers of stearic acid, methyl stearate, and stearyl alcohol on dilute aqueous solutions containing Ca^{2+}, Cu^{2+}, Zn^{2+}, Fe^{3+}, and Al^{3+} ions. They found that only the acid showed a remarkable sensitivity of the π-A isotherms to the pH and the presence of metallic ions in the subphase.

It was noted that in the absence of cations, molecular areas σ_0 did not vary with the pH for stearic acid. When calcium chloride was present in the subphase σ_0 decreased as the pH increased between 4 and 8, and this phenomenon was associated with the formation of calcium distearate in the monolayer.

The presence of Cu^{2+} in the subphase is believed to cause the formation of a liquid-condensed fluid (pH < 5) and a solid-condensed film at pH 5.2 – 5.5, presumably due to the formation of copper distearate. As the pH is increased above 5.5 the films become solid-expanded (brittle) and this fact is associated with the formation of the copper monostearate (see equation 3.3).

$$\text{Cu-distearate} \xrightarrow{\text{pH} > 5.5} \text{Cu(OH)stearate} \qquad (3.3)$$

The presence of Zn^{2+} causes the same effects in the stearic acid monolayer as the ones observed for Cu^{2+}, but the change from liquid-condensed to solid-condensed film occurs between pH 5.8 and 6.2, while the formation of solid-expanded films is observed at pH > 7. Fe^{3+} and Al^{3+} were also found to have a profound influence on the behavior of stearic acid, but the results were difficult to interpret.[83]

Jeffers and Daen[88] gave an account of the formation of monolayers of α,ω-dicarboxylic acids with 12, 14, 16, 20, and 24 methylene groups on acidified distilled water (pH 2) and concentrated ammonium sulfate solutions. They found that solubility was a problem for low molecular weight dicarboxylic acids and that stable layers were formed at temperatures above certain values, characteristic for each compound. The presence of salts stabilized the monolayers leading to an increase in the collapse pressure to 16 dynes/cm on ammonium sulfate subphase, compared to 8 dynes/cm on acidified distilled water. No first order transitions were noted in the π-A isotherms. The large areas and the surface potential values at the collapse point indicated that the molecules adopted a horizontal configuration with both carboxylic acids anchored to the subphase and very little vertical bowing of the hydrocarbon chain before collapse. The isotherms were very reproducible at a given compression rate, but were strongly dependent on the latter. This fact suggested that the monolayers were metastable, and not in equilibrium.

The studies of ionized polymer monolayers (e.g. protein films) evidenced the fact that the pH and the salt content of the subphase influence the behavior of these films. It

was noted that these monolayers expanded when ionized and that a plateau observed was followed by a pressure rise upon compression, but no kinetic studies were attempted. Complicated kinetics and slow approach to equilibrium are major difficulties when ionized and non-ionized polymer layers are studied and the results are interpreted.

In the light of the facts presented in this chapter and in Chapter 1.1.2 it is expected that the presence of metal cations such as Ca^{2+} and Ni^{2+} in the subphase, as well as pH changes will have a marked effect on the behavior of succinyl- and NTA-functional silicones at air-water interfaces.

Chapter 3.2 will present an account of the surface pressure-area measurements performed for these compounds on several aqueous subphases.

3.2 Monolayers of Silicone Chelators and Succinyl-Functional Silicones

3.2.1 Isotherm Shapes and Assignments of Transitions

The pressure-area isotherms obtained for succinyl- and NTA-functional silicones were assigned type numbers according to their similarity with the four basic types of isotherms observed for end-functional silicones by Korberstein and coworkers (see Chapter 1.1.2 for details). Two numbers were attributed to isotherms that had intermediate shapes, with the first number representing the shape closest in resemblance (i.e. a 23 type isotherm has a shape intermediate between a type 2 and a type 3 isotherm, with more similarities to type 2).

All measurements were obtained as pressure (dynes/cm) – area (m^2/mg) curves. The areas were calculated as $Å^2$/molecule by using experimental molecular weight values obtained from ^{1}H-NMR spectra for the end-functional silicones, and values calculated from manufacturer specifications for pendant-functional silicones respectively. Since these values are approximative, and the determination of molecular areas at collapse is also a subject to uncertainty, the values determined for molecular areas at collapse F are approximate and should be regarded with caution.

The isotherms of the lowest molecular weight compounds NTA-DMS-A11 and SUCC-DMS-A11 (Figures 3-3 and 3-4) are rather featureless, exhibiting similarities with curves obtained for small molecules such as fatty acids. Both isotherms, of type 34 for SUCC-DMS-A11 and 43 for NTA-DMS-A11, feature transitions A and B with the latter less pronounced for NTA-DMS-A11. Regions A-B and B-F present steep slopes (A-B less steep than B-F) that suggest "condensed" monolayer states[17].

The isotherms of larger molecular weight functional silicones exhibit more features and similarities to the behavior of non-functional PDMS behavior. As the molecular weight increases, a transition from type 4 to 2 isotherms is noted for both succinyl- and NTA-silicones. The isotherms of SUCC-AMS-152 and NTA-AMS-152, even though belonging to the highest molecular weight samples, resemble type 3 curves (common for lower MW), probably due to the fact that the molecules have a higher degree of functionalization, which leads to a stronger, multiple point anchoring of the molecule to the subphase.

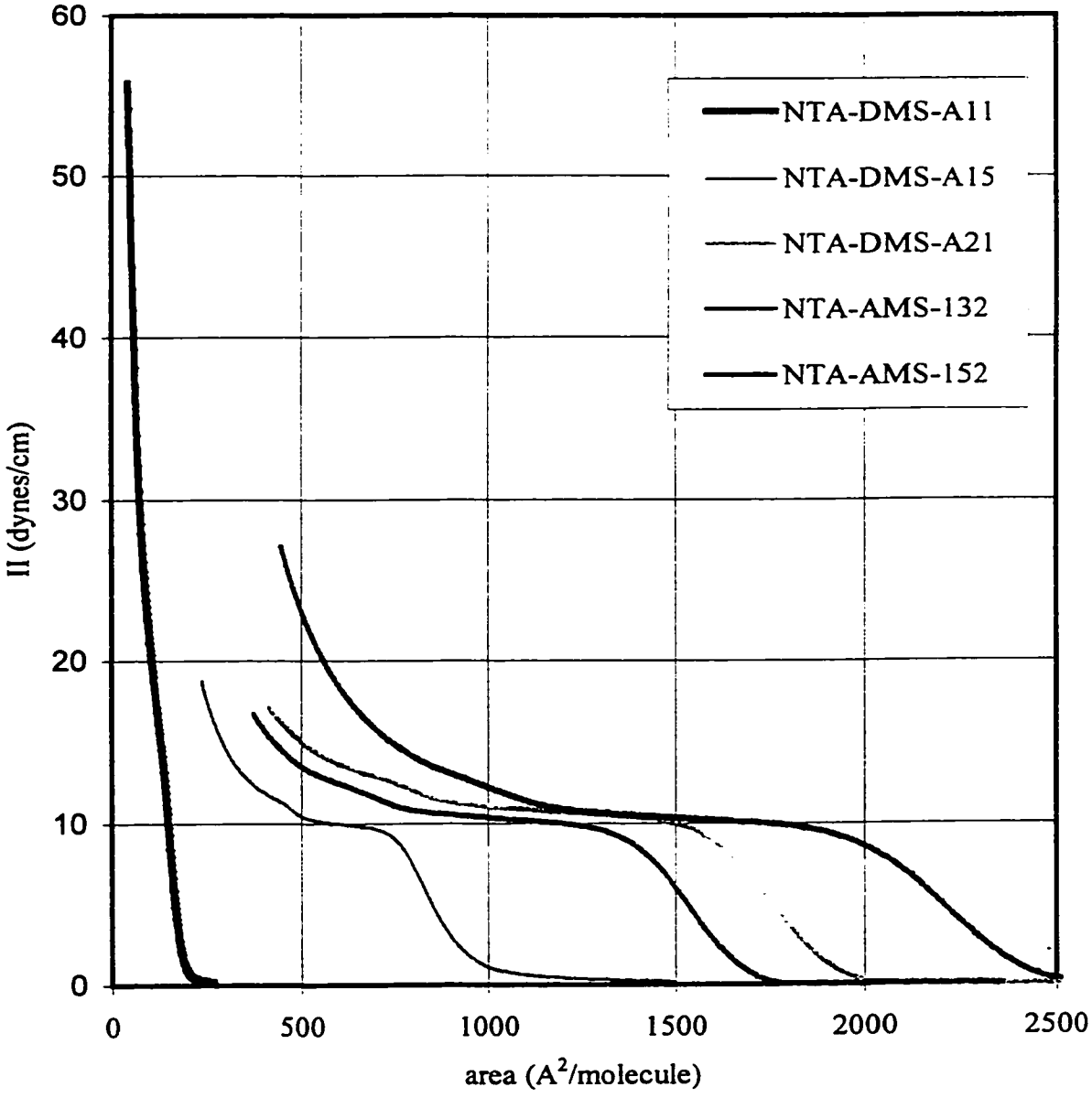

Figure 3-3: Surface pressure measurements on water subphase for NTA-DMS-A11, NTA-DMS-A15, NTA-DMS-A21, NTA-AMS-132, and NTA-AMS-152.

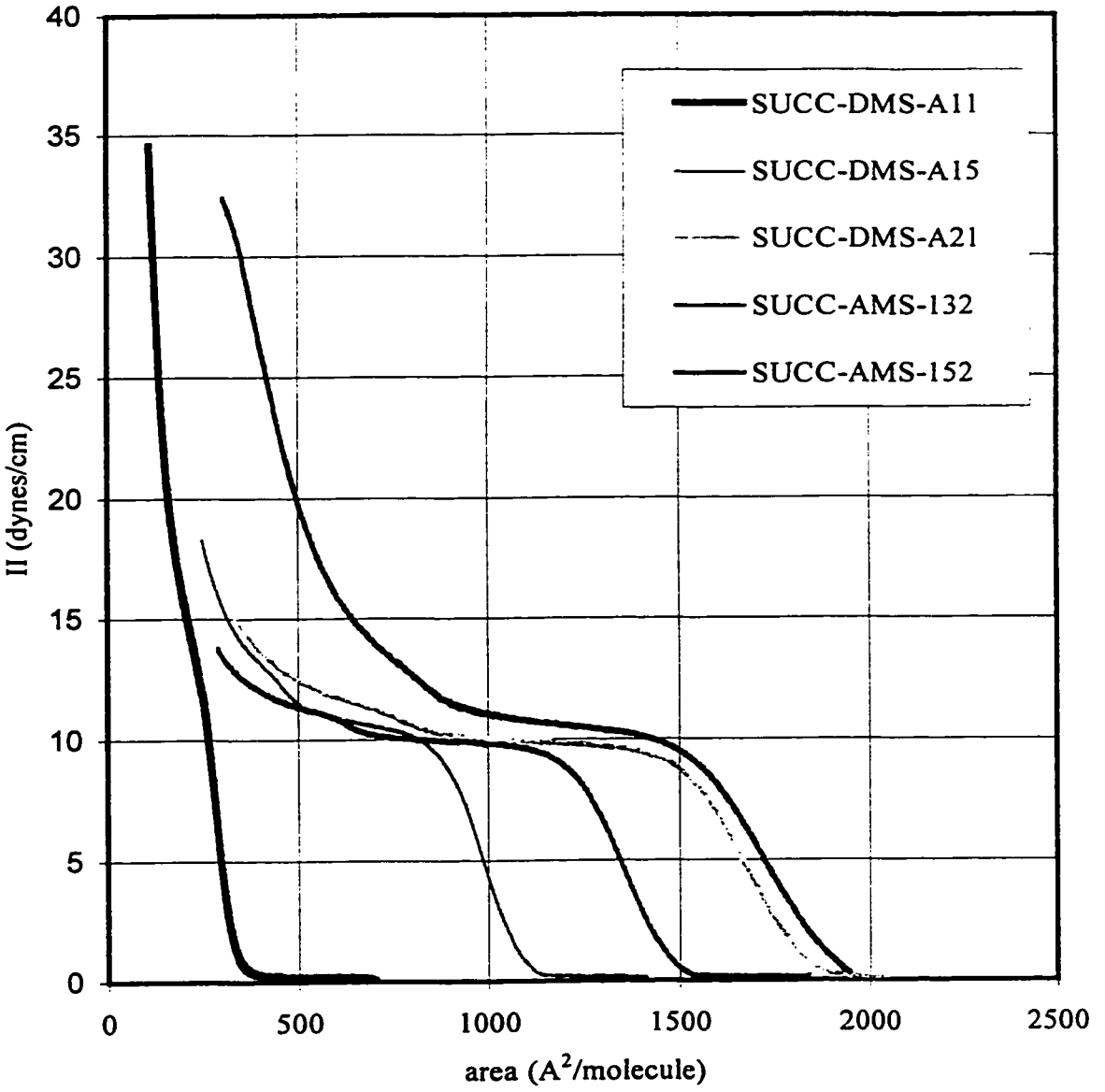

Figure 3-4: Surface pressure measurements on water subphase for SUCC-DMS-A11, SUCC-DMS-A15, SUCC-DMS-A21, SUCC-AMS-132, and SUCC-AMS-152.

Compounds NTA-DMS-A15, -DMS-A21, -AMS-132, -AMS-152, and the corresponding succinyl derivatives exhibit transitions A – D, associated with interactions between individual monomers and water subphase, as well as transitions E and F (collapse), which are attributed to changes in orientation involving the entire molecule, as a consequence of the hydrophilic group anchoring the molecule to the subphase[24]. The slopes for the regions A – B of the succinyl-functional silicones appear to be steeper than the ones of the corresponding NTA-functional compounds. This fact suggests that succinyl-silicones pack in a tighter arrangement than the NTA-silicones during this step.

The fact that the positions of transitions A – D (Figure 1-5) are relatively independent of the molecular weight is supported by the values determined for ratio B/A, C/A, and D/A (see Table 3-1). For example, B/A values are quite similar for all the compounds investigated, on a given subphase. The differences observed can be accounted for by the influence exerted by functional groups (i.e. end-group effects). The positions of transitions E and F (Figure 1-5) are dependent on the areas per molecule occupied by each type of compound.

Low molecular weight compounds SUCC-DMS-A11 and NTA-DMS-A11 exhibited significant hysteresis on all subphases with the largest differences between the compression and the expansion isotherms on $NiCl_2$ and $NaHCO_3$-$CaCl_2$ subphases. Hysteresis was much less pronounced for higher molecular weight compounds and was noticeable especially between transitions A and B. Several factors could account for these observations: too rapid compression and expansion rate, partial dissolution of oligomers in the subphase during the period of the experiment, and/or relaxation of layer during

expansion via a different mechanism than folding and packing during compression. Some dissolution of polymer in the subphase could be partially accountable for the magnitude of the hysteresis observed for the low-molecular weight isomers. Korberstein and coworkers[24] reported that the only point of significant hysteresis was recorded between transitions C and D for end-functional polysiloxane oligomer layers compressed and expanded at a barrier speed of 4 mm/min. Since the present experiments were performed using a barrier speed of 10 mm/min, it is possible that the polymer layer is not in a state of equilibrium during the compression and expansion. This point could be clarified by performing additional experiments at very slow barrier speeds.

Table 3-1: Pressure-Area Isotherms for Succinyl- and NTA-Functional Silicones on a Water Subphase.

Silicone	M_n	n [b]	n/m [c]	Isoth. Type	Area Ratios			P_B mN/m	P_F mN/m	F Å^2/molecule
					B/A	C/A	D/A			
SUCC-DMS-A11	1100	8	4	34	0.64	N/A	N/A	11.8	34.6	110
SUCC-DMS-A15	3400	40-41	20	23	0.68	0.46	0.38	10.3	18.3	247
SUCC-DMS-A21	5500	68-69	34	2	0.72	0.47	0.37	9.5	15.7	320
SUCC-AMS-132	5160 [a]	63-64 [a]	39	2	0.71	0.44	0.39	9.7	13.8	289
SUCC-AMS-152	7935 [a]	92-93 [a]	21	32	0.71	0.48	0.40	10.2	32.4	305
NTA-DMS-A11	1530	8-9	4	43	0.69	N/A	N/A	12.2	55.8	42
NTA-DMS-A15	5230	58	29	23	0.73	0.51	0.45	9.6	18.6	237
NTA-DMS-A21	6860	80	40	23	0.76	0.46	0.38	10.0	17.2	411
NTA-AMS-132	5560 [a]	63-64 [a]	39	2	0.73	0.47	0.36	9.8	16.8	370
NTA-AMS-152	9000 [a]	92-93 [a]	21	32	0.74	0.46	0.39	9.9	27.1	444

a) calculated from manufacturer specifications
b) n = number of dimethylsiloxy units in the backbone
c) m = number of functional groups per molecule

3.2.2 Molecular Weight and Functional Group Effects

In Chapter 3.2.1 it was mentioned that as the molecular weight of the succinyl- and NTA-end-functional polysiloxanes increases, the isotherm shapes change from type 4 to type 2 (see Figures 3-3 and 3-4 for NTA- and succinyl-functional silicones respectively). These observations are similar to the ones of Korberstein[24] and were attributed to the decreased overlap between molecular (regions E-F) and monomer (regions A-D) transitions. The onset of transition E, which is associated with the upright orientation of molecules in the monolayer, takes place closer to transition B for the low molecular weight oligomers. This is probably due to the fact that shorter molecules cannot form extended helices (A – B) that can be further compressed (B – C), and adopt an upright position while in an extended *cis-trans* conformation. Pressure at transition B for the lowest molecular weight compounds (SUCC-DMS-A11 and NTA-DMS-A11) is slightly, but significantly higher than for higher molecular weight compounds with the same functional groups. This resistance to transition B can be interpreted as being a consequence of the strong interaction between the end groups and the aqueous subphase.

Pendant-functional group compounds SUCC-AMS-132 and NTA-AMS-132 have molecular weights intermediate between the corresponding DMS-A15 and DMS-A21 derivatives and degrees of functionalization close to DMS-A21. Their isotherms are quite similar to the ones measured for the above-mentioned end-functional compounds. SUCC-AMS-152 and NTA-AMS-152 have the highest molecular weights and their backbones are more heavily functionalized. As a consequence their isotherms present both the A – D

transitions typical for non-functional silicones, as well as high pressures at collapse characteristic for strongly anchored low molecular weight end-functional silicone oligomers. These observations demonstrate that the density of functional group per chain, together with the molecular weight of the oligomer have an important effect on the surface behavior of the compounds studied.

Molecular weight exerts an important influence on pressure and area at collapse. It is noted that the pressure at collapse decreases as the molecular weight increases for both succinyl- and NTA-end-functional polysiloxane oligomers (see Table 3-1 and Figures 3-3 and 3-4). For example, for the succinyl-end functional series the pressure at collapse decreases from 34.6 mN/m (SUCC-DMS-A11) to 15.7 mN/m (SUCC-DMS-A21). This difference is even more dramatic for NTA-end-functional compounds. Collapse pressures for NTA-DMS-A11 and NTA-DMS-A21 is 55.8 and 17.2 mN/m, respectively. The position of the collapse point is determined by the balance that exists between the entropy loss from chain orientation and close packing and the enthalpy of the head group interaction with the aqueous subphase[24]. When the backbone becomes sufficiently large, the effect of the end groups is offset by the interactions of the backbone units with the subphase and with each other. Thermal motion in larger oligomers becomes disruptive and the chains cannot become fully ordered and extended. The collapse occurs before the chains become fully extended and the chain length does not effect the collapse pressure. This situation is observed for the end-functional compounds SUCC-DMS-A15, -DMS-A21, NTA-DMS-A15, and NTA-DMS-A21. The collapse pressure values are influenced not only by molecular weight (chain length), but also by

the type and positioning of the functional groups. The presence of tricarboxylic acid-water soluble groups ensures better anchoring of the polymer to the aqueous subphase, compared to the monocarboxylic acid groups. As a consequence, the resistance to collapse increases with on exception (SUCC-AMS-132).

The presence of a multiple tethering functional group pendant from the backbone of SUCC-AMS-152 and NTA-AMS-152 also leads to better anchoring of the film to the subphase and results in a significant increase of collapse pressure, in spite of the fact that these polymers have the highest molecular weights.

Areas at collapse are affected by the same factors that influence the collapse pressures, namely: molecular weight, type and position (pendant from the backbone or at its end) of functional groups, compression rates, and composition of the aqueous phase. The last factor will be discussed in Chapter 3.2.3. Previous papers (for a more detailed account, see reference 24 and literature cited therein) suggested that end-functional polydimethylsiloxane molecules packed in a compressed monolayer can adopt three types of conformations: extended *cis-trans* conformation (calculated cross-sectional area of 52 $Å^2$), Damaschun helix (6 backbone atoms per unit cell; 96 $Å^2$ calculated cress-sectional area), and extended helix (obtained from Damaschun helix by rotating 37° away from the trans-conformation along each backbone bond; 72 $Å^2$ calculated cross-sectional area).

Higher-molecular weight NTA- and SUCC- functional silicones could also adopt helical conformations upon compression, while the lowest members of the series under the same conditions would be more likely to pack in an extended *cis-trans* conformation. It is noted that areas at collapse increase with increasing molecular weight for NTA-

functional silicones. A similar trend is noted for succinyl-functional polysiloxanes, with the exception of SUCC-AMS-152, which exhibits a lower area per molecule at collapse (Table 3-1).

NTA-DMS-A11 exhibits a molecular cross-sectional area at collapse of 42 $Å^2$/molecule, which is lower than the 52 $Å^2$ for extended cis-trans configuration. A partial loss of oligomer from the monolayer through dissolution of lower molecular weight species in the aqueous subphase would lead to apparently lower area per molecule at collapse. It is also possible that at the point of collapse the molecules remaining in the monolayer are short enough to pack tightly in an extended fully oriented cis-trans conformation having one end strongly anchored to the water subphase and the other end at the monolayer-air interface. Multiple hydrogen bonds between carboxylic acid groups and between water and the carboxylic acid groups could contribute to a better packing of molecules in the monolayer, hence lower areas per molecule at the collapse, and stronger tethering to the subphase, hence high pressure at collapse.

SUCC-DMS-A11 has the same number of monomer units in the backbone as NTA-DMS-A11, and one succinyl group at each end. It exhibits an area at collapse of 110 $Å^2$/molecule, which corresponds to the formation of a Damaschun helix or an extended helix with structural defects, with one carboxylic acid group in the subphase and the other at the air-film interface. The relatively high area at collapse of 34.6 mN/m suggests good anchoring to the subphase.

For compounds NTA-DMS-A15, -DMS-A21, -AMS-132, and -AMS-152 the areas at collapse increase with the increase in molecular weight. The values are much higher than the cross-sectional areas of a Damaschun helix, which suggests that at collapse the molecules are not fully extended or oriented. The formation of looped structures with molecules having both ends anchored to the subphase cannot be excluded.

High collapse pressure (27.1 mN/m) combined with a large area at collapse (444 $Å^2$/molecule) for NTA-AMS-152 are consistent with molecules having multiple anchoring to the subphase. Succinyl functional silicones present a similar trend for area at collapse values, with the exception of SUCC-AMS-152. This abnormality cannot be explained at this point.

3.2.3 Effects of Metal Cations Present in the Aqueous Subphase

We have anticipated that the behavior of NTA- and succinyl-functional polysiloxane monolayers at the air-water interface can be altered by the presence of metal cations in the subphase. In order to verify this hypothesis, π-A isotherms were measured on aqueous subphases containing $5x10^{-4}$ M $NiCl_2$ (pH 6.8 – 7.0), $5x10^{-4}$ M $CaCl_2$ (pH 7.9, $NaHCO_3$ solution), and $NaHCO_3$ (pH 7.9). Tables 3-2 to 3-4 summarize the experimental results.

Table 3-2: Pressure-Area Isotherms for Succinyl- and NTA-Functional Silicones on Water/$NiCl_2$ Subphase.

Silicone	Isotherm Type	Area Ratios			P_B (mN/m)	P_F (mN/m)
		B/A	C/A	D/A		
SUCC-DMS-A11	3	0.68	N/A	N/A	12.3	39.2
SUCC-DMS-A15	23	0.67	0.45	0.38	10.4	16.1
SUCC-DMS-A21	21	0.72	0.45	0.40	9.5	17.4
SUCC-AMS-132	21	0.70	0.44	0.38	9.5	14.6
SUCC-AMS-152	23	0.85	0.55	0.46	10.1	34.3
NTA-DMS-A11	43	0.66	N/A	N/A	15.5	57.8
NTA-DMS-A15	23	0.69	0.47	0.38	9.7	17.4
NTA-DMS-A21	23	0.63	0.45	0.38	10.1	18.0
NTA-AMS-132	21	0.70	0.46	0.39	10.0	15.9
NTA-AMS-152	32	0.74	0.48	0.40	9.8	30.4

Figures 3-5 to 3-8 present π-A isotherms for two NTA-end-functional and two succinyl-end functional oligomers of low and high molecular weights for aqueous subphases. It was noted that the isotherm shapes were similar to the ones obtained on the water subphase. The ratios C/A and D/A for the monomer transitions were essentially unaffected by the presence of Ca^{2+} or Ni^{2+} in the subphase at the pH used in these experiments, with the exceptions of compounds SUCC-AMS-152 and NTA-DMS-A15 for which a small pH effect was also noted. Some variations for B/A ratios were also

noted. P_B values were not affected by the presence of cations, with the exception of NTA-DMS-A11, possibly due to the strong effect of the end-groups. The increase in P_B by 3 – 5 mN/m observed for this compound when the pH was changed or Ni^{2+} was present might be due to a resistance to transition B (associated with helix formation), caused by complexation of the metal and stronger anchoring to the subphase.

Table 3-3: π-A Isotherms for Succinyl- and NTA-Functional Silicones on $NaHCO_3$ (pH 7.9) Subphase.

Silicone	M_n	Isotherm Type	Area Ratios			P_B (mN/m)	P_F (mN/m)
			B/A	C/A	D/A		
SUCC-DMS-A11	1100	34	0.69	N/A	N/A	12.4	26.9
SUCC-DMS-A15	3400	23	0.66	0.47	N/A	10.8	19.7
SUCC-DMS-A21	5500	2	0.77	0.49	0.42	9.8	22.1
SUCC-AMS-132	5160[a)]	2	0.65	0.45	0.40	10.0	18.3
SUCC-AMS-152	7935[a)]	32	0.80	0.49	0.42	10.2	37.3
NTA-DMS-A11	1530	43	0.66	N/A	N/A	16.8	53.3
NTA-DMS-A15	5230	2	0.67	0.38	0.36	10.3	13.1
NTA-DMS-A21	6860	23	0.70	0.44	0.36	10.2	16.4
NTA-AMS-132	5560[a)]	32	0.68	0.43	0.38	10.5	17.0
NTA-AMS-152	9000[a)]	32	0.74	0.46	0.39	9.6	26.9

a) calculated from manufacturer specifications

Table 3-4: π-A Isotherms Isotherms for Succinyl- and NTA-Functional Silicones on $NaHCO_3/CaCl_2$ (pH 7.9) Subphase.

Silicone	M_n	Isotherm Type	Area Ratios			P_B (mN/m)	P_F (mN/m)
			B/A	C/A	D/A		
SUCC-DMS-A11	1100	4	0.64	N/A	N/A	13.9	50.0
SUCC-DMS-A15	3400	23	0.65	0.45	0.39	10.4	23.2
SUCC-DMS-A21	5500	2	0.70	0.43	0.37	9.8	18.2
SUCC-AMS-132	5160[a)]	2	0.69	0.45	0.39	9.5	16.5
SUCC-AMS-152	7935[a)]	3	0.86	0.54	0.45	10.3	39.6
NTA-DMS-A11	1530	43	N/A	N/A	N/A	N/A	53.5
NTA-DMS-A15	5230	23	0.69	0.44	0.38	9.8	13.4
NTA-DMS-A21	6860	2	0.72	0.47	0.37	10.0	16.0
NTA-AMS-132	5560[a)]	21	0.69	0.45	0.38	10.2	15.7
NTA-AMS-152	9000[a)]	32	0.75	0.48	0.40	9.3	31.2

a) calculated from manufacturer specifications

The change in the solution pH from 6.8 – 7.0 (water) to 7.9 – 8.0 ($NaHCO_3$ solution) has a small but noticeable influence on the isotherms of both NTA- and succinyl-functionalized silicones. The collapse pressure P_F for NTA-derivatives decreases at higher pH values. It is quite likely that the pH at the interface is actually lower than in the subphase[82], and that a significant number of the carboxylic acid groups (pK_a 1.9, 2.49, and 9.73 respectively) in the tricarboxylic acid anchoring component of the polymer are

ionized. As more carboxylic acid groups are ionized the electrostatic repulsive forces between these negatively charged groups will destabilize the cohesion of the monolayer. By contrast, the collapse pressures for succinyl-compounds increase at higher pH in the subphase. In this case too, the pH at the interface is lower than in the subphase, but fewer carboxyl groups are present at the interface (only one per end-group). It is conceivable that there is a balance between the ionized and non-ionized COOH-groups which is responsible for the increased cohesion of the monolayer due to attractive ion-dipole forces in a manner similar to the stabilization of stearic acid monolayers at pH 8 as explained in Chapter 3.1.2.

The presence of Ni^{2+} or Ca^{2+} in the subphase has a marked effect on the surface behavior of both NTA- and succinyl-functional silicones and on the collapse pressure of functional silicones of all molecular weights and degrees of functionalization, as illustrated in Tables 3-2 to 3-4 and Figures 3-5 to 3-8. Unfortunately it is very difficult to explain the results obtained from these measurements. Nickel and calcium increase the collapse pressure of succinyl-functional silicones by 0.8 – 4.6 mN/m and 2.5 – 15.4 mN/m respectively (with the exception of SUCC-DMS-A15). Formation of nickel and calcium carboxylates could be responsible for the increase of the anchoring of the oligomer to the surface. On the other hand, these compounds might have decreased solubility in the subphase and could cause the formation of condensed "solid"-like monolayers that have higher viscosity and resistance to shear. Since these measurements were performed at relatively high barrier rates, kinetic effects play an important role and

the last assumption seems plausible. Future experiments will be needed in order to clarify this point.

The behavior of NTA-functional oligomers on Ni^{2+} and Ca^{2+} subphases was quite different from the one exhibited by succinyl-functional silicones. Ca^{2+} decreased P_F of NTA-silicones by 1.1 – 5.2 mN/m (with the exception of NTA-AMS-132, for which an increase of 4.1 mN/m was noted, while Ni^{2+} exerted contradictory effects on P_F values. It is reasonable to assume that these differences are due to the presence of an increased number of COOH moieties per functional group in the NTA-silicones versus succinyl-silicones, but the exact nature of these differences remains to be established.

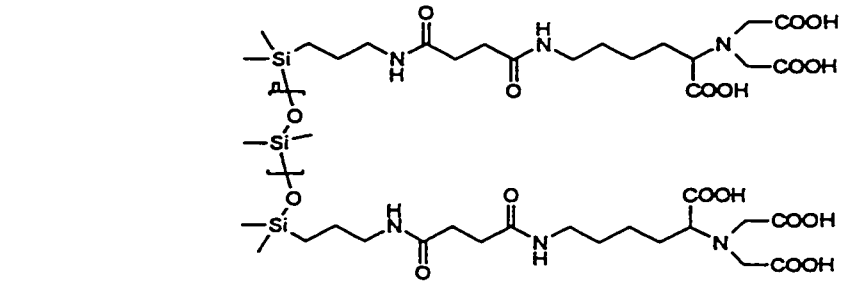

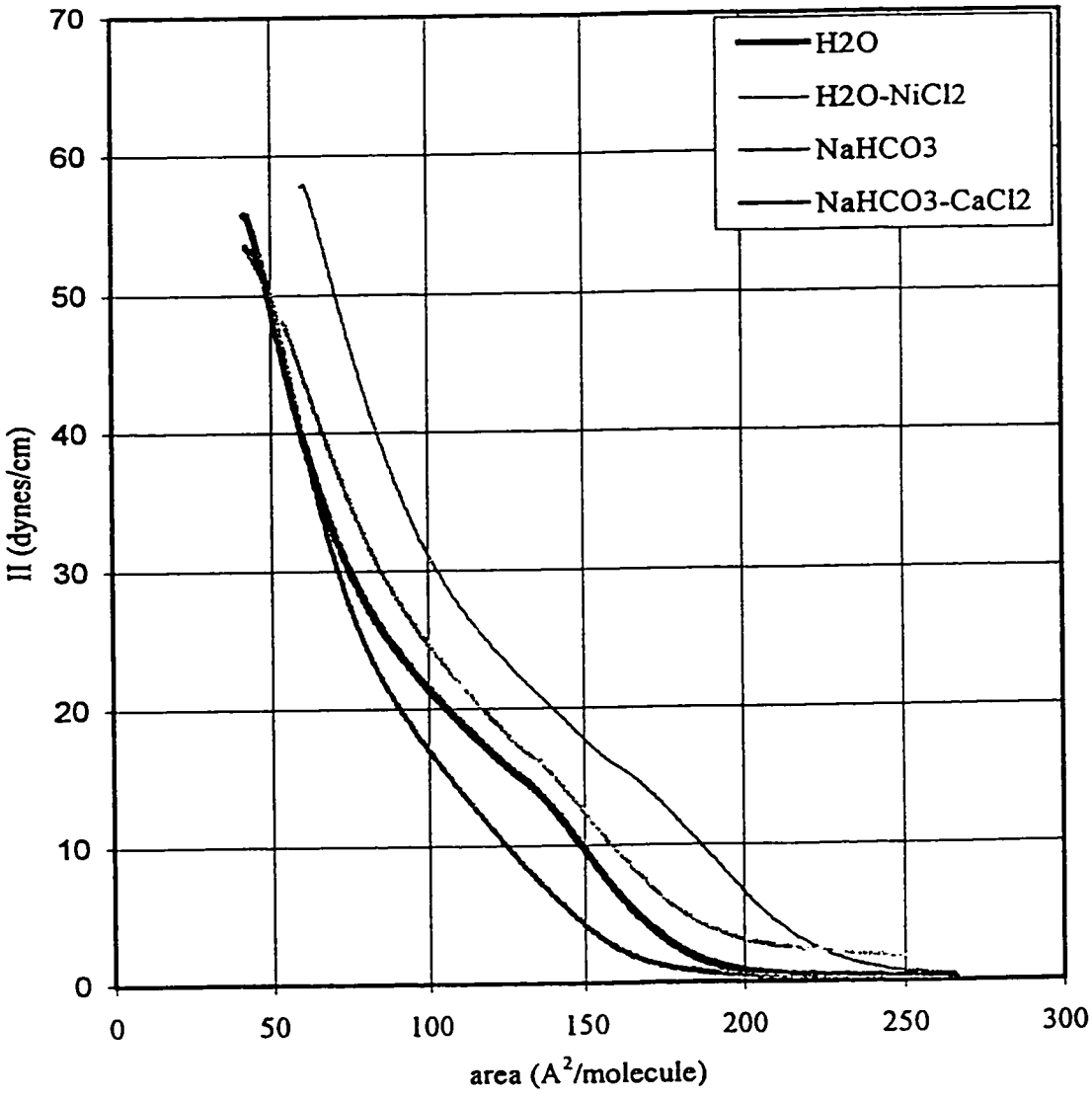

Figure 3-5: Surface Pressure Measurements on Various Aqueous Subphases for NTA-DMS-A11 (M_n = 1530).

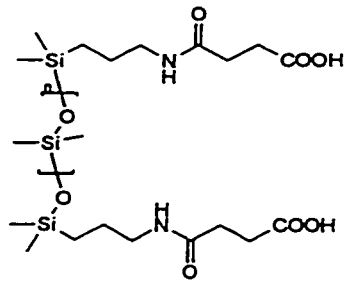

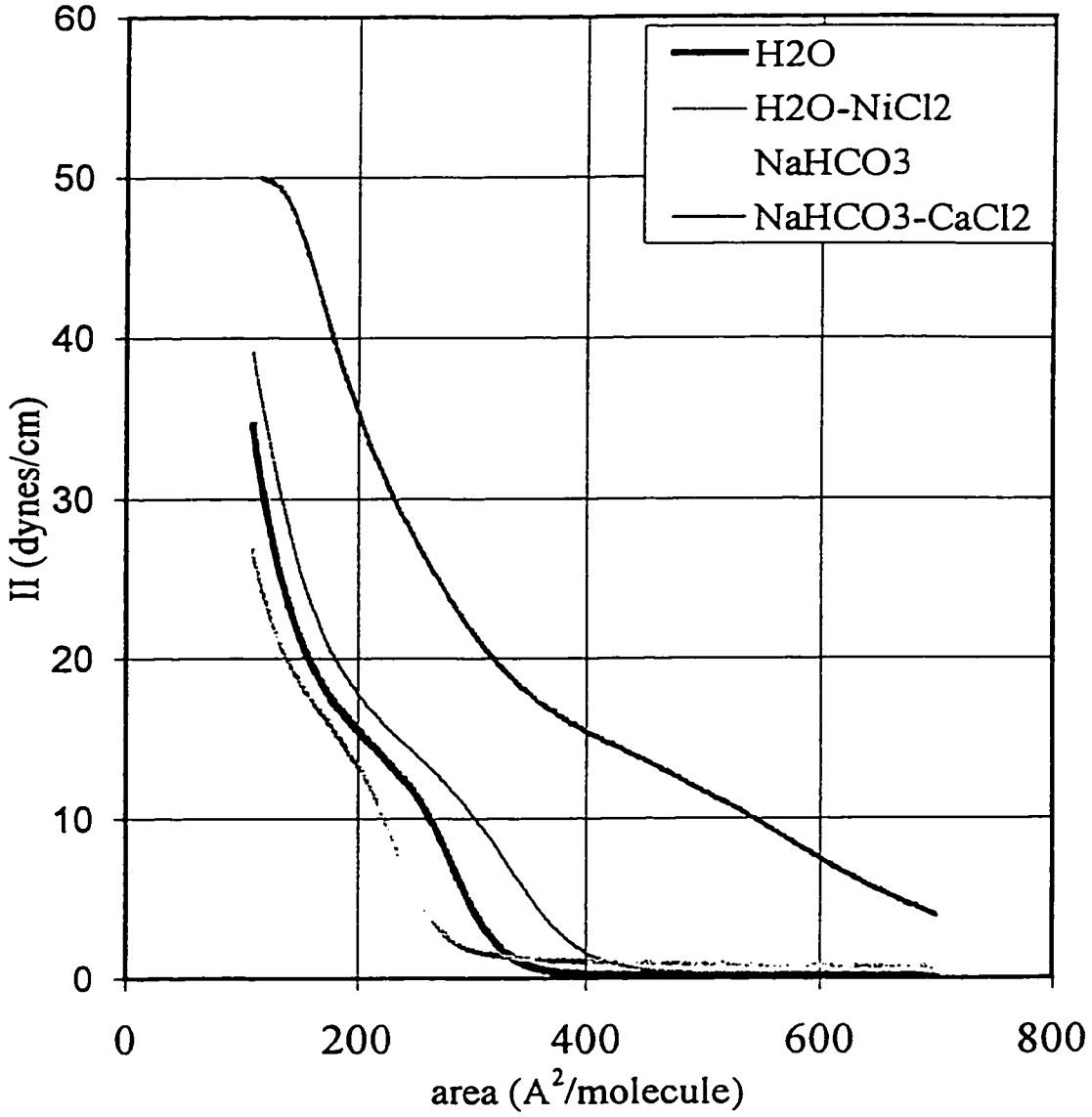

Figure 3-6: Surface Pressure Measurements on Various Aqueous Subphases for SUCC-DMS-A11 (M_n = 1100).

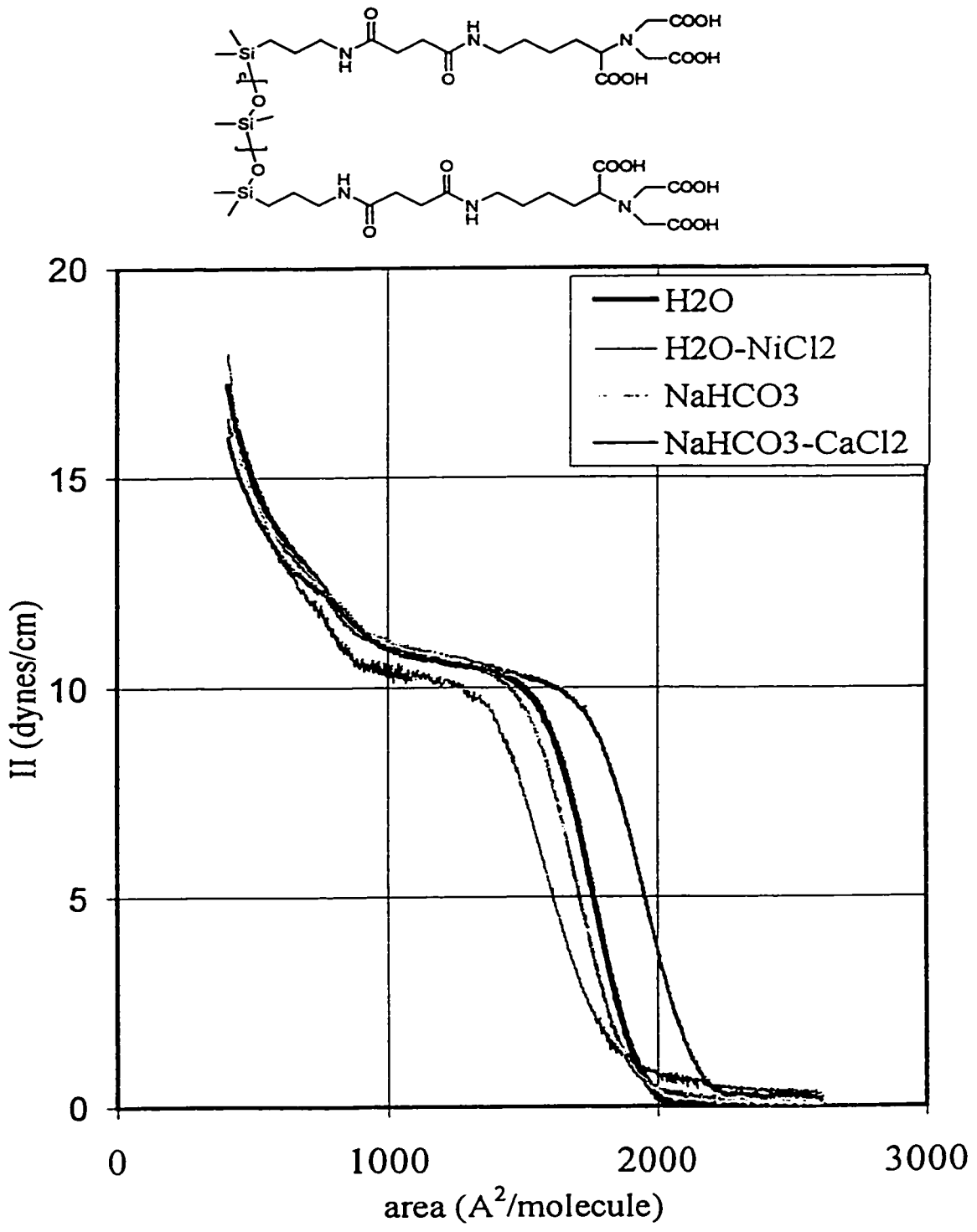

Figure 3-7: Surface Pressure Measurements on Various Aqueous Subphases for NTA-DMS-A21 (M_n = 6860).

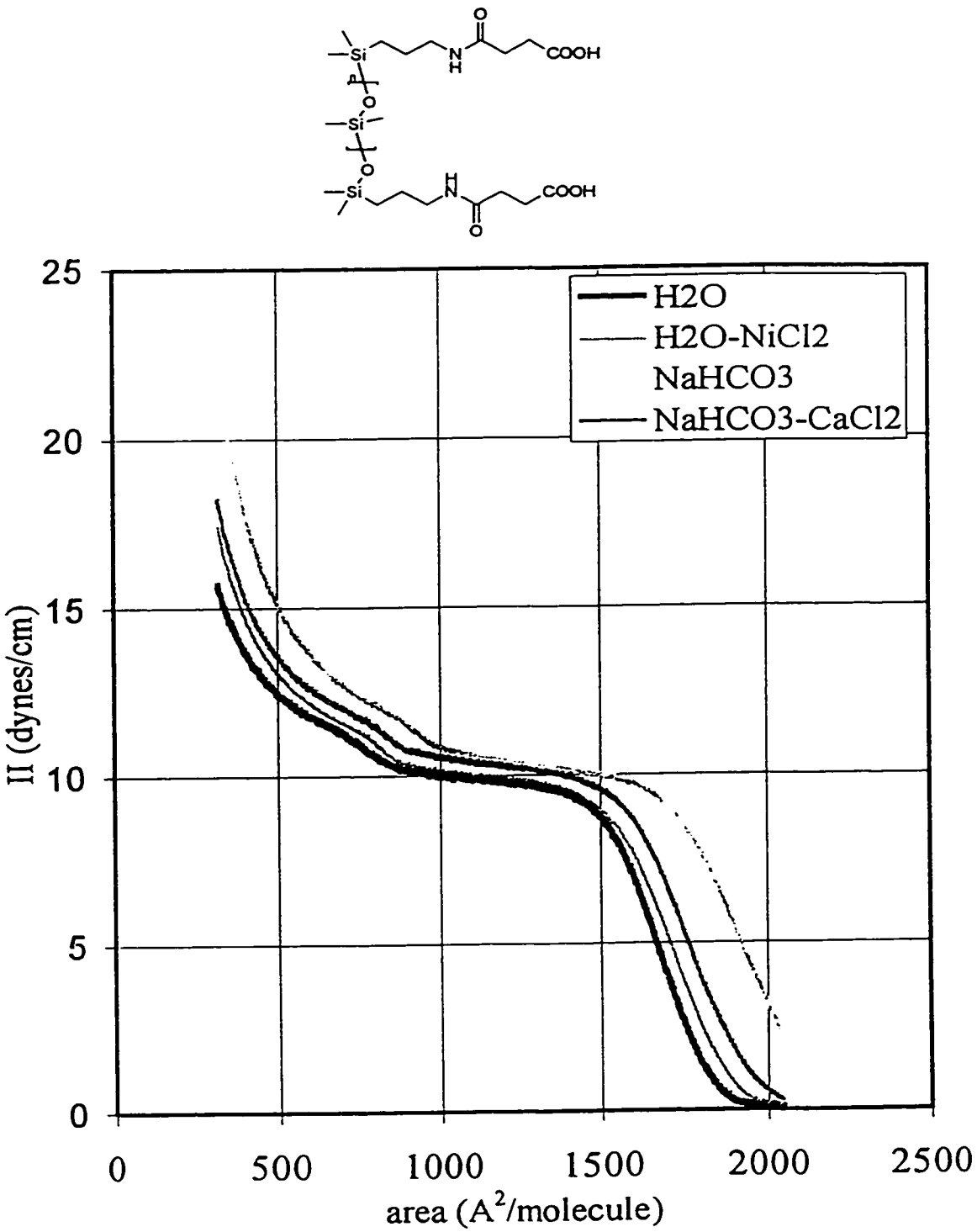

Figure 3-8: Surface Pressure Measurements on Various Aqueous Subphases for SUCC-DMS-A21 (M_n = 5500).

3.2.4 Concluding Remarks

Compounds NTA-DMS-A11 and SUCC-DMS-A11 reduced the surface tension of water by 55 and 35 mN/m respectively and exhibited featureless isotherms, where monomer-related transitions A-D overlapped with transitions E-F involving entire molecules. At the collapse point F these molecules are closely packed in an extended *cis-trans* conformation with one end of the chain in the aqueous subphase, as suggested by the corresponding values of areas at collapse (42 and 110 $Å^2$). The presence of multiple carboxyl groups per chain-end increased the anchoring of the oligomers to the surface and led to higher pressures at collapse.

Higher molecular weight end-functional compounds NTA-DMS-A15, -A21, SUCC-DMS-A15, and -A21 exhibited monomer-associated transitions A-D, which corresponded to the formation of zigzag structures with every other backbone atom at the surface (A-B), followed by the formation of extended helices which could be compressed without a significant increase in surface pressure (B-C). Transitions D-F were very close to each other due to the fact that large oligomers underwent collapse without prior vertical orientation of the chain or complete coiling into helical structures. Thermal motion of the chain segments in higher molecular weight oligomers is sufficiently large to lead to structural defects in these structures. Low pressures at collapse (15-18 mN/m) and large areas at collapse (230-410Å) exhibited by these compounds were consistent with this behavior.

Pendant-functional group polysiloxane oligomers NTA-AMS-152 and SUCC-AMS-152 exhibited relatively high collapse pressures (27 and 32 mN/m respectively), which could be explained by the fact that the molecules had multiple anchoring points to the surface. The large areas at collapse (305 and 444 $Å^2$) showed by these compounds suggested the fact that the molecules formed helical structures with some structural defects.

The study of silicone-chelator monolayers is complicated by a multitude of factors that affect the behavior of the insoluble film at the air-water interface. Partial ionization, complexation, complex stability, solubility in the subphase, pH, ionic strength, nature of counterions, structure of ionic double layer, effects of ions on water-microstructure, interactions between siloxane chains, between subphase and siloxane chains, polymer conformations in the film, viscosity, resistance to shear, and experimental conditions (temperature, compression rate) are several of these factors. In order to understand better the surface behavior of the succinyl- and NTA-silicones, systematic investigations of the effects of the above factors are needed. The surface pressure experiments can be complemented by other experimental techniques, such as surface potential determination, isotope labeling of metal cations in order to investigate quantitatively their incorporation in the film, and deposition on solid surfaces (formation of Langmuir-Blodgett-films).

So far we demonstrated that the newly synthesized silicone chelators and succinyl-functional polysiloxanes have the ability to form insoluble films at the air-water interface. The surface pressure-area isotherms of the NTA-functional silicones exhibited

marked differences compared to the ones of monocarboxylic acid-functional silicones. The properties of these films could be modified by selecting the composition of the subphase, the molecular weight, morphology, and density of functional groups per chain.

4 Organofunctional Silanes as Dual Coupling Agents for Wood-Polyolefin Interface Modification

4.1 Synthesis of Vinylsilanes Used in Model Studies of Polyolefin Functionalization

As seen in Chapter 3, functional silicones could be successfully used to stabilize liquid-air interfaces, due to the remarkable surface activity of the silicone backbone and the presence of particular structural features (chelating groups) of these compounds. However, when the stabilization of hydrophobic-hydrophilic interfaces in solid materials, such as wood-polyolefin composites, is desired, functional polydimethylsiloxanes have very limited utility, due to the fact that stronger interactions are needed in order to improve the adhesion of such inherently incompatible materials. Small molecular weight functional vinylsilanes with moieties (e.g. anhydride, hydroxyl, amino) able to form covalent and ionic or hydrogen bonds with the two substrates (wood, polyolefin) seem more suitable for interface stabilization in this case. Vinylsilanes can be covalently grafted to polyolefins (polyethylene PE, polypropylene PP) via peroxide initiated grafting (see Chapter 1.3). This changes the nature of the polymer surface from hydrophobic to hydrophilic. The further adhesion to wood via hydrogen bonds can be ensured by the presence of OH or NH_2 groups as structural features of the vinylsilane. These polar groups can form hydrogen bonds with hydroxyl groups from cellulose or lignin, helping

in the reinforcement of the interface, or can react with other compounds added for the same purpose, improving the adhesion of wood to polyolefin. If a stronger attachment to wood is desired, covalent bond formation between wood and coupling agent could be utilized (see Chapter 1.1.4) (Figure 4-1).

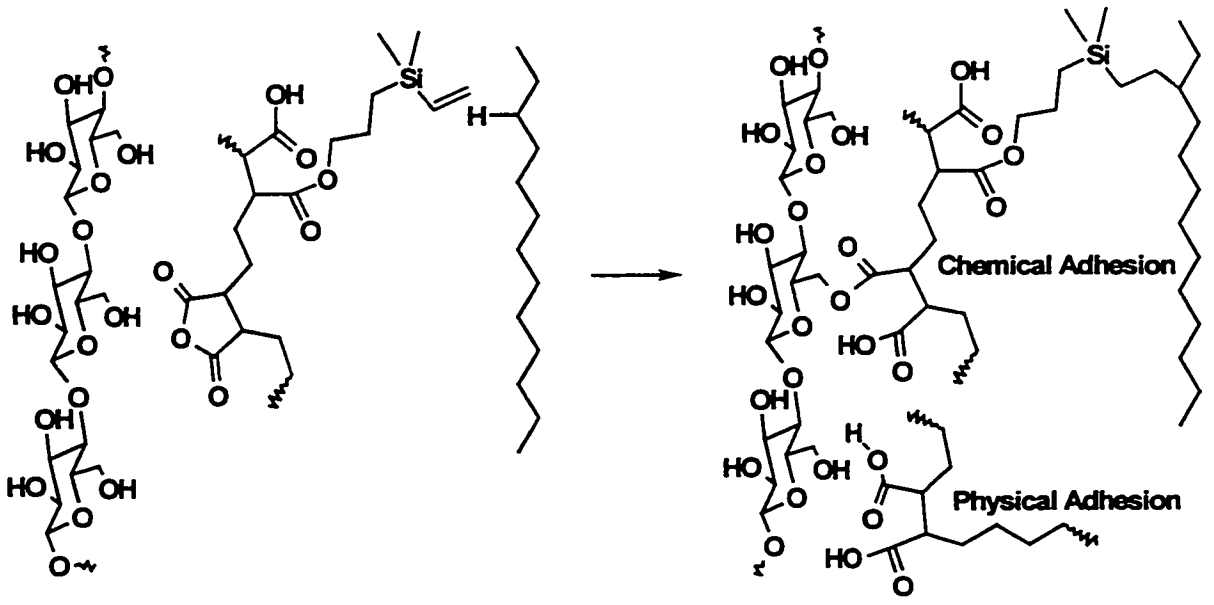

Figure 4-1: Wood-PE composite reinforced by a bifunctional coupling agent.

A dual-functionality coupling agent has two functional groups: one capable of forming covalent bonds with the cellulose in wood, and the other capable of forming covalent bonds with polyethylene. The use of coupling agents of this type in wood-PE composites is expected to improve the adhesion between the two components and to lead to better mechanical properties. In this chapter the synthesis of new compounds that

could act as coupling agents is presented, followed by a study of some mechanical properties of wood-PE that contain one of the vinylsilane-based coupling agents synthesized.

As mentioned in Chapter 1.3, vinylalkyl- and arylsilanes were selected for radical grafting to polyethylene due to their chemical stability to hydrolysis, an area that - to our knowledge - has not been explored. Several different vinylsilanes were chosen as model compounds. Dimethyl-2-phenylethyl-vinylsilane **1** is a trialkylvinylsilane that is stable to hydrolysis and a wide variety of reagents. The phenyl group was introduced in order to aid in the quantification of grafting by ^{1}H-NMR. Dimethyl-1-naphthylvinylsilane **2** and 1-dimethylvinylsilyl-4-[*N*,*N*-bis(trimethylsilyl)amino]naphthalene **3** both contain a naphthyl group which is useful for UV detection and NMR quantification. Compound **3** also contains a protected amino group, which could serve for further modification in order to transform it into a suitable coupling agent, capable of forming covalent bonds with the wood. **1** was readily prepared by the hydrosilylation of styrene with chlorodimethylsilane, followed by the addition of vinylmagnesium bromide, and a final purification using silica gel chromatography (Figure 4-2). **2** and **3** were obtained from their respective bromonaphthalenes (Figure 4-2). It was necessary to protect the amino group amino-4-bromonaphthalene by bis-trimethylsilylation. Treatment with butyllithium, followed by the addition of chlorodimethylvinylsilane led to products **2** and **3**, which were purified by distillation under high vacuum. Repeated attempts to remove the TMS groups in compound **3** using a variety of reagents failed, leading instead to the cleavage of the naphthyl-Si and vinyl-Si bonds. As a consequence, compound **3** was used

as its bis(trimethylsilyl)amine form. This resistance to hydrolysis is not common for mono-and disubstituted silazanes ($RR'NSiMe_2$, R,R′ = H, alkyl, aryl, silyl) but is common with trisubstituted silazanes ($RR'NSiMe_2$, R ≠ H)[89,90].

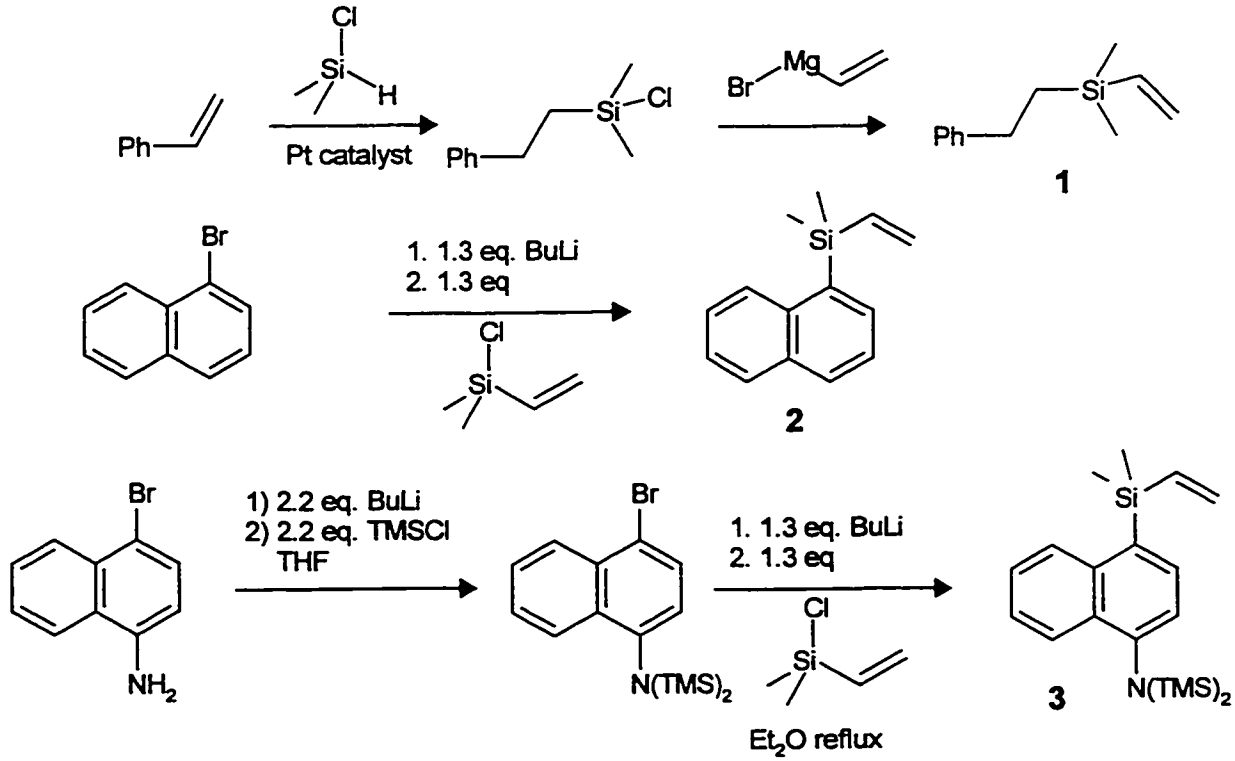

Figure 4-2: Synthesis of model vinylsilanes.

4.2 Model Studies of Radical Grafting of Alkyl- and Arylvinylsilanes onto Squalane Using Peroxide Initiators

4.2.1 Crosslinking of Squalane Using Peroxides

In order to explore the chemistry involved in the radical grafting of vinylsilanes **1**, **2**, and **3** onto low density polyethylene, linear low density polyethylene and polypropylene, we selected squalane **4** ($C_{30}H_{62}$, 2,6,10,15,19,23-hexamethyltetracosane) as a model hydrocarbon substrate[91,92]. The use of **4** facilitated structural characterization and kinetic studies of the grafting process.

Table 4-1: Peroxides used to initiate crosslinking, homopolymerization, and grafting.

Trade Name	General Name	Formula	Conc.	T [°C]	$t_{1/2}$ [hr.]	1 hr Half-Life [°C]
Luperox 500R	Dicumyl Peroxide (DCP)	$[Ph\text{-}C(CH_3)_2\text{-}O\text{-}]_2$	0.2M in Decane	115 130 145	13 2.2 0.42	137
Lucidol-98	Benzoyl Peroxide (BPO)	$[Ph\text{-}COO\text{-}]_2$	0.2M in Benzene	80 90 100	2.5 0.55 0.18	91
Di-*t*-Butyl Peroxide	Di-*t*- Butyl Peroxide (BOOB)	$[(CH_3)_3C\text{-}O]_2$	0.2M in Decane	130 145 160	9.3 1.6 0.3	149
Lupersol 101	2,5-Dimethyl-2,5-di(*t*-butyl peroxy) hexane	$[(CH_3)_3C\text{-}OO\text{-}C(CH_3)_2\text{-}CH_2\text{-}]_2$	0.2M in Dodecane	115 130 145	19 3.2 0.6	140
Lupersol 130	2,5-Dimethyl-2,5-di(*t*-butyl peroxy) hex-3-yne	$[(CH_3)_3C\text{-}OO\text{-}C(CH_3)_2\text{-}C\equiv]_2$	0.2M in Dodecane	130 145 160	11 2.1 0.42	152

The radical reactivity of each of the starting materials, particularly the initiator efficiency for hydrogen abstraction, the crosslinking of the model hydrocarbons, and the homopolymerization of the vinylsilanes were examined. Five commercial peroxides including a diacyl peroxide and four dialkyl peroxides, were used as initiators: benzoyl peroxide (BPO), di-*t*-butyl peroxide (BOOB), dicumyl peroxide (DCP), 2,5-bis(*t*-butylperoxy)-2,5-dimethylhexane (Lupersol 101 L101), and 2,5-bis(*t*-butylperoxy)-2,5-dimethyl-3-hexyne (Lupersol 130 L130). Table 4-1[93] presents some of the specifications of these initiators.

Squalane was treated with the peroxide initiators in a 9:1 weight ratio. The presence of higher molecular weight species (dimers, trimers) was clear from the appearance of several new peaks corresponding to species having higher molecular weights, and larger polydispersities in the gel permeation chromatograms (Table 4-2). The % wt. of these species was estimated using the signal areas in the ^{1}H-NMR spectra. A comparison between ^{13}C- and ^{13}C-DEPT NMR spectra of squalane and crosslinked squalane showed that almost no change had occurred, pointing to the formation of dimers, trimers, and ruling out the possibility of isomerization of squalane. Previous researchers have described extensive isomerization processes of the alkane and grafted products, leading to shorter backbones and multiple branching, under such radical conditions.[63,64] Our NMR data are inconsistent with such isomerizations occurring. The CH peaks at 28 and 23.2 ppm (typical for the squalane) seemed unmodified. No new CH_2- or quaternary C- peaks were observed, while three new CH- peaks could be seen at 31.3, 31.5 and 32.6 ppm, respectively. Lupersol 101, 130 and BOOB showed similar

efficiency for crosslinking, leading to the same weight percent of higher molecular weight species. It was also noted that the benzyloxy (acyloxy type) radical was less efficient (only 9% of the reaction mixture consisted of crosslinked squalane) than the cumyloxy (alkyloxy type) radical in this process, which led to 20 % higher molecular weight species.

A general reaction mechanism for the crosslinking of hydrocarbons initiated by alkoxy type peroxides is presented in Figure 4-3.

Table 4-2: Crosslinking of squalane initiated by peroxides.

Initiator	% Wt Init.	Mol Ratio 4 : Init	Mol Ratio 4 : RO·	$\overline{M}_n$	$\overline{M}_w / \overline{M}_n$	% crosslinked (by wt.)
-	-	-	-	848	1.04	0
L 130	10	5.43:1	1.36:1	1100	1.32	36
L 101	10	5.53:1	1.38:1	1100	1.27	31
L 101	0.5	47.7:1	11.85:1	787	1.07	3
BOOB	10	2.76:1	1.38:1	1200	1.33	39
DCP	10	5.38:1	2.69:1	1000	1.17	20
BPO	10	5.12:1	2.56:1	900	1.10	9

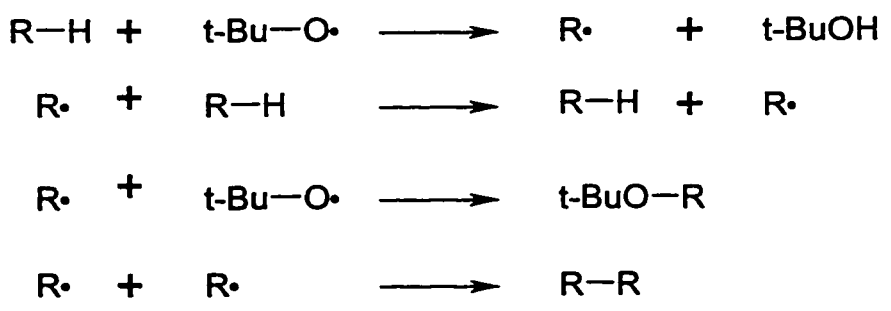

Figure 4-3: Crosslinking of hydrocarbons by peroxides

4.2.2 Homopolymerization of Model Vinylsilanes Using Peroxide Initiators

Although the radical grafting of H_2C=CH-Si(OEt)$_3$ onto PE is a commercial technology[94] and some structural studies were previously performed on the PE-*g*-H_2C=CH-Si(OEt)$_3$ polymer, it was important to establish that the alkyl- and alkylarylvinysilanes **1-3** would similarly graft onto PE. Prior to this, we decided to examine the facility with which **1** underwent homopolymerization. Reactions initiated by BOOB, and Lupersols 101 and 130, respectively, produced relatively low molecular weight oligomers (2-6 units) (Figure 4-4). The GPC results showed unambiguously the presence of higher molecular weight species. The percent of unreacted vinyl groups was determined from the ^{1}H-NMR spectrum by integrating the remaining vinyl-H signals using the phenyl-H signals as a reference. This spectrum also showed several broad signals in the 0-0.5, 0.7-2.0, and 2.7-2.9 ppm regions, confirming the presence of several types of CH- and CH_2- groups from oligomers and initiator-oligomer adducts.

The appearance of the ^{13}C- and ^{13}C-DEPT spectra were consistent with the presence of significant amounts of initiator-oligomer adducts. Several new quaternary C peaks between 60 and 88 ppm, as well as CH_3 peaks in the 30-31.5 ppm region corresponded to structural units that could be attributed to the alkoxy groups (e.g. ≡C-C$(CH_3)_2$O· and $(CH_3)_3$CO· in the Lupersol 130 initiated reaction). The presence of several

new CH- and CH_2- peaks was also noted in the region between 14 and 32 ppm in the ^{13}C- and ^{13}C-DEPT spectra (not shown).

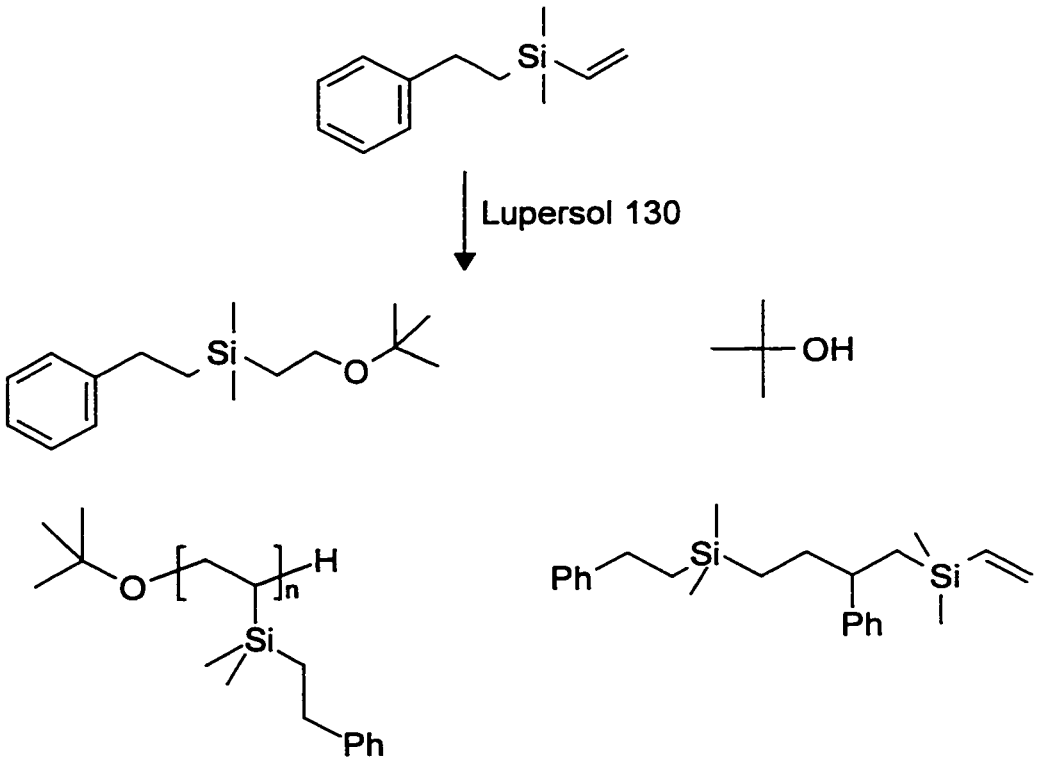

Figure 4-4: Reaction products from the homopolymerization of compound **1**.

Gradient COSY-45 H-H, gradient HSQC H-C, gradient HMBC H-C-C, and gradient H-C-Si chemical shift correlation spectra confirmed the presence of various structural units belonging to the products presented in Figure 4-4 (data not shown).

In addition to radical vinyl polymerization, some side reactions occurred to a small extent: these took place via the abstraction of benzylic hydrogen. At low peroxide concentrations (entry 1, Table 4-3), the homopolymerization still occurred to a significant

extent. This was confirmed by the fact that 27-28 mol % of the vinylsilane reacted when 32.5 moles of monomer were present for each mole of alcoxy radical generated. Even when high peroxide concentrations were used (20-25% by wt.), total vinyl consumption could not be achieved (Table 4-3).

Table 4-3: Homopolymerization reactions of compounds **1**, **2**, and **3**.

Entry	Monomer (M)	Initiator (I)	Initiator. Conc. (wt.%)	Mol Ratio M:I	$\overline{M}_n$	$\overline{M}_w/\overline{M}_n$	%Si-Vi reacted
1	**1**	L 101	0.5	130:1	400	1.91	27.6
2	**1**	L 101	26.5	4:1	2000	3.14	88.3
3	**1**	L 130	22.9	5:1	1700	2.42	81.4
4	**1**	BOOB	5.8	1.7:1	-	-	82.6
5	**2**	L 101	0.5	138:1	500	1.19	53.8
6	**2**	L 101	23.9	4.4:1	900	1.54	80.8
7	**2**	L 130	23.7	4:1	700	1.47	61.2
8	**3**	L 101	24.7	2:1	1300	1.38	95.4
9	**3**	L 101	25.7	2:1	1000	2.04	90.3

Vinylsilanes **2** and **3** also underwent oligomerization (2-6 monomer units, Table 4-3) when initiated with Lupersols 101 and 130, respectively. Again, complete consumption of the vinyl groups could not be achieved, for two reasons: short kinetic chain lengths for the radical polymerization of vinylsilanes[56,57,58], and some chain termination by disproportionation. Low concentrations of peroxide (entry 5, Table 4-3) still led to 53.8 % mol consumption of compound **2**, confirming the fact that the homopolymerization occurred to an even greater extent than in the case of vinylsilane **1**. Complex mixtures of products were obtained in all cases. Consistent with previous work[55], ^{1}H and ^{13}C NMR demonstrated that radical initiator-vinylsilane adducts were

present in the product mixture. Figure 4-5 presents possible reactions occurring during the homopolymerization of vinylsilanes initiated by *t*-BuO· radicals.

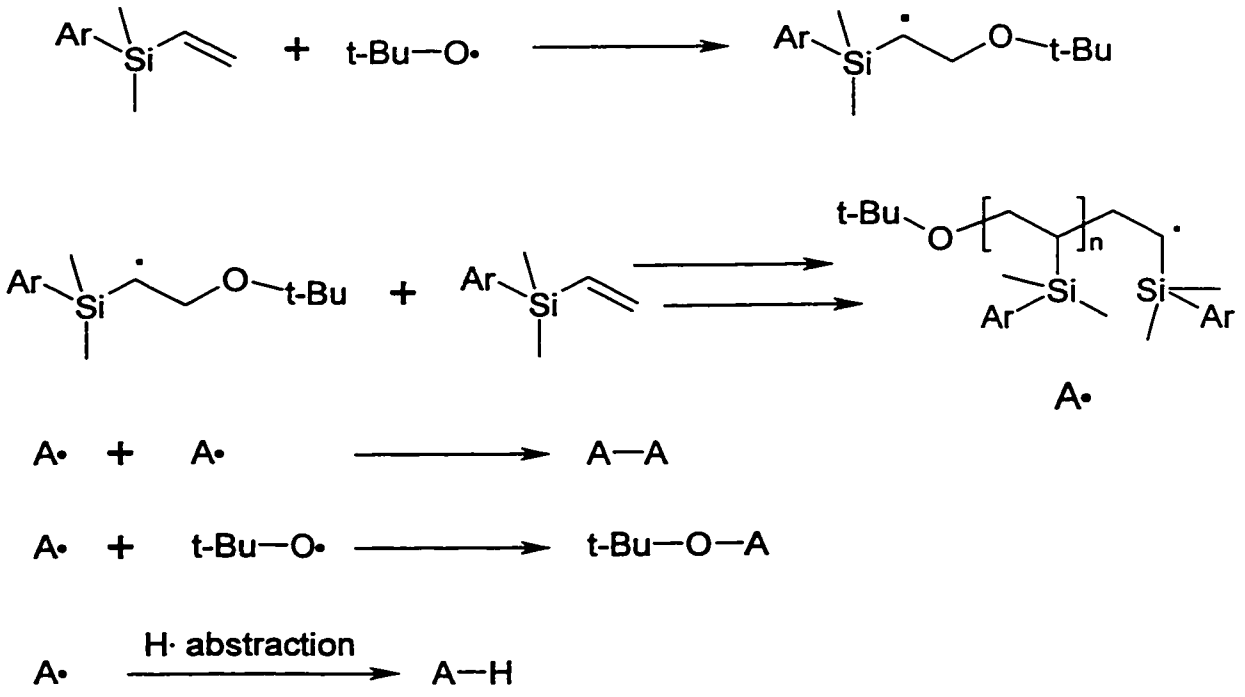

Figure 4-5: Homopolymerization of vinylsilanes.

4.2.3 Peroxide-Initiated Grafting of Model Vinylsilanes onto Squalane

The effect of the initiator on the grafting of vinylsilanes **1**, **2**, and **3** to squalane was examined. The efficiency of grafting was highly dependent upon the type of vinylsilane used, the amount of initiator and the reaction temperature. Attempts to

remove unreacted starting materials (squalane and vinylsilanes) from the product mixtures by vacuum distillation (P <0.1 mmHg) at various temperatures between 80 and 200°C led to extensive degradation, presumably due to various decomposition side reactions initiated thermally and by peroxide traces, as well as backbone isomerization. Therefore, all the reaction mixtures were analysed without separation.

Table 4-4: Experimental results for the vinylsilanes **1-3** grafting onto squalane.

Entry	Monomer (M)	Initiator (I)	Wt%. HMW species	4 : M : I	Mol% Vinyl reacted	$\overline{M}_n$	$\overline{M}_w/\overline{M}_n$
1	1	L 130	70	1:1:0.22	98	1600	2.11
2	1	BOOB	76	1:1:0.53	100	2000	3.54
3	1	DCP	55	1:1:0.22	80	1200	1.51
4	1	BPO	29	1:1:0.28	80	900	1.19
5	1	L 101	65	1:1:0.24	96	1500	1.86
6	1	L 101	-	8.5:1:0.075	<<5	700	1.15
7	2	L 130	ND	1:1:0.26	100	1300	1.45
8	2	L 101	ND	1:1:0.24	100	1100	1.43
9	2	L 101	ND	8.5:1:0.075	88.4	900	1.08
10	3	L 130	ND	1:1:0.32	100	1400	1.68
11	3	L 101	ND	1:1:0.32	100	1300	1.51

ND- not quantified by GPC.

GPC analysis led to semi-quantitative values for the weight percent of products formed in the reaction mixtures. The mol percent of vinyl groups reacted was determined from the ^{1}H-NMR spectra in the same manner described in the homopolymerization experiments.

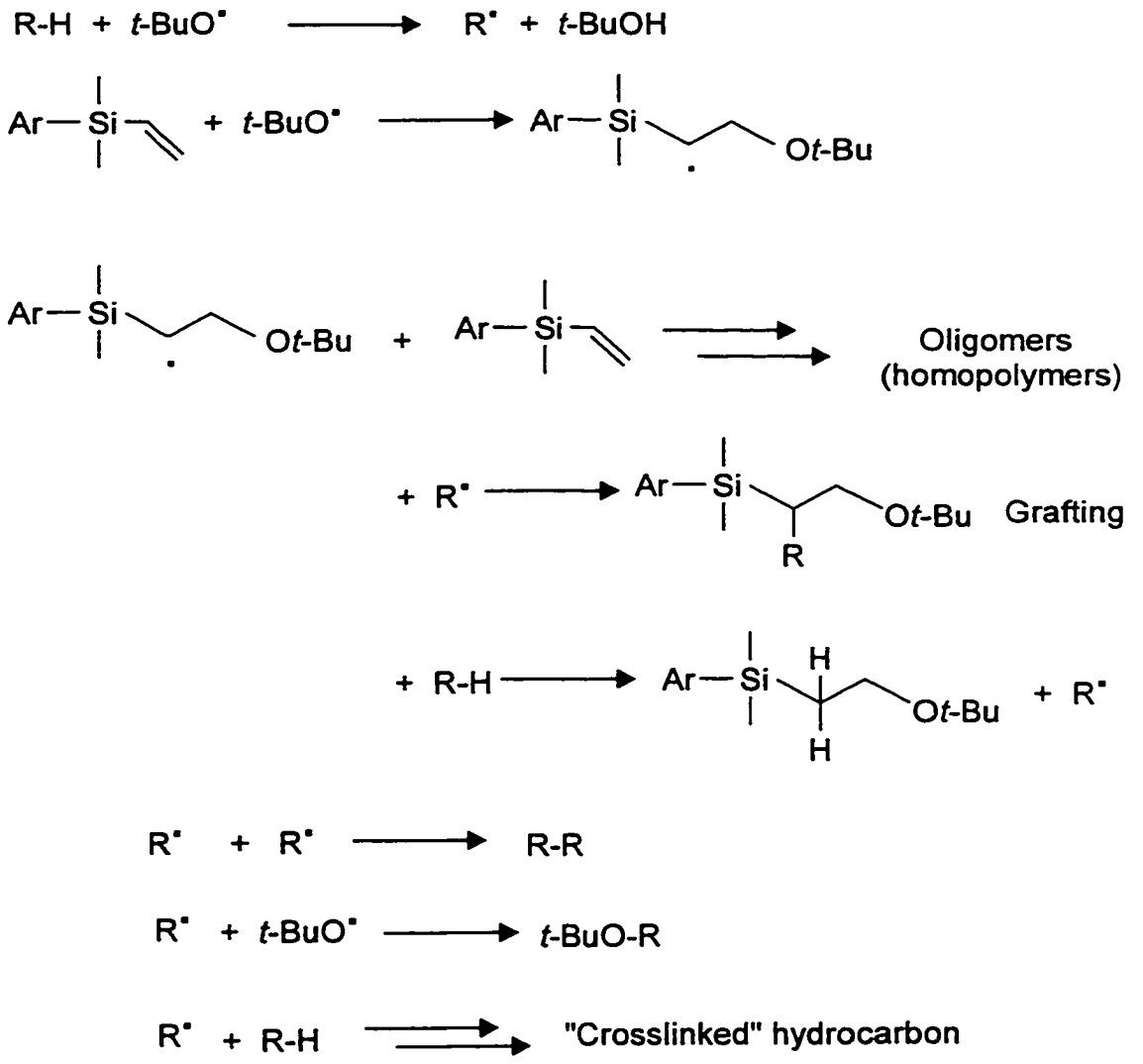

Figure 4-6: Possible reactions during the grafting of vinylsilanes onto squalane.

^{1}H-NMR spectra showed the presence of RO-oligomer adducts. ^{13}C and ^{13}C-DEPT-NMR spectra were difficult to interpret. A comparison was made between data

obtained by crosslinking of **4**, homopolymerization of **1** and the grafting of **1** onto **4**. A few completely new aliphatic signals for CH_2 and CH_3 groups were present, as well as weak, new quartenary carbon atoms, supporting the hypothesis that grafting took place.

It was observed that the mole percent of vinyl groups consumed in the grafting of compound **1** to squalane initiated by Lupersols and BOOB (entries 1,2,5 Table 4-4) was 7 to 18% higher than the corresponding values in the homopolymerization of compound **1** (entries 2,3, and 4, Table 4-3) when similar ratios of monomer to initiator were used. This fact suggested that the vinyl bonds were consumed not only by RO· addition and olefin polymerization (as in homopolymerization) but also by addition of squalane radicals generated by H· abstraction (i.e., grafting). On the other hand, when entry 1, Table 4-3, was compared with entry 6, Table 4-4, it was noted that even though in the grafting experiment the ratio vinylsilane **1**: initiator (Lupersol 101) was roughly 9.8 times higher than in the homopolymerization of **1** experiment, the vinyl group consumption in the grafting process of **1** to squalane was very small. This fact suggested that the radical initiated hydrogen abstraction from squalane followed by the recombination of the radicals generated were the predominant reactions at low peroxide concentrations for this case.

GPC data were of limited use for the characterization of the reaction mixtures obtained from grafting. The only reliable data were the values of mol% vinyl consumption, which was quantitative for experiments with high peroxide concentrations.

A comparison with the values obtained in the homopolymerization experiments showed that in the case of monomer **2**, 20-40% more vinyl groups were consumed in the

grafting experiments than homopolymerization. This suggested that the vinyl groups were consumed not only by RO· addition and olefin polymerization, but also by combination with squalane radicals formed by hydrogen abstraction. A similar conclusion could be drawn for monomer **3**, although a smaller increase in vinyl consumption (5-10 mol%) was observed.

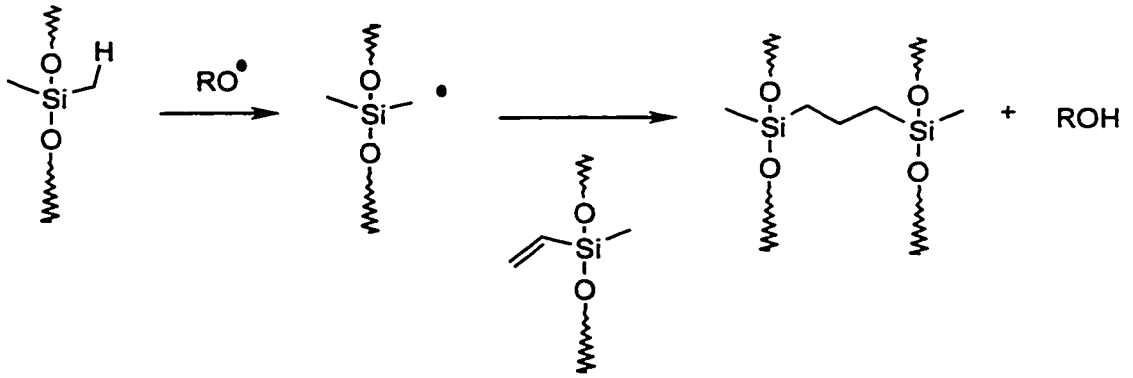

Figure 4-7: Crosslinking of methylsilicones with vinylsilicones.

In an additional experiment, the grafting of **2** and **3** was attempted on durene (1,2,4,5-tetramethylbenzene) in order to compare the selectivity of the initiator towards radical addition to a vinyl bond *versus* benzylic hydrogen abstraction. The intensity of the methyl signal in the proton NMR spectrum was only slightly diminished and no other evidence for benzylic abstraction was found. It could therefore be deduced that the vinyl groups are significantly more reactive under these radical reactions than the benzylic carbon-hydrogen bond.

Many attempts were made to purify the reaction products of grafting. In particular, it was hoped that vinylsilane homopolymer and crosslinked squalane could be separated from grafting products. The grafting of maleic anhydride to squalane[91,92] for example, leads to grafted materials that phase separate. Unfortunately, the grafted materials derived from compounds **1**, **2**, and **3** remained soluble in squalane. It was, therefore, not possible to exclude completely crosslinked squalane and oligomeric vinylsilanes as by-products of the grafting reaction (Figure 4-6). However, several factors pointed to efficient grafting, including the greater conversion of vinyl groups in the grafting than in the homopolymerization reactions, the ineffective radical crosslinking of squalane, and the low efficiency of homopolymerization reactions of vinylsilanes[95], which is well known.

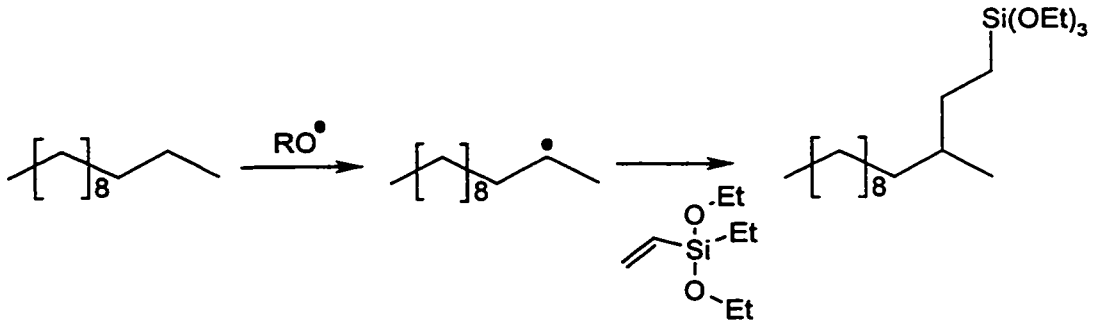

Figure 4-8: Radical grafting of vinyltriethoxysilane onto dodecane.

This situation is analogous to the radical crosslinking reactions used to make silicone elastomers. Methylsilicones efficiently crosslink with vinylsilicones to give typically 3 carbon bridges between adjacent silicone chains.[96] The reaction proceeds with

so-called "vinyl specific" radical initiators such as BOOB and the Lupersols. Essentially, each vinyl group undergoes grafting/crosslinking (Figure 4-7) with little competition from vinyl/vinyl radical recombination and some competition from CH_2•/CH_2• radical recombination (some 2 carbon bridges, and rarely, 4 carbon bridges are evidenced)[96]. One proposed mechanism involves generation of a carbon radical from a methyl group, addition to the vinyl group, and chain transfer. An analogous process has recently been proposed for the grafting of vinyltriethoxysilane onto the model hydrocarbon dodecane[63] (Figure 4-8). In the grafting reaction of **1**, **2**, and **3**, once hydrogen abstraction has taken place, in analogy with silicone crosslinking, vinyl grafting should efficiently follow.

4.2.4 Solution Grafting of Model Vinylsilane 3 onto Polyethylene

Silane **3** was grafted onto PE in 1,2,4-trichlorobenzene-solution using BOOB as a radical source. The reaction was carried out at 165°C for 10½ hours under an inert gas atmosphere. In order to assess the possibility of thermal initiation of grafting, a control experiment was carried out, using the same conditions, but without BOOB as a reaction component.

In contrast to PE, silane **3** and its oligomers are soluble in acetone, so PE could be precipitated by addition of acetone. Soxhlet-extraction with the same solvent was performed in order to remove impurities that were not covalently bound. Finally, the product was vacuum dried and thin films of the polymer were analyzed by fluorescence

spectroscopy. Identical fluorescence spectra were found for pure PE films (PE) and films obtained from the experiment without radical initiator (PE1) with λ_{exc} values of 214, 250 and 338 nm. By contrast, the film made out of PE treated with silane **3** and initiator (PEGR) exhibited sharp emissions at 350, 370 and 390 nm for excitation at λ = 250 nm (Figure 4-9) typical for the naphthyl group and consistent with grafting.

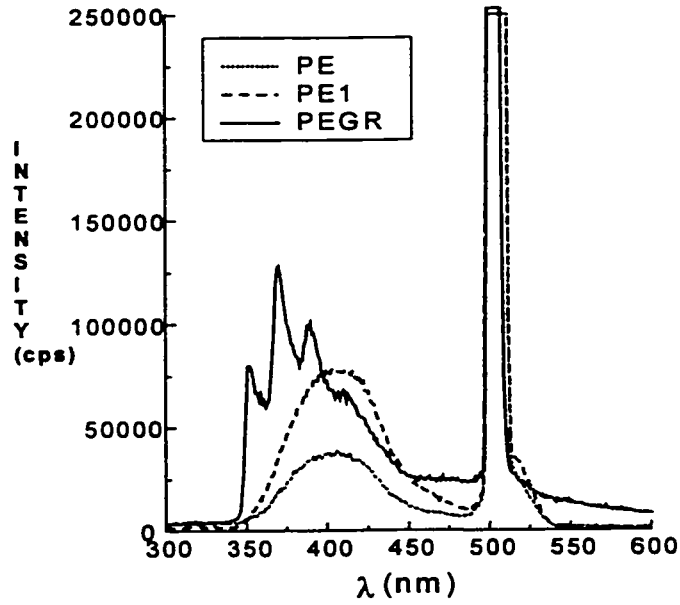

Figure 4-9: Fluorescence spectra of polyethylene films.

4.3 Wood-Polyethylene Composites

The experiments presented in Chapter 4.2 were encouraging with respect to the ability of vinylsilanes to graft onto polyolefin mimics (squalane, **4**) and polyethylene itself. However, the naphthylvinylsilanes used as grafting agents proved to be surprisingly susceptible to aryl-Si bond cleavage under mild, acidic conditions. This chemical instability is expected to have a negative effect on the reinforcement of wood-polyethylene composites with compound **3**. Therefore, we chose to examine compounds containing the requisite vinylsilane functionality that were synthetically more accessible and for which comparison could be directly made with commercial coupling agents. Maleated polyethylenes and polypropylenes are frequently used as coupling agents for wood composites, as noted in Chapter 1.3. Maleic anhydride groups are hydrolyzed by water present in the wood.[65] The resulting carboxylic acids can form hydrogen bonds with polar groups on the wood surface (physical adhesion). Maleic anhydride may additionally form ester linkages with hydroxyl groups (cellulosic or lignin-derived) on wood surfaces (chemical adhesion).

We reasoned that the maleate ester formation reaction could also serve as a vehicle to insert the vinylsilane, which could then react under radical conditions with a polyolefin. An appropriate compound, (γ-hydroxypropyl)vinyldimethylsilane **5**, was synthesized by the hydrosilylation of allyltrimethoxysilane with Me_2SiClH and subsequent Grignard addition of vinylmagnesium bromide to the chlorosilane, followed by purification on silica gel chromatography (Figure 4-10).

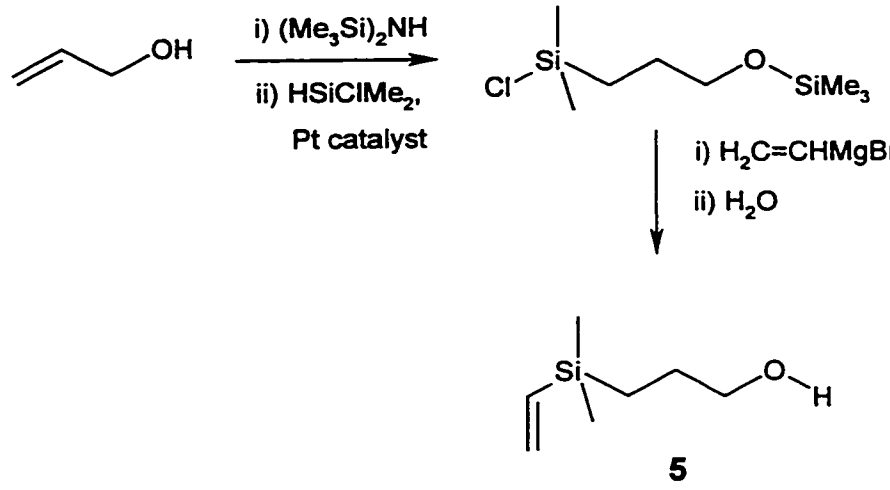

5

Figure 4-10: Synthesis of 3-vinyldimethylsilylpropanol **5**.

It was anticipated that if **5** was combined with a commercially available maleated polypropylene or ethylene, in substoichiometric quantities, a bifunctional coupling agent would result that could graft via ionic chemistry to wood and via radical chemistry to polyethylene (Figure 4-1). To examine this question, low density polyethylene, wood flour, maleated polypropylene, Lupersol 130 and **5** were mixed and melt injected into standard ASTM dog-bone shaped tensile specimens and the properties of the resulting composites measured. The variables of interest that were investigated included the presence and quantity of initiator and **5** (Table 4-5). No attempt was made to ensure that the esterification reaction between the maleated polypropylene and **5** occurred. The composites produced were examined for tensile strength and impact resistance (Table 4-6).

It was noted that the presence of both silane **5** and peroxide (entry 8, Table 4-6) improved the tensile strength of wood-PE composite (entry 2, Table 4-6) even when added in small amounts. Still, the performance of formulations found as entries 5 and 9

was not as good as that of the composition containing the commercial coupling agent MA-*g*-PE and peroxide (entry 7, Table 4-6). The presence of additives, especially peroxide had a negative impact over modulus (tensile strength), with the formulation containing only MA-*g*-PE and silane performing best. From the flexural test results it could be observed that the presence of both silane and peroxide (entry 8) led to higher peak stress values compared with wood-PE (entry 2), and to similar performances as the formulations 7 and 9. Compositions 8 and 9 performed best in the impact tests, but the improvements were marginal compared to entry 7.

Table 4-5: Sample Composition for Wood-Polyethylene Composites.

Entry	Composition	Wt. Ratio
1	PE	
2	PE : Wood	70 : 30
3	PE : Wood : L130	70 : 30 : 0.5
4	PE : Wood : PE-*g*-MA	70 : 30 : 1
5	PE : Wood : Silane	70 : 30 : 1
6	PE : Wood : PE-*g*-MA : Silane	70 : 30 : 0.5 : 0.5
7	PE : Wood : PE-*g*-MA : L130	70 : 30 : 1 : 0.5
8	PE : Wood : L130 : Silane	70 : 30 : 0.5 : 1
9	PE : Wood : PE-*g*-MA : L130 : Silane	70 : 30 : 0.5 : 0.5 : 0.5

Note: PE = polyethylene; L130 = Lupersol 130; PE-*g*-MA = polyethylene-*graft*-maleic anhydride; Silane= (3-hydroxypropyl)dimethylvinylsilane, **5**.

These results were encouraging to a degree. The composite formed using the commercial coupling agent only (entry 4, Table 4-6) showed poorer modulus and impact strength than the analogous formula containing silane and maleated PE (entry 9, Table 4-6). The possibility that this arose from both ionic and radical grafting was suggested by the fact that the presence of radicals (that can lead to grafting in analogy with the reactions described in Table 4-4) improved the performance of the maleated PE in the

absence of silane. The amounts of silane coupling agent used were kept very low and this could be a reason why the improvements noted were rather small. Unfortunately the cost of the reagent made the use of larger amounts not feasible for further testing.

Table 4-6: Mechanical Test Results for Wood-Polyethylene Composites.

	TENSILE STRENGTH		**FLEXURAL TEST**			
Entry	**Ultimate Tensile Strength MPa**	**Modulus GPa**	**Peak Stress Mpa**	**Modulus Gpa**	**Unnotched Izod impact j/m**	**Izod impact j/m**
1	20.30± 0.32	0.582± 0.068	30.71± 1.43	0.866± 0.067	866.10± 117.77	67.78± 3.27
2	10.97± 0.29	0.776± 0.032	21.79± 0.30	0.747± 0.014	109.32± 8.10	34.98± 2.47
3	14.58± 0.15	0.605± 0.031	26.02± 0.30	0.734± 0.021	296.45± 22.40	78.84± 4.90
4	15.04± 0.51	0.706± 0.036	25.79± 0.47	0.754± 0.015	255.61± 10.80	57.53± 7.24
5	10.98± 0.13	0.683± 0.032	21.13± 0.18	0.670± 0.015	127.29± 12.31	37.19± 5.98
6	14.45± 0.41	0.719± 0.037	25.82± 0.24	0.772± 0.009	219.19± 14.85	53.19± 2.14
7	15.88± 0.09	0.677± 0.031	26.66± 0.24	0.775± 0.011	315.15± 29.91	79.96± 6.44
8	14.50± 0.33	0.621± 0.028	25.88± 0.17	0.711± 0.016	356.14± 29.03	89.80± 8.50
9	15.64± 0.17	0.667± 0.026	26.54± 0.30	0.757± 0.009	347.55± 26.52	84.89± 2.04

4.4 Summary

This chapter presented the synthesis of several vinyl/alkyl- and arylsilanes that were used as model compounds for the study of vinysilane grafting onto squalane, initiated by several alcoxide-based radicals. Squalane was used in order to mimic the behavior of polypropylene and low-density polyethylene. Nuclear magnetic resonance spectroscopy and gel permeation chromatography were used in order to analyze the reaction mixtures. It was proved that, with the experimental conditions used, the grafting of the vinylsilanes **1**, **2**, and **3** onto the hydrocarbon substrate took place preferentially over homopolymerization. Furthermore, the synthesis of (γ-hydroxypropyl)vinyl-dimethyl-silane **5** and its ability to act a dual-coupling agent *in situ* in combination with a low molecular weight polyethylene-*g*-maleic anhydride was presented. This coupling agent was used in order to improve adhesion in wood-polyethylene composites. Mechanical tests were performed in order to compare the properties of such composites with similar materials containing polyethylene-alt-maleic anhydride and / or peroxides as adhesion promotors.

In conclusion, radical chemistry involving vinylsilanes **1**, **2**, **3**, and **5** could be successfully employed in the functionalization of chemically inert R-H substrates (hydrocarbons, polyolefins). In the cases of compounds **1**, **2**, and **3**, the grafting of the model vinylsilanes studied was more efficient than their homopolymerization. Compound **3** was found to be the most reactive towards grafting and the presence of the naphthyl group proved to be a convenient means for the characterization of grafting, especially

onto PE substrates. Compound **5** formed a new *in situ* coupling agent for wood-PE composites and along with Lupersol 130 served to provide some mechanical property improvements for this material.

5 General Conclusions and Future Work

We synthesized several new vinylalkyl- and aryl-silanes and grafted them successfully to squalane and polyethylene by employing peroxide initiators. Although the grafted products could not be separated from the reaction mixtures, their formation could be inferred from ^{1}H- and ^{13}C-NMR, as well as GPC. We established that under these conditions grafting takes place preferentially over vinylsilane homopolymerization.

The combined use of low quantities of γ-hydroxypropylvinyldimethylsilane and polyethylene-*graft*-maleic anhydride with Lupersol 130 led to a marginal improvement of mechanical properties in wood-polyethylene composites containing approximately 30 wt% wood flour. It is expected that an increase of the amount of coupling agent to 2 – 5 % will lead to better reinforcement of the composites.

We established a viable synthetic methodology for the synthesis of a new class of amphiphilic silicones bearing nitrilotriacetic acid chelating moieties, starting with commercially available aminopropyl-functional poly(dimethylsiloxanes). Five new compounds were synthesized, having various molecular weights and NTA groups either at the ends of or pendant from, the polysiloxane backbone. These products were characterized by ^{1}H-, ^{13}C-, and ^{29}Si-NMR, electrospray-mass spectrometry, and gel permeation chromatography.

These materials combined the high surface activity and hydrophobicity of the polydimethylsiloxane backbone with the metal-binding properties and water solubility of nitrilotriacetic acid, and formed oriented insoluble films (monolayers) when spread out on aqueous subphases. The presence of metal cations (Ca^{2+}, Ni^{2+}) capable of forming complexes with the NTA moieties, as well as the modification of the subphase pH produced small but noticeable changes in the surface behavior of the film, as evidenced by surface-pressure measurements. These changes were difficult to interpret and correlate with specific polymer conformations induced by calcium-NTA- or nickel-NTA-complex formation. The surface-pressure isotherms of chelating silicones were found to be similar to compounds having similar backbones and monocarboxylic acid functional groups synthesized by us and by other researchers. Low molecular weight silicone chelator NTA-DMS-A11 had one functional group strongly anchored to the subphase and exhibited upright oriented, closely packed chains in an extended *cis-trans* conformation. Higher molecular weight silicone-chelators exhibited a behavior consistent with the formation of expanded helical structures that readily underwent collapse upon further compression.

Further studies will be necessary in order to elucidate the nature of the interactions between silicone-chelator molecules in the insoluble film and a variety of aqueous subphases. A systematic study on the influence of pH, nature of counterions, ionic strength, and compression rates, together with the use of other surface investigation techniques will provide the information needed to fully understand the surface behavior

of NTA-chelators. A quantitative determination of the amounts of metal cations incorporated in the film upon complexation will also be needed for future studies.

Silicone-chelators could be used to form Langmuir-Blodgett films with properties that can be tailored by selecting the molecular weight, the placement of chelating groups (pendant from or at the ends of the backbone), as well as the solid surface (e.g., some inorganic minerals).

6 General Experimental Methods

6.1 Chemical Reagents

N^{ε}-Benzyloxycarbonyl-L-lysine (99%, Bachem), bromoacetic acid (97%, Aldrich), palladium on activated charcoal (Degussa type E101NE/W, wet/Pd 10% dry weight basis, water 50%, Aldrich), Celite (Aldrich), benzyl bromide (98%, Aldrich), cesium carbonate (99%, Aldrich), di-*t*-butyl pyrocarbonate (99%, Aldrich), anhydrous *N*,*N*-dimethylformamide (99.8%, Aldrich), trifluoroacetic acid (99+%, Aldrich), succinic anhydride (99%, Aldrich), *N*-hydroxysuccinimide (97%, Aldrich), 1-(3-dimethylaminopropyl)-3-ethylcarbodiimide hydrochloride (98%, Aldrich), 4-nitrobenzyl chloride (99%, Aldrich), hydrogen bromide (30% solution in acetic acid, Aldrich), allyl alcohol (99%, Aldrich), 1-amino-4-bromonaphthalene (97%, Aldrich), *n*-butyllithium (1.6 M solution in hexanes, Aldrich), benzoyl peroxide (97%, Aldrich), *t*-butyl peroxide (95%, Fluka), 2,5-bis(*t*-butylperoxy)-2,5-dimethylhexane (Lupersol 101 (L101), 90%, Aldrich), 2,5-bis(*t*-butylperoxy)-2,5-dimethyl-3-hexyne (Lupersol 130 (L130), 90%, Aldrich), chlorotrimethylsilane (redistilled, 99+%, Aldrich), dicumyl peroxide (98%, Aldrich), 1,1,1,3,3,3-hexamethyldisilazane (99.9%, Aldrich), platinum-divinyl-tetramethyldisiloxane complex (Karstedt's catalyst) in xylene (Gelest), low density polyethylene injection mold grade PE 2114 (DuPont), polyethylene-*graft*-maleic anhydride (M_w 15,000; M_n 5,700, Aldrich), squalane (99%, Aldrich), styrene (99 %,

Aldrich), and vinylmagnesium bromide (1.0 M solution in tetrahydrofuran, Aldrich), were used as received. Bio-Rad Laboratories supplied Bio-beads S-X1 (divinylbenzene crosslinked styrene). Toyopearl HW-40C gel filtration was supplied by Supelco (Sigma-Aldrich Canada Ltd.)

Amino-functionalized silicones were purchased from Gelest Inc., with the following specifications:

-Aminopropyl-terminated polydimethylsiloxanes:

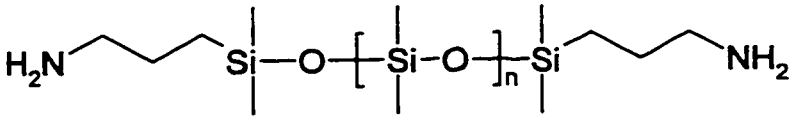

Code	Viscosity (cSt)	Molecular weight*	Mol % amine (NH_2)
DMS-A11	10 - 15	850 - 900	3.2 - 3.8
DMS-A15	50 - 60	3,000	1.0 – 1.2
DMS-A21	100 - 120	5,000	0.6 – 0.7

* relative to polystyrene standards

-Aminopropylmethylsiloxane – Dimethylsiloxane Copolymers:

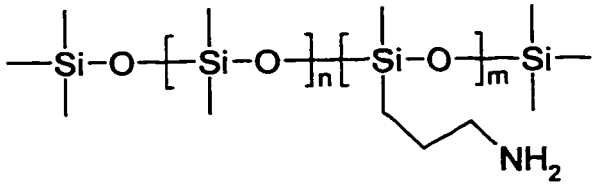

Code	Viscosity (cSt)	Molecular weight*	Mol % Amine (NH_2)
AMS-132	80 – 100	4,500 – 5,500	2 – 3
AMS-152	150 – 260	7,000 – 8,000	4 – 5
AMS-162	80 - 120	4,000 - 5,000	6 – 7

Triethylamine (99%, Aldrich) was dried over KOH pellets, distilled and stored over molecular sieves (4 Å). Methylene chloride (98%, Aldrich) was distilled from calcium hydride. 1,1,1-Trichloroethane (reagent grade, Caledon) was filtered using a type HA 0.45μm Millipore filter. Chlorodimethylsilane (97%, Aldrich), chloro-dimethylvinylsilane (97%, Gelest), and chlorotrimethylsilane (98%, Aldrich) were distilled under an inert (nitrogen) atmosphere and stored over molecular sieves. 1-Bromonaphthalene (98%, Aldrich) was distilled under reduced pressure and stored over molecular sieves. Diethyl ether (99.9%, Aldrich) was distilled over lithium aluminum hydride. Tetrahydrofuran (99%, Aldrich) was first distilled from lithium aluminum hydride and then from potassium/benzophenone. Sodium bicarbonate, potassium hydroxide, and sodium hydroxide were obtained from BDH Chemicals. Acetic acid and hydrochloric acid were obtained from Fischer Scientific. The NMR solvents D_2O, $CDCl_3$, CD_2Cl_2, CD_3OD, and CD_3CN were obtained from Cambridge Isotope Laborotories.

A Milli-Q purification system (Waters Associates, Millford, Massachusetts) was used to deionize and further purify distilled water.

6.2 General Procedures

All syntheses were carried out in dry apparatus under a dry nitrogen atmosphere utilizing conventional bench-top techniques.

6.3 Compound Characterization

6.3.1 Nuclear Magnetic Resonance Spectroscopy

^{1}H-NMR Fourier spectra were recorded on a Bruker DRX-500 (500 MHz) spectrometer, Bruker AC-300 (300 MHz) spectrometer or Bruker AC-200 (200 MHz) spectrometer. ^{13}C and ^{29}Si-NMR were performed on a Bruker DRX-500 spectrometer (at 125.7 MHz and 99.3 MHz for carbon and silicon, respectively), a Bruker AC-200 spectrometer (at 50.3 MHz for carbon), and a Bruker AC-300 spectrometer (at 75.4 MHz and 59.60 MHz for carbon and silicon, respectively). Two dimensional ^{1}H-, ^{13}C-, and ^{1}H-^{1}H chemical shift correlation experiments were recorded on a Bruker DRX-500 spectrometer. Chemical shifts for ^{1}H-NMR spectra are reported with respect to the following standards: residual chloroform set at 7.24 ppm, $CDHCl_2$ set at 5.32 ppm, CD_2HOD set at 3.30 ppm, the HDO peak at 4.67 ppm, and tetramethylsilane set at 0 ppm. ^{13}C-NMR spectra are reported with respect to the following standards: chloroform set at 77 ppm, methylene chloride set at 53.8 ppm, and tetramethylsilane set at 0 ppm. Chemical shifts for ^{29}Si-NMR spectra are reported with respect to tetramethylsilane set at

0 ppm. Coupling constants (*J*) are recorded in hertz (Hz). The abbreviations s = singlet, d = doublet, t = triplet, dd = doublet of doublets, m = multiplet, are used in reporting the spectra.

6.3.2 Mass Spectrometry

6.3.2.1 Chemical Ionization and Electron Impact

Chemical ionization (CI), with ammonia as the reagent gas (NH_3-CI), and electron impact (EI) mass spectra were recorded on a VG Analytical ZAB-E double focusing mass spectrometer. Low-resolution spectra were recorded for routine sample analysis of non-polar samples where appropriate. Typical experimental conditions were: electron energy 70 eV, source temperature 200°C, source pressure 2×10^{-6} mbar for EI and 4×10^{-5} mbar for CI. Mass spectra were reported as percent intensity (%) *versus* mass/charge (m/z) ratio.

6.3.2.2 Electrospray Ionization Mass Spectrometry

Pneumatically-assisted ESMS was performed on a Micromass Quattro-LC Triple Quadrupole mass spectrometer with dichloromethane, dichloromethane: methanol (50/50) or methanol as the mobile phase at a flow rate of 15 μL/min, with use of a Brownlee Microgradient syringe pump. Samples were dissolved in dichloromethane:

methanol (50/50) or pure methanol. For analysis in the negative mode ammonia or NH_4OAc was added, for analysis in the positive mode formic acid was added.

6.3.3 Other Spectroscopy

Infrared spectra in the 4000 – 400 cm^{-1} region were recorded on a Bio Rad FTS-40 Fourier transform spectrometer. Solid samples were prepared as KBr pellets (1-5 % w/w). Ultraviolet spectra were recorded on a Hewlett-Packard 8451 diode array spectrometer.

6.3.4 Gel Permeation Chromatography

The molecular weight distributions of oligomers, grafted products, and functional silicones were analyzed using a Waters Gel Permeation Chromatograph equipped with a Waters 410 Differential Refractive Index detector. Two Waters Styragel HR-4E (7.8x300 mm) columns in series were utilized with 1,1,1-trichloroethane as solvent flowing at 1 mL/min for functional silicone analysis. Narrow molecular weight polydimethylsiloxane standards (Polymer Laboratories) were used for calibration of the chromatographic system. Two Jordi mixed bed columns in series and 1,1,1-trichloroethane flowing at 1 mL/min was used for the analysis of squalane – vinylsilane grafted compounds and low molecular weight oligomers. For these compounds narrow molecular weight polystyrene standards (Polymer Laboratories) were used for calibration.

6.3.5 Surface Pressure Measurements

Surface pressure-area (π-A) experiments were conducted on a commercial (KSV-5000) teflon trough with a length of 475.0 mm, a width of 150.0 mm, and a movable barrier. The measurements were made using a filter paper Wilhelmy plate connected to a microelectronic feedback system for surface pressure control. Thermostated water was used for temperature control. Pressure / area diagrams were obtained by isothermal compression and expansion. All materials were spread from 0.9-1.8 mg/mL solutions in chloroform or chloroform: methanol (9/1) solutions. 15 minutes was allowed before compression of the monolayers began and a compression speed of 10 mm/min was used.

6.3.6 Mechanical Tests

The mechanical properties of all the samples were measured with an Sintech Tester (Model 20). The impact strength (Izod, un-notched) was tested with a Tinius Olsen Impact Tester. The results are the average of measurements on six samples (ASTM D-638).

6.4 Experimental Procedures

6.4.1 Silicone Chelator Syntheses (Chapter 2)

N^{α},N^{α}-Bis(carboxymethyl)-N^{ε}-(benzyloxycarbonyl)-L-lysine [N^{ε}-Z-NTA].

N^{ε}-(Benzyloxycarbonyl)-L-lysine (14.00 g, 0.050 mol) was dissolved in 2M NaOH (125 mL, 0.250 mol) with stirring and cooled to 0°C. Bromoacetic acid (27.80 g, 0.200 mol) was added gradually with stirring and the pH of the solution was adjusted to 12.5 – 13.0 by NaOH additions. After 2 h the reaction mixture was warmed to room temperature and the reaction was allowed to continue overnight. Several pH adjustments were necessary in order to maintain a pH value above 12. The reaction mixture was heated to 50°C for 4 h with stirring and pH adjustments. After cooling to room temperature the product was precipitated from the solution by adding 1N HCl to pH 1.8, filtered, and dried overnight under high vacuum at 50°C. A white solid (18.85 g, 0.048 mol, 95%) was obtained (m.p. 171 - 174°C).

^{1}H-NMR (DMSO-d_6, 200. MHz) δ 9.19 (s, br, 3H, CO_2H), 7.33 (m, 5H, Ph), 7.24 (t, J = 4.8 Hz, 1H, N*H*), 4.99 (s, 2H, PhCH_2), 3.46 (s, 4H, HO_2CCH_2), 3.32 (m, 1H, HO_2CCHCH_2), 2.95 (m, 2H, ZNHCH_2), 1.57 (m, 2H, HO_2CCHCH_2), 1.36 (m, 4H, $ZNHCH_2CH_2CH_2$); ^{13}C-NMR (D_2O: CD_3CN (1:1), 50.3 MHz) δ 175.4 (CO_2H), 175.1 (2 x CO_2H), 158.4 (HN*C*=O), 138.0 (Ph), 129.6 (Ph), 129.1 (Ph), 128.8 (Ph), 67.2 (HO_2CCHCH_2), 66.6 (2 x HO_2CCH_2), 55.5 (PhCH_2), 41.2 (ZNHCH_2), 30.0 (HO_2CCHCH_2), 29.7 ($ZNHCH_2CH_2$), 24.2 ($ZNHCH_2CH_2CH_2$); ESMS (-ve mode + 1

drop 0.2 % NH_4OH): m/z (% intensity), 395 (100) [M$^-$]; FT-IR (KBr): ν (cm^{-1}) 3377 (COO-H), 3024 (CH), 2942 (CH), 1728 (C=O), 1698 (N-C=O), 1536 (N-C=O).

N^{α},N^{α}-Bis(carboxymethyl)-L-lysine [NTA].

N^{ε}-Z-NTA (9.35 g, 0.027 mol) was dissolved in 1N NaOH (60 mL, 0.060 mol), a spatula tip of 10% Pd/C was added, and hydrogenation was conducted at normal pressure and room temperature overnight. The catalyst was removed by vacuum filtration through a Celite pad. The clear colourless filtrate was acidified to pH 2 by dropwise addition of concentrated HCl, followed by the removal of solvent *in vacuo*. The crude solid obtained was triturated with 3 x 250-mL hot methanol. The solvent was removed *in vacuo* and the product was dried under vacuum at 50°C overnight: yield 5.24 g (0.020 mol, 83.3 %) white solid.

^{1}H-NMR (CD_3OD: D_2O (1:1), 200.13 MHz) δ 3.84 (s, 5H, 2 x CH_2CO_2H, C$H$$CO_2H$), 2.90 (t, 2H, J = 6.9 Hz, H_2NCH_2), 1.82 (m, 2H, HO_2CCHCH_2), 1.56 (m, 4H, $H_2NCH_2CH_2CH_2$); ^{13}C-NMR (CD_3OD: D_2O (1:1), 50.32 MHz) δ 173.2 (CO_2H), 171.4 (2x CO_2H), 68.8 ($CHCO_2H$), 56.3 (2 x CH_2CO_2H), 40.2 (H_2NCH_2), 27.7 (CH_2), 27.5 (CH_2), 24.2 (CH_2); ESMS (-ve mode + 1 drop 0.1 % NH_4OH): m/z (% intensity), 261 (100) [M$^-$]; FT-IR (KBr): ν (cm^{-1}) 3561 (COO-H), 3005 (CH), 2963 (CH), 1734 (C=O), 1627 (C=O).

N^{α},N^{α}-Bis(carboxymethyl)-N^{ε}-(*tert*-butyloxycarbonyl)-L-lysine cesium-salt [N^{ε}-Boc-NTA-Cs-salt].

N^{α},N^{α}-Bis(carboxymethyl)-L-lysine (4.150 g, 15.8 mmol) was added to a mixture of cesium carbonate (7.746 g, 23.8 mmol), water (25 mL), and dioxane (25 mL). The

solution was cooled to 0°C and di-*tert*-butyl dicarbonate (3.457 g, 15.8 mmol) was added with stirring. The reaction was continued at room temperature for 45 min and the pH of the solution was maintained at a value of 8.5 by addition of small amounts of cesium carbonate. Complete disappearance of N^{α},N^{α}-bis(carboxymethyl)-L-lysine was shown by TLC on silica-gel (95% EtOH: H_2O (7:3), ninhydrin). The organic solvent was removed *in vacuo* and the residual water was removed by lyophilization yielding the product as a white powder. The product (as a Cs-salt) was used in the next step without further purification. TLC in 95% EtOH: H_2O (7:3), ninhydrin: $R_{f\,(prod.)} = 0.40$, $R_{f\,(start.\ mat.)} = 0.25$.

N^{α},N^{α}-Bis(carboxymethyl)-N^{ε}-(*tert*-butyloxycarbonyl)-L-lysine tribenzyl ester [N^{ε}-Boc-NTA-Bn-ester].

Benzyl bromide (1.436 g, 1 mL, 8.4 mmol) was added to a stirred suspension of N^{ε}-boc-NTA-Cs-salt (1.880 g, 2.0 mmol) in anhydrous DMF (50 mL). The reaction was continued at room temperature overnight under nitrogen atmosphere and vigorous stirring. DMF was removed *in vacuo* (<1 mm Hg) at 45 – 50°C. The product was purified by silica gel chromatography with hexanes / ethyl acetate (80:20) as eluant. The solvents were removed *in vacuo* yielding a pale yellow oil (0.563 g, 0.9 mmol, 44.5%). TLC in hexanes / ethyl acetate (80:20), ninhydrin: $R_f = 0.09$.

^{1}H-NMR ($CDCl_3$, 200.13 MHz) δ 7.25 (m, 16H, 3 x Ph + N*H*), 5.01 (m, 6H, 3x CH_2Ph), 3.63 (s, 4H, 2 x CH_2CO_2Bn), 3.39 (t, 1H, J = 5.1 Hz, C*H*CO_2Bn), 2.94 (m, 2H, NHCH_2), 1.60 (m, 2H, NCH_2CH_2), 1,37 (s, 9H, Boc), 1.33 (m, 4H, CH_2CH_2CH); ^{13}C-NMR ($CDCl_3$, 50.32 MHz) δ 172.3 (CH*C*O_2Bn), 171.0 (2 x CH_2CO_2Bn), 155.9 (NH*C*=O), 135.7 (Ph), 135.6 (2 x Ph), 128.4 (Ph), 128.2 (Ph), 126.8 (Ph), 78.9 (*C*Me_3), 66.3 (2 x

CH_2Ph), 65.1 (NCH), 64.7 (CH_2Ph), 52.7 (2 x NCH_2), 40.2 ($NHCH_2$), 30.0 (CH_2), 29.4 (CH_2), 28.4 (3 x CH_3), 23.0 (CH_2); ESMS (+ve mode + MeOH): m/z (% intensity), 633 (100 %) [M^+].

N^{α},N^{α}-Bis(carboxymethyl)-L-lysine tribenzyl ester [NTA-Bn-ester].

N^{α},N^{α}-Bis(carboxymethyl)-N^{ε}-(*tert*-butyloxycarbonyl)-L-lysine tribenzyl ester (1.625 g, 2.6 mmol) in trifluoroacetic acid (20 mL) was stirred under a nitrogen atmosphere at room temperature. After 45 min the reaction was complete as shown by TLC on silica gel in hexanes/ ethyl acetate (70:30) (ninhydrin and UV detection). After solvent removal *in vacuo* (< 1 mm Hg) a clear oil was obtained (1.680 g, 100% yield, product is the TFA salt), which was used in the next step without further purification. TLC in hexanes/ethyl acetate (70:30): $R_{f\,(start.\,mat.)} = 0.25$, $R_{f\,(product)} = 0.00$.

^{1}H-NMR ($CDCl_3$, 200.13 MHz) δ 7.32 (m, 15H, Ph), 5.10 (m, 6H, 3 x CH_2Ph), 3.59 (m, 4H, 2 x NCH_2), 3.53 (m, 1H, NCH), 3.05 (m, 2H, H_2NCH_2), 1.75–1.43 (m, 6H, $H_2NCH_2CH_2CH_2CH_2$).

N^{α},N^{α}-Bis(carboxymethyl)-N^{ε}-succinyl-L-lysine tribenzyl ester [SUCC-NTA-Bn-ester].

Succinic anhydride (0.257 g, 2.6 mmol) was added to a stirred solution of N^{α},N^{α}-bis(carboxymethyl)-L-lysine tribenzyl ester TFA salt (1.680 g, 2.6 mmol) and triethylamine (2.5 mL) in dry methylene chloride (30 mL) under nitrogen atmosphere at room temperature. More triethylamine was added in order to maintain basic conditions (pH 8.5 on wet litmus paper). After 3.5 h the reaction was complete as evidenced by thin layer chromatography on silica gel in methylene chloride / acetic acid (99.8:0.02),

detected by UV-light and molybdenum reagent. The organic phase was washed with 1N HCl (80 mL) and brine (3 x 80 mL) and dried over anhydrous sodium sulfate. Solvent removal *in vacuo* yielded the product as a clear colourless oil (1.422 g, 2.3 mmol, 87.5%). TLC in CH_2Cl_2 / AcOH (99.8: 0.02): $R_{f\,(start.\,mat.)} = 0.38$, $R_{f\,(product)} = 0.13$, $R_{f\,(succinic\,anh.)} = 0.90$.

^{1}H-NMR ($CDCl_3$, 200.13 MHz) δ 7.31 (m, 15H, 3x Ph), 6.39 (s, 1H, N*H*), 5.05 (m, 6H, CH_2Ph), 3.65 (s, 4H, 2 x NCH_2), 3.47 (t, 1H, J = 4.6 Hz, NC*H*), 3.17 (m, 2H, NHCH_2), 2.62 (m, 2H, HO_2CCH_2), 2.45 (m, 2H, $HO_2CCH_2CH_2$), 1.67 (m, 2H, NCHCH_2) 1.43 (m, 4H, $NHCH_2CH_2CH_2$); ^{13}C-NMR ($CDCl_3$, 50.32 MHz) δ 175.3 (C=O), 172.9 (C=O), 172.6 (C=O), 171.4 (2 x BnOC=O), 135.6 (Ph), 135.5 (Ph), 128.5 (Ph), 128.3 (Ph), 128.2 (Ph), 128.1 (Ph), 66.5 (2 x CH_2Ph), 66.4 (CH_2Ph), 64.1 (NCH), 52.9 (2 x NCH_2), 39.4 ($NHCH_2$), 30.6 (CH_2), 30.3 (CH_2), 29.4 (CH_2), 27.7 (CH_2), 22.4 (CH_2); FT-IR (neat): ν (cm^{-1}) 3369 (COO-H), 3036 (CH), 2950 (CH), 1737 (C=O), 1635 (N-C=O), 1554 (N-C=O); ES-MS (+ve mode in MeOH): m/z (% intensity), 633 (100) [M^+].

N^{α},N^{α}-Bis(carboxymethyl)-N^{ε}-succinimidylsuccinyl-L-lysine tribenzyl ester [N^{ε}-SSU-NTA-Bn-ester].

N-Hydroxysuccinimide (0.780 g, 6.7 mmol) in dry 1,2-dimethoxyethane (80 mL) was added to N^{α},N^{α}-bis(carboxymethyl)-N^{ε}-succinyl-L-lysine tribenzyl ester (4.234 g, 6.7 mmol) in dry methylene chloride (80 mL) under a nitrogen atmosphere. After cooling to 0°C 1-ethyl-3-(3-dimethylaminopropyl)-carbodiimide hydrochloride (1.311 g, 6.7 mmol) was added with stirring. After 4 h the solution was gradually warmed to room temperature and the reaction continued overnight. The solvents were removed *in vacuo*.

Silica gel chromatography in hexanes/ ethyl acetate (15:85) (UV and molybdenum reagent visualization) yielded the product as colourless oil (3.676 g, 5.8 mmol, 87%).

TLC in hexanes: ethyl acetate (15:85): $R_{f\,(product)} = 0.13$.

^{1}H-NMR ($CDCl_3$, 200.13 MHz) δ 7.31 (m, 15H, 3 x Ph), 6.09 (s, 1H, N*H*), 5.07 (m, 6H, CH_2Ph), 3.68 (s, 4H, 2 x NCH_2), 3.47 (t, 1H, J = 7.5 Hz, NC*H*), 3.17 (m, 2H, NHCH_2), 2.95 (t, 2H, J = 7.3 Hz, NHS-O_2CCH_2), 2.74 (s, 4H, NHS), 2.55 (t, 2H, J = 7.3 Hz, NHS-O_2CCH_2CH_2), 1.67 (m, 2H, NCHCH_2) 1.43 (m, 4H, NHCH_2CH_2CH_2); ^{13}C-NMR ($CDCl_3$, 50.32 MHz) δ 172.5 (C=O), 171.2 (2x C=O), 169.9 (C=O), 169.0 (2 x BnOC=O), 168.2 (C=O), 135.6 (Ph), 135.5 (Ph), 128.5 (Ph), 128.3 (Ph), 128.1 (Ph), 66.4 (3 x CH_2Ph), 64.2 (NCH), 52.8 (2 x NCH_2), 39.1 (NHCH_2), 30.6 (CH_2), 29.4 (CH_2), 28.0 (CH_2), 26.9 (CH_2), 25.5 (2 x CH_2), 22.5 (CH_2); FT-IR (neat): ν (cm^{-1}) 3387 (COO-H), 3036 (CH), 2946 (CH), 1816 (C=O), 1786 (C=O), 1740 (C=O), 1674 (C=O), 1544 (N-C=O); ES-MS (+ve mode in MeOH): m/z (% intensity), 730 (100) [M^+].

N^{α},N^{α}-Bis(carboxymethyl)-L-lysine tribenzyl ester-terminated polydimethyl-siloxane DMS-A11 [NTA-DMS-A11-Bn-Ester].

Aminopropyl-terminated poly-dimethylsiloxane DMS-A11 (0.394 g, 0.5 mmol) was added to a stirred solution of N^{α},N^{α}-bis(carboxymethyl)-N^{ε}-succinimidylsuccinyl-L-lysine tribenzyl ester (0.720 g, 1.0 mmol) in dry methylene chloride (40 mL) under a nitrogen atmosphere. After stirring for 5 h at room temperature the solvent was removed *in vacuo*. Silica gel chromatography using methylene chloride/methanol (97:3) yielded the product as a clear pale yellow solid (0.900 g, 0.4 mmol, 95%). TLC in CH_2Cl_2 / MeOH (97:3): $R_{f\,(product)} = 0.14 - 0.40$, $R_{f\,(NHS\text{-}OH)} = 0.04$, $R_{f\,(DMS\text{-}A11)} = 0$, $R_{f\,(NHS\text{-}ester\ start.\ mat.)} = 0.58$.

^{1}H-NMR ($CDCl_3$, 200.13 MHz) δ 7.31 (m, 30H, 6 x Ph), 6.20 (s, br, 4H, N*H*), 5.06 (m, 12H, CH_2Ph), 3.67 (s, 8H, 4 x NCH_2), 3.47 (t, 2H, J = 7.5 Hz, 2 x NC*H*), 3.15 (m, 8H, 4 x NHCH_2), 2.46 (s, 8H, 2 x O=CCH_2CH_2C=O), 1.65 (m, 4H, 2 x NCHCH_2) 1.43 (m, 12H, 2 x SiCH$_2$CH_2, 2 x NHCH$_2$CH_2CH_2), 0.49 (m, 4H, 2 x SiCH_2), 0.04 (m, ~55H, SiCH_3); ^{13}C-NMR ($CDCl_3$, 50.32 MHz) δ 172.5 (C=O), 172.3 (C=O), 172.1 (C=O), 171.2 (C=O), 135.7 (Ph), 135.6 (Ph), 128.5 (Ph), 128.3 (Ph), 128.1 (Ph), 66.4 (6 x *C*H$_2$Ph), 64.4 (2 x N*C*H), 52.8 (4 x N*C*H$_2$), 42.5 (2 x NH*C*H$_2$), 39.2 (2 x NH*C*H$_2$), 32.0 (2 x *C*H$_2$), 31.8 (2 x *C*H$_2$), 29.7 (2 x *C*H$_2$), 28.4 (2 x *C*H$_2$), 23.4 (2 x *C*H$_2$), 22.8 (2 x *C*H$_2$), 15.4 (2 x *C*H$_2$), 1.2 (*C*H$_3$), 1.0 (*C*H$_3$), 0.3 (*C*H$_3$), 0.1 (*C*H$_3$); ^{29}Si-NMR (CH_2Cl_2, 59.63MHz, TMS ext. std): δ 7.22, -20.9, -21.50, -22.10; FT-IR (neat): ν (cm^{-1}) 3301 (COO-H), 2962 (CH), 1743 (C=O), 1642 (N-C=O), 1549 (N-C=O), 1261 (Si-CH$_3$), 1091 (Si-O), 1028 (Si-O), 801 (Si-CH$_3$); ES-MS (+ve mode in MeOH + 1 drop 0.1 % HCOOH): singly charged ion series with peaks from 1478 [M$^+$, n = 0] to 2364 [M$^+$, n = 11]; doubly charged ion series with peaks from 739 [M^{2+}, n = 0] to 1407 [M^{2+}, n = 18].

N^{α},N^{α}-Bis(carboxymethyl)-L-lysine terminated polydimethylsiloxane DMS-A11 [NTA-DMS-A11].

N^{α},N^{α}-Bis(carboxymethyl)-L-lysine tribenzyl ester-terminated polydimethylsiloxane DMS-A11 (0.506 g, 0.2 mmol) was dissolved in dry 1,2-dimethoxyethane (40 mL), 10% palladium on charcoal (a spatula tip) was added, and hydrogenation at room temperature and normal pressure was allowed to proceed for 8 h. The completion of the reaction was shown by the disappearance of the starting material as checked by thin layer chromatography using methylene chloride / methanol (93:7). The catalyst was removed

by filtration through a Celite pad and the solvent was removed *in vacuo* yielding the product as a pale yellow clear solid (0.370 g, 0.2 mmol, 100%).

^{1}H-NMR (CD_3OD, 200.13 MHz) δ 3.64 (s, 8H, 4 x NC*H*$_2$), 3.47 (t, 2H, J = 6.8 Hz, 2 x NC*H*), 3.15 (m, 8H, 4 x NHC*H*$_2$), 2.45 (s, 8H, 2 x O=CC*H*$_2$C*H*$_2$C=O), 1.70 (m, 4H, 2 x NCHC*H*$_2$), 1.52 (m, 12H, 2 x SiCH$_2$C*H*$_2$, 2 x NHCH$_2$C*H*$_2$C*H*$_2$), 0.56 (m, 4H, 2 x SiC*H*$_2$), 0.08 (m, ~60H, SiC*H*$_3$); ^{13}C-NMR (CD_3OD, 50.32 MHz) δ 175.8 (C=O), 174.6 (C=O), 66.6 (2 x NCH), 55.3 (4 x NCH$_2$), 43.6 (2 x NHCH$_2$), 40.1 (2 x NHCH$_2$), 32.4 (4 x CH$_2$), 30.7 (2 x CH$_2$), 29.9 (2 x CH$_2$), 24.7 (2 x CH$_2$), 24.4 (2 x CH$_2$), 16.4 (2 x CH$_2$), 1.4 (CH$_3$), 0.3 (CH$_3$); FT-IR (neat): ν (cm^{-1}) 3297 (COO-H), 2963 (CH), 1730 (C=O), 1646 (N-C=O), 1553 (N-C=O), 1261 (Si-CH$_3$), 1090 (Si-O), 1029 (Si-O), 801 (Si-CH$_3$); ES-MS (-ve mode in CH_2Cl_2 / MeOH + 1 drop 0.25mM NH_4OAc): singly charged ion series with peaks from 936 [M^-, n = 0] to 2120 [M^-, n = 16]; doubly charged ion series with peaks from 467 [M^{2-}, n = 0] to 1209 [M^{2-}, n = 20].

N^α,N^α-Bis(carboxymethyl)-L-lysine tribenzyl ester-terminated polydimethylsiloxane DMS-A15 [NTA-DMS-A15-Bn-Ester].

Aminopropyl-terminated polydimethylsiloxane DMS-A15 (1.340 g, 0.5 mmol) was added to a stirred solution of N^α,N^α-bis(carboxymethyl)-N^ε-succinimidylsuccinyl-L-lysine tribenzyl ester (0.720 g, 1.0 mmol) in dry methylene chloride (40 mL) under a nitrogen atmosphere. After stirring for 5 h at room temperature a small amount of aminopropylmethylsiloxane-dimethylsiloxane copolymer AMS-162 (0.500 g) was added in order to react with excess NHS-activated starting material and the stirring was continued for 15 min. The solvent was removed *in vacuo*. Silica gel chromatography

using methylene chloride/methanol (95:5) yielded the product as a clear pale yellow solid (1.136 g, 55 %). TLC in CH_2Cl_2 / MeOH (95:5): $R_{f\,(product)}$ = 0.08 – 0.24, $R_{f\,(NHS\text{-}OH)}$ = 0.02, $R_{f\,(DMS\text{-}A15)}$ = 0.00, $R_{f\,(AMS\text{-}162\text{-}NTA\text{-}Bn\text{-}ester)}$ = 0.00.

^{1}H-NMR ($CDCl_3$, 200.13 MHz) δ 7.31 (m, 30H, 6 x Ph), 6.21 (s, br, 4H, N*H*), 5.06 (m, 12H, CH_2Ph), 3.67 (s, 8H, 4 x NCH_2), 3.47 (t, 2H, J = 7.3 Hz, 2 x NC*H*), 3.16 (m, 8H, 4 x NHCH_2), 2.47 (s, 8H, 2 x O=CCH_2CH_2C=O), 1.66 (m, 4H, 2 x NCHCH_2) 1.46 (m, 12H, 2 x SiCH$_2$CH_2, 2 x NHCH$_2$CH_2CH_2), 0.50 (m, 4H, 2 x SiCH_2), 0.06 (m, ~330H, SiCH_3); ^{13}C-NMR ($CDCl_3$, 50.32 MHz) δ 172.5 (C=O), 172.3 (C=O), 172.1 (C=O), 171.2 (C=O), 135.7 (Ph), 135.6 (Ph), 128.6 (Ph), 128.3 (Ph), 128.2 (Ph), 66.4 (6 x *C*H$_2$Ph), 64.4 (2 x N*C*H), 52.8 (4 x NCH$_2$), 42.5 (2 x NHCH$_2$), 39.2 (2 x NHCH$_2$), 32.0 (2 x *C*H$_2$), 31.8 (2 x *C*H$_2$), 29.7 (2 x *C*H$_2$), 28.4 (2 x *C*H$_2$), 23.5 (2 x *C*H$_2$), 22.8 (2 x *C*H$_2$), 15.4 (2 x *C*H$_2$), 1.7 (*C*H$_3$), 1.0 (*C*H$_3$), 0.3 (*C*H$_3$), 0.1 (*C*H$_3$); FT-IR (neat): ν (cm^{-1}) 3299 (COO-H), 2964 (CH), 1746 (C=O), 1641 (N-C=O), 1550 (N-C=O), 1261 (Si-CH$_3$), 1092 (Si-O), 1021 (Si-O), 800 (Si-CH$_3$); ES-MS (+ve mode in MeOH + 1 drop 0.2 % HCOOH): doubly charged ion series with peaks from 1407 [M^{2+}, n = 18] to 2291 [M^{+}, n = 41]; triply charged ion series with peaks from 1260 [M^{3+}, n = 31] to 1851 [M^{3+}, n = 55]; GPC: M_n = 2137, M_w = 2398, PD = 1.12.

N^{α},N^{α}-Bis(carboxymethyl)-L-lysine-terminated polydimethylsiloxane DMS-A15 [NTA-DMS-A15].

N^{α},N^{α}-Bis(carboxymethyl)-L-lysine tribenzyl ester-terminated polydimethylsiloxane DMS-A15 (0.547 g, 0.1 mmol) was dissolved in dry 1,2-dimethoxyethane (25 mL), 10% palladium on charcoal (a spatula tip) was added, and hydrogenation at room temperature

and normal pressure was allowed to proceed for 8 h. The completion of the reaction was shown by the disappearance of the starting material as checked by thin layer chromatography using methylene chloride / methanol (93 : 7). The catalyst was removed by filtration through a Celite pad and the solvent was removed *in vacuo* yielding the product as a pale yellow clear solid (0.397 g, 0.1 mmol, 95.4 %).

^{1}H-NMR (CD_3OD, 200.13 MHz) δ 3.62 (s, 8H, 4 x NCH_2), 3.49 (t, 2H, J = 7.0 Hz, 2 x NCH), 3.13 (m, 8H, 4 x NHCH_2), 2.69 (s, 8H, 2 x O=CCH_2CH_2C=O), 1.76 (m, 4H, 2 x NCHCH_2), 1.52 (m, 12H, 2 x SiCH$_2$CH_2, 2 x NHCH$_2$CH_2CH_2), 0.59 (m, 4H, 2 x SiCH_2), 0.09 (m, ~360H, SiCH_3); ^{13}C-NMR (CD_3OD, 50.32 MHz) δ 175.8 (C=O), 174.6 (C=O), 66.6 (2 x NCH), 55.3 (4 x NCH_2), 43.6 (2 x NHCH_2), 40.1 (2 x NHCH_2), 32.5 (4 x CH_2), 30.7 (2 x CH_2), 29.9 (2 x CH_2), 24.7 (2 x CH_2), 24.4 (2 x CH_2), 16.4 (2 x CH_2), 1.5 (CH_3), 0.4 (CH_3); FT-IR (neat): ν (cm^{-1}) 3290 (COO-H), 2964 (CH), 1729 (C=O), 1642 (N-C=O), 1261 (Si-CH$_3$), 1091 (Si-O), 1020 (Si-O), 800 (Si-CH$_3$); ES-MS (-ve mode in CH_2Cl_2 / MeOH): doubly charged ion series with peaks from 1096 [M^{2-}, n = 17] to 2392 [M^{2-}, n = 52]; triply charged ion series with peaks from 756.5 [M^{3-}, n = 18] to 1545 [M^{3-}, n = 51].

N^{α},N^{α}-Bis(carboxymethyl)-L-lysine tribenzyl ester-terminated polydimethylsiloxane DMS-A21 [NTA-DMS-A21-Bn-Ester].

Aminopropyl-terminated poly-dimethylsiloxane DMS-A21 (1.125 g, 0.2 mmol) was added to a stirred solution of N^{α},N^{α}-bis(carboxymethyl)-N^{ε}-succinimidylsuccinyl-L-lysine tribenzyl ester (0.365 g, 0.5 mmol) in dry methylene chloride (60 mL) under a nitrogen atmosphere. After stirring for 5 h at room temperature a small amount of

aminopropylmethylsiloxane-dimethylsiloxane copolymer AMS-162 (0.500 g) was added in order to react with excess NHS-activated starting material and the stirring was continued for 15 min. The solvent is removed *in vacuo*. Silica gel chromatography using methylene chloride/methanol (95:5) yielded the product as a clear pale yellow solid (1.010 g, 0.17 mmol, 70 %). TLC in CH_2Cl_2 / MeOH (95:5): $R_{f\,(product)}$ = 0.07 – 0.29, $R_{f\,(NHS\text{-}OH)}$ = 0.02, $R_{f\,(DMS\text{-}A15)}$ = 0.00, $R_{f\,(AMS\text{-}162\text{-}NTA\text{-}Bn\text{-}ester)}$ = 0.00.

^{1}H-NMR ($CDCl_3$, 200.13 MHz) δ 7.30 (m, 30H, 6 x Ph), 6.15 (s, br, 4H, N*H*), 5.07 (m, 12H, CH_2Ph), 3.67 (s, 8H, 4 x NCH_2), 3.45 (t, 2H, *J* = 7.1 Hz, 2 x NC*H*), 3.16 (m, 8H, 4 x NHCH_2), 2.47 (s, 8H, 2 x O=CCH_2CH_2C=O), 1.66 (m, 4H, 2 x NCHCH_2) 1.44 (m, 12H, 2 x SiCH$_2$CH_2, 2 x NHCH$_2$CH_2CH_2), 0.50 (m, 4H, 2 x SiCH_2), 0.06 (m, ~490H, SiCH_3); ^{13}C-NMR ($CDCl_3$, 50.32 MHz) δ 172.5 (C=O), 172.3 (C=O), 171.2 (C=O), 135.7 (Ph), 135.6 (Ph), 128.6 (Ph), 128.3 (Ph), 128.1 (Ph), 66.4 (6 x *C*H$_2$Ph), 64.4 (2 x NCH), 52.8 (4 x NCH_2), 42.6 (2 x NHCH_2), 39.2 (2 x NHCH_2), 31.7 (4 x *C*H$_2$), 29.7 (2 x *C*H$_2$), 28.3 (2 x *C*H$_2$), 23.4 (2 x *C*H$_2$), 22.8 (2 x *C*H$_2$), 15.4 (2 x *C*H$_2$), 1.7 (*C*H$_3$), 1.0 (*C*H$_3$), 0.3 (*C*H$_3$), 0.1 (*C*H$_3$); ^{29}Si-NMR (CH_2Cl_2, 59.63MHz, TMS ext. std): δ 7.10, -19.19, -22.03, -22.76; FT-IR (neat): ν (cm^{-1}) 3299 (COO-H), 2964 (CH), 1746 (C=O), 1642 (N-C=O), 1550 (N-C=O), 1261 (Si-CH$_3$), 1092 (Si-O), 1021 (Si-O), 801 (Si-CH$_3$); ES-MS (+ve mode in MeOH + 1 drop 0.2 % HCOOH): doubly charged ion series with peaks from 1407 [M^{2+}, n = 18] to 2291 [M^{+}, n = 41]; triply charged ion series with peaks from 1260 [M^{3+}, n = 31] to 1851 [M^{3+}, n = 55]; GPC: M_n = 1922, M_w = 2813, PD = 1.46.

N^{α},N^{α}-Bis(carboxymethyl)-L-lysine-terminated polydimethylsiloxane DMS-A21 [NTA-DMS-A21].

N^{α},N^{α}-Bis(carboxymethyl)-L-lysine tribenzyl ester-terminated polydimethylsiloxane DMS-A15 (1.010 g, 0.2 mmol) was dissolved in dry 1,2-dimethoxyethane (25 mL), 10% palladium on charcoal (a spatula tip) was added, and hydrogenation at room temperature and normal pressure was allowed to proceed for 8 h. The completion of the reaction was shown by the disappearance of the starting material as checked by thin layer chromatography using methylene chloride / methanol (93:7). The catalyst was removed by filtration through a Celite pad and the solvent was removed *in vacuo* yielding the product as a pale yellow clear solid (0.832 g, 0.2 mmol, 93%).

^{1}H-NMR ($CDCl_3$ / CD_3OD (1:1), 200.13 MHz) δ 3.64 (s, 8H, 4 x NCH_2), 3.48 (m, 2H, 2 x NC*H*), 3.14 (m, 8H, 4 x NHCH_2), 2.44 (s, 8H, 2 x O=CCH_2CH_2C=O), 1.68 (m, 4H, 2 x NCHCH_2), 1.49 (m, 12H, 2 x $SiCH_2CH_2$, 2 x $NHCH_2CH_2CH_2$), 0.52 (m, 4H, 2 x SiCH_2), 0.06 (m, ~490H, SiCH_3); ^{13}C-NMR ($CDCl_3$ / CD_3OD (1:1), 50.32 MHz) δ 174.6 (C=O), 173.2 (C=O), 66.6 (2 x NCH), 52.5 (4 x NCH_2), 41.6 (2 x $NHCH_2$), 38.1 (2 x $NHCH_2$), 30.7 (2 x CH_2), 28.8 (2 x CH_2), 28.5 (2 x CH_2), 27.8 (CH_2), 22.4 (2x CH_2), 22.2 (2x CH_2), 14.5 (2x CH_2), -0.1 (CH_3), -1.2 (CH_3), -3.0 (CH_3); FT-IR (neat): ν (cm^{-1}) 3300 (COO-H), 2963 (CH), 1730 (C=O), 1643 (N-C=O), 1549 (N-C=O), 1261 ($Si-CH_3$), 1091 (Si-O), 1020 (Si-O), 798 ($Si-CH_3$); ES-MS (-ve mode in CH_2Cl_2 / MeOH): doubly charged ion series with peaks from 1096 [M^{2-}, n = 17] to 2249 [M^{2-}, n = 48].

N^{α},N^{α}-Bis(carboxymethyl)-L-lysine tribenzyl ester pendant polydimethyl-siloxane AMS-132 [NTA-AMS-132-Bn-Ester].

Aminopropylmethylsiloxane-dimethylsiloxane copolymer AMS-132 (1.377 g, 0.3 mmol, 0.46 meq NH_2) was added to a stirred solution of N^{α},N^{α}-bis(carboxymethyl)-N^{ϵ}-succinimidylsuccinyl-L-lysine tribenzyl ester (0.403 g, 0.6 mmol) in dry methylene chloride (50 mL) under a nitrogen atmosphere. After stirring for 5 h at room temperature a small amount of aminopropylmethylsiloxane-dimethylsiloxane copolymer AMS-162 (0.2 g) was added in order to react with excess NHS-activated starting material and the stirring was continued for 15 min. The solvent was removed *in vacuo*. Silica gel chromatography using methylene chloride/methanol (95:5) yielded the product as a clear pale yellow solid (0.783 g, 0.15 mmol, 54%). TLC in CH_2Cl_2 / MeOH (95:5): $R_{f\,(product)}$ = 0.10 – 0.22, $R_{f\,(AMS\text{-}132)} = 0$.

^{1}H-NMR ($CDCl_3$, 200.13 MHz) δ 7.30 (m, 15H, 3 x Ph), 6.10 (s, br, 2H, N*H*), 5.06 (m, 6H, CH_2Ph), 3.67 (s, 4H, 2 x NCH_2), 3.44 (t, 1H, J = 6.9 Hz, NC*H*), 3.19 (m, 4H, 2 x NHCH_2), 2.46 (s, 4H, O=CCH_2CH_2C=O), 1.65 (m, 2H, NCHCH_2) 1.40 (m, 6H, SiCH$_2$CH_2, NHCH$_2$CH_2CH_2), 0.47 (m, 2 H, SiCH_2), 0.05 (m, ~205H, SiCH_3); ^{13}C-NMR ($CDCl_3$, 50.32 MHz) δ 172.5 (C=O), 171.2 (C=O), 135.7 (Ph), 128.6 (Ph), 128.3 (Ph), 128.2 (Ph), 66.4 (3 x CH_2Ph), 64.5 (NCH), 52.8 (2 x NCH_2), 42.4 (NHCH_2), 39.2 (NHCH_2), 31.8 (2 x CH_2), 29.7 (CH_2), 28.4 (CH_2), 23.5 (CH_2), 22.8 (CH_2), 15.4 (CH_2), 1.7 (CH_3), 1.0 (CH_3), 0.3 (CH_3); FT-IR (neat): ν (cm^{-1}) 3300 (COO-H), 2965 (CH), 1747 (C=O), 1642 (N-C=O), 1550 (N-C=O), 1262 (Si-CH_3), 1091 (Si-O), 1021 (Si-O), 801

(Si-CH_3); GPC: M_n = 3311, M_w = 5566, PD = 1.68 (from ^{1}H-NMR, MW = 5251, n = 53, m = 1.63, calculated for 2.5% NH_2).

N^{α},N^{α}-Bis(carboxymethyl)-L-lysine pendant polydimethylsiloxane AMS-132 [NTA-AMS-132].

N^{α},N^{α}-Bis(carboxymethyl)-L-lysine tribenzyl ester pendant polydimethylsiloxane AMS-132 (0.783 g, 0.15 mmol) was dissolved in dry 1,2-dimethoxyethane (25 mL), 10% palladium on charcoal (a spatula tip) was added, and hydrogenation at room temperature and normal pressure was allowed to proceed for 8 h. The completion of the reaction was shown by the disappearance of the starting material as checked by thin layer chromatography using methylene chloride/methanol (93:7). The catalyst was removed by filtration through a Celite pad. A thick gel-like material separated upon solvent removal *in vacuo*. This gel was dissolved in methylene chloride (20 mL) and water (20 mL) was added to this solution with stirring. The product precipitated upon methylene chloride removal *in vacuo*. The precipitation was repeated with 20 mL CH_2Cl_2 and 20 mL water. After drying *in vacuo* (< 0.1 mm Hg) the final product was obtained as a white solid (0.332 g, 0.07 mmol, 47%).

^{1}H-NMR ($CDCl_3$ / CD_3OD (1:1), 200.13 MHz) δ 3.59 (m, 4H, 2 x NCH_2), 3.48 (m, 1H, NCH), 3.13 (m, 4H, 2 x NHCH_2), 2.45 (s, 4H, O=CCH_2CH_2C=O), 1.70 – 1.40 (m, 8H, NCHCH_2 + SiCH$_2$CH_2 + NHCH$_2$CH_2CH_2), 0.53 (m, 2H, SiCH_2), 0.04 (m, ~367H, SiCH_3); ^{13}C-NMR ($CDCl_3$ / CD_3OD (1:1), 50.32 MHz) δ 173.8 (C=O), 172.3 (C=O), 64.6 (NCH), 53.4 (2 x NCH_2), 41.3 (NHCH_2), 38.0 (NHCH_2), 30.3 (2 x CH_2), 28.5 (2 x CH_2), 27.7 (CH_2), 22.1 (CH_2), 13.6 (CH_2), -0.2 (CH_3), -0.5 (CH_3); FT-IR (neat): ν (cm^{-1})

3337 (COO-H), 2964 (CH), 1728 (C=O), 1644 (N-C=O), 1261 (Si-CH_3), 1092 (Si-O), 1021 (Si-O), 800 (Si-CH_3) (from ^{1}H-NMR, MW = 4838, n = 53, m = 1.63, calculated for 2.5% NH_2).

N^{α},N^{α}-Bis(carboxymethyl)-L-lysine tribenzyl ester pendant polydimethylsiloxane AMS-152 [NTA-AMS-152-Bn-Ester].

Aminopropylmethyl-siloxane-dimethylsiloxane copolymer AMS-152 (1.233 g, 0.16 mmol, 0.72 meq NH_2) was added to a stirred solution of N^{α},N^{α}-bis(carboxymethyl)-N^{ε}-succinimidylsuccinyl-L-lysine tribenzyl ester (0.584 g, 0.8 mmol) in dry methylene chloride (50 mL) under a nitrogen atmosphere. After stirring for 5 h at room temperature a small amount of aminopropylmethylsiloxane-dimethylsiloxane copolymer AMS-162 (0.2 g) was added in order to react with excess NHS-activated starting material and the stirring was continued for 15 min. The solvent was removed *in vacuo*. Silica gel chromatography using methylene chloride / methanol (95:5) yielded the product as a clear pale yellow solid (0.604 g, 0.06 mmol, 37%). TLC in CH_2Cl_2 / MeOH (95:5): $R_{f\,(product)} = 0.08 - 0.25$, $R_{f\,(AMS\text{-}132)} = 0$.

^{1}H-NMR ($CDCl_3$, 200.13 MHz) δ 7.30 (m, 15H, 3 x Ph), 6.12 (s, br, 2H, N*H*), 5.06 (m, 6H, CH_2Ph), 3.67 (s, 4H, 2 x NCH_2), 3.44 (t, 1H, J = 7.4 Hz, NC*H*), 3.15 (m, 4H, 2 x NHCH_2), 2.46 (s, 4H, O=CCH_2CH_2C=O), 1.64 (m, 2H, NCHCH_2) 1.40 (m, 6H, SiCH$_2$CH_2, NHCH$_2$CH_2CH_2), 0.47 (m, 2 H, SiCH_2), 0.05 (m, ~175H, SiCH_3); ^{13}C-NMR ($CDCl_3$, 50.32 MHz) δ 172.5 (C=O), 171.2 (C=O), 135.7 (Ph), 128.6 (Ph), 128.3 (Ph), 128.2 (Ph), 66.4 (3 x CH_2Ph), 64.5 (NCH), 52.8 (2 x NCH_2), 42.4 (NHCH_2), 39.2 (NHCH_2), 31.9 (2 x CH_2), 29.7 (CH_2), 28.4 (CH_2), 23.2 (CH_2), 22.8 (CH_2), 14.7 (CH_2),

1.8 (CH_3), 1.0 (CH_3), 0.3 (CH_3); FT-IR (neat): ν (cm^{-1}) 3301 (COO-H), 2965 (CH), 1747 (C=O), 1642 (N-C=O), 1550 (N-C=O), 1261 (Si-CH_3), 1091 (Si-O), 1019 (Si-O), 801 (Si-CH_3); GPC: M_n = 3487, M_w = 5082, PD = 1.45 (from ^{1}H-NMR, MW = 12.300, n = 121, m = 4.35, calculated for 4.5% NH_2).

N^{α},N^{α}-Bis(carboxymethyl)-L-lysine pendant polydimethylsiloxane AMS-152 [NTA-AMS-152].

AMS-152 (0.600 g, 0.06 mmol) was dissolved in dry 1,2-dimethoxyethane (25 mL), 10% palladium on charcoal (a spatula tip) was added, and hydrogenation at room temperature and normal pressure was allowed to proceed for 8 h. The completion of the reaction was shown by the disappearance of the starting material as checked by thin layer chromatography using methylene chloride / methanol (93:7). The catalyst was removed by filtration through a Celite pad. A thick gel-like material separated upon solvent removal *in vacuo*. This gel was dissolved in methylene chloride (20 mL) and water (20 mL) was added to this solution with stirring. The product precipitated upon methylene chloride removal *in vacuo*. The precipitation was repeated with 20 mL CH_2Cl_2 and 20 mL water. After drying *in vacuo* (< 0.1 mm Hg) the final product was obtained as a white solid (0.160 g, 0.02 mmol, 33%).

^{1}H-NMR (CD_3OD, 500.13 MHz) δ 3.61 (m, 4H, 2 x NCH_2), 3.46 (m, 1H, NC*H*), 3.14 (m, 4H, 2 x NHCH_2), 2.45 (s, 4H, O=CCH_2CH_2C=O), 1.70 – 1.50 (m, 8H, NCHCH_2 + SiCH$_2$CH_2 + NHCH$_2$CH_2CH_2), 0.54 (m, 2H, SiCH_2), 0.09 (m, ~120H, SiCH_3); ^{13}C-NMR (CD_3OD, 125.76 MHz) δ 175.9 (C=O), 174.6 (C=O), 66.8 (NCH), 55.6 (NCH_2), 54.8 (NCH), 43.5 (NHCH_2), 40.1 (NHCH_2), 32.5 (CH_2), 30.7 (CH_2), 29.9 (CH_2), 28.0 (2 x

CH_2), 24.3 (CH_2), 15.8 (CH_2), 2.0 (CH_3), 1.5 (CH_3); FT-IR (neat): ν (cm^{-1}) 3303 (COO-H), 2963 (CH), 1737 (C=O), 1644 (N-C=O), 1568 (N-C=O), 1262 (Si-CH_3), 1098 (Si-O), 1023 (Si-O), 808 (Si-CH_3) (from ^{1}H-NMR, MW = 8400, n = 85, m = 4.35, calculated for 4.5% NH_2).

N^{α},N^{α}-Bis(carboxymethyl)-L-lysine tribenzyl ester pendant-polydimethylsiloxane AMS-162 [NTA-AMS-162-Bn-Ester].

Aminopropylmethyl-siloxane-dimethyl-siloxane copolymer AMS-162 (1.100 g, 0.24 mmol, 0.9 meq NH_2) was added to a stirred solution of N^{α},N^{α}-bis(carboxymethyl)-N^{ϵ}-succinimidylsuccinyl-L-lysine tribenzyl ester (0.660 g, 0.9 mmol) in dry methylene chloride (50 mL) under a nitrogen atmosphere. After stirring for 5 h at room temperature the solvent was removed *in vacuo*. Silica gel chromatography using methylene chloride/methanol (95:5) yielded the product as a clear pale yellow solid (1.200 g, 0.18 mmol, 73.8%).

^{1}H-NMR ($CDCl_3$, 200.13 MHz) δ 7.30 (m, 15H, 3 x Ph), 6.11 (s, br, 2H, N*H*), 5.06 (m, 6H, CH_2Ph), 3.67 (s, 4H, 2 x NCH_2), 3.44 (t, 1H, *J* = 7.5 Hz, NC*H*), 3.18 (m, 4H, 2 x NHCH_2), 2.46 (s, 4H, O=CCH_2CH_2C=O), 1.66 (m, 2H, NCHCH_2) 1.44 (m, 6H, SiCH$_2$CH_2, NHCH$_2$CH_2CH_2), 0.48 (m, 2 H, SiCH_2), 0.05 (m, ~86H, SiCH_3); ^{13}C-NMR ($CDCl_3$, 50.32 MHz) δ 172.5 (C=O), 172.2 (C=O), 172.1 (C=O), 171.2 (C=O), 135.7 (Ph), 135.6 (Ph), 128.5 (Ph), 128.3 (Ph), 128.2 (Ph), 66.4 (3 x CH_2Ph), 64.5 (NCH), 52.8 (2 x NCH_2), 42.4 (NHCH_2), 39.2 (NHCH_2), 31.9 (CH_2), 31.7 (CH2), 29.7 (CH_2), 28.5 (CH_2), 23.2 (CH_2), 22.8 (CH_2), 14.7 (CH_2), 1.8 (CH_3), 1.0 (CH_3), 0.5 (CH_3), -0.6 (CH3);

FT-IR (neat): ν (cm^{-1}) 3299 (COO-H), 2963 (CH), 1746 (C=O), 1642 (N-C=O), 1550 (N-C=O), 1261 (Si-CH_3), 1091 (Si-O), 1021 (Si-O), 801 (Si-CH_3); GPC: M_n = 2143, M_w = 4178, PD = 1.95 (from ^{1}H-NMR, MW = 5,900, n = 47, m = 3.7, calculated for 6.5% NH_2).

Succinyl-Terminated Polydimethylsiloxane DMS-A11 [SUCC-DMS-A11].

Succinic anydride (1.600 g, 16 mmol) and aminopropyl terminated polydimethylsiloxane DMS-A11 (7.200 g, 8 mmol) were dissolved in 200 mL dry methylene chloride and triethylamine (10 mL) was added. The solution was stirred under nitrogen at room temperature overnight. The organic phase was washed with 1M HCl (2x 150 mL) and water (4 x 150 mL). After drying over anhydrous sodium sulfate the solvent was removed *in vacuo*, yielding a pale yellow oil (8.360 g, 95 %).

^{1}H-NMR ($CDCl_3$, 200.13 MHz) δ 3.17 (q, 4H, J = 6.4 Hz, 2 x $SiOCH_2CH_2CH_2NH$), 2.60 (m, 4H, 2 x $O{=}CCH_2$), 2.50 (m, 4H, 2 x $O{=}CCH_2$), 1.48 (m, 4H, 2 x $SiOCH_2CH_2$), 0.48 (m, 4H, 2 x $SiOCH_2$), 0.03 (m, ~65H, $SiCH_3$); ^{13}C-NMR ($CDCl_3$, 50.32 MHz) δ 176.4 (2 x O-*C*=O), 172.4 (2 x NH-*C*=O), 42.7 (2 x $SiOCH_2CH_2CH_2NH$), 30.7 (2 x $OC(O)CH_2$), 29.9 (2 x $NC(O)CH_2$), 23.3 (2 x $SiOCH_2CH_2$), 15.3 (2 x $SiOCH_2$), 1.0 ($SiCH_3$), 0.1 ($SiCH_3$); ^{29}Si-NMR (CH_2Cl_2, 59.63MHz, TMS ext. std): δ 7.23, -19.33, -21.31, -22.04; FT-IR (neat): ν (cm^{-1}) 3305 (COO-H), 2964 (CH), 1709 (C=O), 1651 (N-C=O), 1557 (N-C=O), 1261 (Si-CH_3), 1020 (Si-O), 802 (Si-CH_3); GPC: neg. signal (RI det.): M_n = 1687, M_w = 1908, PD = 1.13; pos. signal (RI det.): M_n = 543, M_w = 562, PD = 1.03.

Succinimidyl-Terminated Succinyl-Polydimethylsiloxane DMS-A11 [SSU-DMS-A11].

To a stirred solution of succinyl terminated polydimethylsiloxane (2.870 g, 2.5 mmol) in dry methylene chloride (40 mL), which was cooled at 0°C, was added *N*-hydroxysuccinimide (0.640 g, 5.0 mmol) in dry dimethoxyethane (15 mL), followed by 1-ethyl-3-(3-diethylaminopropyl)carbodiimide hydrochloride (0.960 g, 5.0 mmol) in 25 mL dry dimethoxyethane. The solution was stirred under nitrogen for 2 h at 0°C and overnight at room temperature. The solvents were removed *in vacuo* and the solid obtained was dissolved in 60 mL methylene chloride. The organic phase was washed with 25 mL 1N HCl, 25 mL water, 25 mL 1N $NaHCO_3$, 3x 25 mL water. After drying over anhydrous Na_2SO_4 the solvent was removed *in vacuo*, yielding a clear colorless oil (3.200 g, 94%). The product was immediately used for the next step.

^{1}H-NMR ($CDCl_3$, 200.13 MHz) δ 3.18 (q, 4H, J = 4.4 Hz, 2 x $SiCH_2CH_2CH_2NH$), 2.95 (t, 4H, J = 4.8 Hz, 2 x NHS-OC(O)CH_2), 2.79 (s, 8H, 2 x NHS), 2.54 (t, 4H, J = 4.8 Hz, 2 x NC(O)CH_2), 1.49 (m, 4H, 2 x $SiCH_2CH_2$), 0.49 (m, 4H, 2 x $SiCH_2$), 0.04 (m, 65H, $SiCH_3$); ^{13}C-NMR ($CDCl_3$, 50.32 MHz) δ 169.7 (2 x O-*C*=O), 168.9 (4 x NHS-*C*=O), 168.2 (2 x N-*C*=O), 42.6 (2 x $SiCH_2CH_2CH_2NH$), 30.9 (2 x NHS-OC(O)CH_2), 28.1 (4 x NC(O)CH_2), 25.5 (4 x NHS), 23.4 (2 x $SiCH_2CH_2$), 15.3 (2 x $SiCH_2$), 1.0 (silicone); FT-IR (neat): ν (cm^{-1}) 3305 (COO-H), 2964 (CH), 1709 (C=O), 1651 (C=O), 1261 (Si-CH_3), 1020 (Si-O) 802 (Si-CH_3).

NTA-DMS-A11 (Route 1).

Succinimidyl-terminated succinylpolydimethyl-siloxane DMS-A11 (0.830 g, 0.7 mmol) dissolved in 1,2-dimethoxyethane (15 mL) was vigorously stirred overnight with N^{α},N^{α}-bis(carboxymethyl)-L-lysine sodium salt (0.510 g, 1.5 mmol) dissolved in water (5 mL). The two layers were separated; the bottom aqueous layer was first evaporated and the solid was purified by dialysis against deionized water using a Spectrapor membrane with a MWCO 500. Lyophilization yielded a white solid (0.172 g, 13.5%).

^{1}H-NMR (CD_3OD, 200.13 MHz) δ 4.14 (s, 8H, 4 x CH_2CO_2H), 4.01 (m, 2H, 2x CHCO$_2$H), 3.64 (m, 8H, 2 x NHCH_2), 2.95 (s, 8H, 2 x O=CCH_2CH_2C=O), 2.24 – 2.00 (m, 16H, 2 x NHCH$_2$CH_2CH_2CH_2, 2 x SiCH$_2$CH_2), 1.06 (m, 4H, 2 x SiCH_2), 0.58 (m, 65H, Si-CH$_3$); ^{13}C-NMR (CD_3OD, 50.32 MHz) δ 175.7 (6 x CO$_2$H), 174.6 (4 x NC=O), 66.6 (2 x CHCO$_2$H), 55.3 (4 x CH$_2$CO$_2$H), 43.6 (2 x NCH$_2$), 40.1 (2 x NCH$_2$), 32.4 (4 x NC(O)CH$_2$), 30.7 (2 x NCH$_2$CH$_2$CH$_2$$CH_2$), 29.9 (2 x NCH$_2$$CH_2$), 24.7 (2 x NHCH$_2CH_2$$CH_2$), 24.4 (2 x SiCH$_2$$CH_2$), 16.4 (2 x Si$CH_2$), 1.4 (silicone), 0.3 (silicone).

Succinyl-Terminated Polydimethylsiloxane DMS-A15 [SUCC-DMS-A15].

Succinic anydride (2.110 g, 21.0 mmol) and aminopropyl-terminated polydimethylsiloxane DMS-A11 (30.000 g, 10.0 mmol) were dissolved in 700 mL dry methylene chloride under a nitrogen atmosphere and dry triethylamine (10 mL) was added. The solution was stirred under nitrogen at room temperature overnight. The organic phase was washed with 1M HCl (2 x 150 mL) and water (4 x 150 mL). After drying over anhydrous sodium sulfate the solvent was removed *in vacuo*, yielding a pale yellow oil (30.780 g, 95%).

^{1}H-NMR ($CDCl_3$, 200.13 MHz) δ 3.22 (q, 4H, J = 6.4 Hz, 2 x $SiCH_2CH_2CH_2NH$), 2.67 (m, 4H, 2 x $O{=}CCH_2$), 2.49 (m, 4H, 2 x $O{=}CCH_2$), 1.52 (m, 4H, 2 x $SiCH_2CH_2$), 0.50 (m, 4H, 2 x $SiCH_2$), 0.05 (m, ~256H, $SiCH_3$); ^{13}C-NMR ($CDCl_3$, 50.32 MHz) δ 172.4 (4 x $C{=}O$), 42.7 (2 x $SiCH_2CH_2CH_2NH$), 30.7 (2 x $OC(O)CH_2$), 30.0 (2 x $NC(O)CH_2$), 23.3 (2 x $SiCH_2CH_2$), 15.3 (2 x $SiCH_2$), 1.8 ($SiCH_3$), 1.0 ($SiCH_3$), 0.1 ($SiCH_3$); FT-IR (neat): ν (cm^{-1}) 3300 (COO-H), 2965 (CH), 1713 (C=O), 1652 (N-C=O), 1557 (N-C=O), 1266 ($Si\text{-}CH_3$), 1005 (Si-O); ES-MS (-ve mode in CH_2Cl_2 / MeOH): doubly charged ion series with peaks from 297 [M^{2-}, n = 2] to 1261 [M^{2-}, n = 28]; GPC: M_n = 1185, M_w = 3552, PD = 3.0 (from ^{1}H-NMR, MW = 3,408, n = 40-41, based on end-group analysis).

Succinyl-Terminated Polydimethylsiloxane DMS-A21 [SUCC-DMS-A21].

Succinic anydride (1.050 g, 10.5 mmol) and aminopropyl-terminated polydimethylsiloxane DMS-A21 (25.000 g, 5.0 mmol) were dissolved in 700 mL dry methylene chloride under nitrogen atmosphere and dry triethylamine (7 mL) was added. The solution was stirred under nitrogen at room temperature overnight. The organic phase was washed with 1M HCl (2x 110 mL) and deionized water (4x 110 mL). After drying over anhydrous sodium sulfate the solvent was removed *in vacuo*, yielding a pale yellow oil (25.860 g, 5.0 mmol, 95 %).

^{1}H-NMR ($CDCl_3$, 200.13 MHz) δ 3.23 (q, 4H, J = 6.7 Hz, 2 x $SiCH_2CH_2CH_2NH$), 2.68 (m, 4H, 2 x $O{=}CCH_2$), 2.49 (m, 4H, 2 x $O{=}CCH_2$), 1.52 (m, 4H, 2 x $SiCH_2CH_2$), 0.51 (m, 4H, 2 x $SiCH_2$), 0.05 (m, ~422H, $SiCH_3$); ^{13}C-NMR ($CDCl_3$, 50.32 MHz) δ 175.3 (2 x $C{=}O$), 172.4 (2 x $C{=}O$), 42.8 (2 x $SiCH_2CH_2CH_2NH$), 30.8 (2 x $OC(O)CH_2$), 30.0 (2 x $NC(O)CH_2$), 23.4 (2 x $SiCH_2CH_2$), 15.4 (2 x $SiCH_2$), 1.8 ($SiCH_3$), 1.0 ($SiCH_3$), 0.1

($SiCH_3$); ^{29}Si-NMR (CH_2Cl_2, 59.63MHz, TMS ext. std): δ 7.16, -21.33, -21.47, -22.14; FT-IR (neat): ν (cm^{-1}) 3300 (COO-H), 2965 (CH), 1715 (C=O), 1651 (N-C=O), 1558 (N-C=O), 1261 (Si-CH_3), 1096 (Si-O), 1024 (Si-O), 801 (Si-CH_3); GPC: M_n = 1369, M_w = 5746, PD = 4.19 (from ^{1}H-NMR, MW = 5,500, n = 68-69, based on end-group analysis).

Succinyl-Pendant Polydimethylsiloxane AMS-132 [SUCC-AMS-132].

Succinic anydride (1.340 g, 13.4 mmol) and aminopropylmethylsiloxane-dimethylsiloxane copolymer AMS-132 (30.000 g, 6.7 mmol, 13.4 meq NH_2) were dissolved in 700 mL dry methylene chloride under a nitrogen atmosphere and dry triethylamine (9.6 mL) was added. The solution was stirred under nitrogen at room temperature overnight. The organic phase was washed with 1M HCl (2 x 50 mL) and deionized water (4 x 90 mL). After drying over anhydrous sodium sulfate, the solvent was removed *in vacuo*, yielding a pale yellow oil (26.850 g, 5.8 mmol, 85.7%).

^{1}H-NMR ($CDCl_3$, 200.13 MHz) δ 3.23 (q, 4H, J = 6.7 Hz, 2 x $SiCH_2CH_2CH_2NH$), 2.64 (m, 4H, 2 x O=CCH_2), 2.50 (m, 4H, 2 x O=CCH_2), 1.52 (m, 4H, 2 x $SiCH_2CH_2$), 0.51 (m, 4H, 2 x $SiCH_2$), 0.05 (m, ~364H, $SiCH_3$); ^{29}Si-NMR (CH_2Cl_2, 59.63MHz, TMS ext. std): δ 6.99, -19.41, -21.65, -21.82, -22.13, -22.45; FT-IR (neat): ν (cm^{-1}) 3300 (COO-H), 2965 (CH), 1716 (C=O), 1648 (N-C=O), 1261 (Si-CH_3), 1090 (Si-O), 1021 (Si-O), 801 (Si-CH_3); GPC: M_n = 1348, M_w = 5101, PD = 1.62 (from ^{1}H-NMR, MW = 7,700, n = 95, m = 1.63, calculated for 2.5% NH_2).

Succinyl-Pendant Polydimethylsiloxane AMS-152 [SUCC-AMS-152].

Succinic anydride (2.250 g, 22.5 mmol) and aminopropylmethylsiloxane-dimethylsiloxane copolymer AMS-152 (35.000 g, 5 mmol, 22.5 meq NH_2) were

dissolved in 700 mL dry methylene chloride under a nitrogen atmosphere and dry triethylamine (16.7 mL) was added. The solution was stirred under nitrogen at room temperature overnight. The organic phase was washed with 1M HCl (2 x 90 mL) and deionized water (4 x 150 mL). After drying over anhydrous sodium sulfate, the solvent was removed *in vacuo*, to yield a pale yellow oil (24.690 g, 3.3 mmol, 66.%).

^{1}H-NMR ($CDCl_3$, 200.13 MHz) δ 3.20 (m, 4H, 2 x $SiCH_2CH_2CH_2NH$), 2.63 (m, 4H, 2 x $O{=}CCH_2$), 2.48 (m, 4H, 2 x $O{=}CCH_2$), 1.52 (m, 4H, 2 x $SiCH_2CH_2$), 0.48 (m, 4H, 2 x $SiCH_2$), 0.05 (m, ~163H, $SiCH_3$); ^{13}C-NMR ($CDCl_3$, 50.32 MHz) δ 176.4 (2 x $C{=}O$), 172.4 (2 x $C{=}O$), 42.5 (2 x $SiCH_2CH_2CH_2NH$), 30.7 (2 x $OC(O)CH_2$), 30.0 (2 x $NC(O)CH_2$), 23.0 (2 x $SiCH_2CH_2$), 14.5 (2 x $SiCH_2$), 1.8 ($SiCH_3$), 1.0 ($SiCH_3$), 0.3 ($SiCH_3$), -0.5 ($SiCH_3$); ^{29}Si-NMR (CH_2Cl_2, 59.63MHz, TMS ext. std): δ 6.97, -19.44, -21.68, -22.16, -22.86; FT-IR (neat): ν (cm^{-1}) 3304 (COO-H), 2965 (CH), 1715 (C=O), 1654 (N-C=O), 1558 (N-C=O), 1262 (Si-CH_3), 1094 (Si-O), 1022 (Si-O), 801 (Si-CH_3); GPC: M_n = 1200, M_w = 3162, PD = 2.63 (from ^{1}H-NMR, MW = 10,600, n = 116, m = 4.5, calculated for 4.5% NH_2).

Succinyl-Pendant Polydimethylsiloxane AMS-162 [SUCC-AMS-162].

Succinic anydride (2.710 g, 27.0 mmol) and aminopropylmethylsiloxane-dimethylsiloxane copolymer AMS-162 (30.000 g, 7.5 mmol, 27 meq NH_2) were dissolved in 700 mL dry methylene chloride under a nitrogen atmosphere and dry triethylamine (18.1 mL) was added. The solution was stirred under nitrogen at room temperature overnight. The organic phase was washed with 1M HCl (2 x 100 mL) and

deionized water (4 x 160 mL). After drying over anhydrous sodium sulfate, the solvent was removed *in vacuo*, to yield a pale yellow oil (22.730 g, 5.2 mmol, 70%). ^{1}H-NMR ($CDCl_3$, 200.13 MHz) δ 3.20 (m, 4H, 2 x $SiCH_2CH_2CH_2NH$), 2.63 (m, 4H, 2 x $O{=}CCH_2$), 2.49 (m, 4H, 2 x $O{=}CCH_2$), 1.53 (m, 4H, 2 x $SiCH_2CH_2$), 0.48 (m, 4H, 2 x $SiCH_2$), 0.05 (m, ~82H, $SiCH_3$); ^{13}C-NMR ($CDCl_3$, 50.32 MHz) δ 176.2 (2 x $C{=}O$), 172.5 (2 x $C{=}O$), 42.5 (2 x $SiCH_2CH_2CH_2NH$), 30.7 (2 x $OC(O)CH_2$), 30.0 (2 x $NC(O)CH_2$), 23.0 (2 x $SiCH_2CH_2$), 14.5 (2 x $SiCH_2$), 1.7 ($SiCH_3$), 1.0 ($SiCH_3$), 0.3 ($SiCH_3$), -0.6 ($SiCH_3$); ^{29}Si-NMR (CH_2Cl_2, 59.63MHz, TMS ext. std): δ 6.98, -19.42, -21.66, -22.15, -22.52; FT-IR (neat): ν (cm^{-1}) 3310 (COO-H), 2959 (CH), 1711 (C=O), 1654 (N-C=O), 1553 (N-C=O), 1261 (Si-CH_3), 1091 (Si-O), 1021 (Si-O), 801 (Si-CH_3); GPC: M_n = 785, M_w = 1709, PD = 2.18 (from ^{1}H-NMR, MW = 5,100, n = 44-45, m = 3.7, calculated for 6.5% NH_2).

3-(Acetamido)propyl-Functionalized Polydimethylsiloxanes – General Procedure. Acetic anhydride (25 μL, 27 mg, 0.24 mmol) and aminopropyl-silicone (0.24 meq NH_2) were dissolved in dry methylene chloride (2 mL) under a nitrogen atmosphere and dry triethylamine (38 μL) was added. The solution was stirred at room temperature overnight. The organic phase was washed with 10% aqueous $NaHSO_4$ (2 mL), deionized water (2 mL), sat. aqueous $NaHCO_3$ (2 mL), and deionized water (3x 2 mL). After drying over anhydrous sodium sulfate the solvent was removed *in vacuo* (< 0.1 mm Hg), yielding a pale yellow oil (70 – 80%).

Acetamidopropyl-DMS-A11 [DMS-A11-ACE].

^{1}H NMR ($CDCl_3$, 200.13 MHz) δ 3.18 (q, 4H, J = 6.3 Hz, 2 x $SiCH_2CH_2CH_2NH$), 1.94 (s, 6H, 2 x $O{=}CCH_3$), 1.49 (m, 4H, 2 x $SiCH_2CH_2$), 0.49 (m, 4H, 2 x $SiCH_2$), 0.03 (m, $SiCH_3$); ^{13}C-NMR ($CDCl_3$, 50.32 MHz) δ 169.9 (2 x $C{=}O$), 42.5 (2 x $SiCH_2CH_2CH_2NH$), 23.5 (2 x $O{=}CCH_3$), 23.2 (2 x $SiCH_2CH_2$), 15.4 (2 x $SiCH_2$), 1.7 ($SiCH_3$), 1.0 ($SiCH_3$), 0.3 ($SiCH_3$), 0.1 ($SiCH_3$); FT-IR (neat): ν (cm^{-1}) 3291 (NH), 2963 (CH), 1653 (N-C=O), 1560 (N-C=O), 1261 (Si-CH_3), 1091 (Si-O), 1027 (Si-O), 801 (Si-CH_3); GPC: M_n = 447, M_w = 920, PD = 2.06 (from ^{1}H-NMR, MW = 990, n = 8).

Acetamidopropyl-DMS-A15 [DMS-A15-ACE].

(Assignments as for (3-acetamidopropyl)-DMS-A11) ^{1}H-NMR ($CDCl_3$, 200.13 MHz) δ 3.19, 1.94, 1.50, 0.51, 0.03; ^{13}C-NMR ($CDCl_3$, 50.32 MHz) δ 169.9, 42.5, 23.5, 23.3, 15.4, 1.7, 1.0, 0.3, 0.1; FT-IR (neat): ν (cm^{-1}) 3295, 2964, 1654, 1561, 1261, 1091, 1021, 800; GPC: M_n = 1817, M_w = 3727, PD = 2.05 (from ^{1}H-NMR, MW = 3,100, n = 37).

Acetamidopropyl-DMS-A21 [DMS-A21-ACE].

(Assignments as for (3-acetamidopropyl)-DMS-A11) ^{1}H-NMR ($CDCl_3$, 200.13 MHz) δ 3.21, 1.95, 1.51, 0.51, 0.05; ^{13}C-NMR ($CDCl_3$, 50.32 MHz) δ 169.9, 42.5, 23.5, 23.3, 15.4, 1.7, 1.0, 0.3, 0.1; FT-IR (neat): ν (cm^{-1}) 3295, 2965, 1654, 1560, 1261, 1094, 1022, 801; GPC: M_n = 3465, M_w = 8527, PD = 2.46 (from ^{1}H-NMR, MW = 5,200, n = 66).

Acetamidopropyl-AMS-132 [AMS-132-ACE].

(Assignments as for (3-acetamidopropyl)-DMS-A11) ^{1}H-NMR ($CDCl_3$, 200.13 MHz) δ 3.21, 1.95, 1.54, 0.51, 0.04; ^{13}C-NMR ($CDCl_3$, 50.32 MHz) δ 169.9, 42.3, 23.2 (2 x C),

14.7, 1.7, 1.0, 0.3, -0.5; FT-IR (neat): ν (cm^{-1}) 2965, 1655, 1557, 1262, 1095, 1024, 801; GPC: M_n = 3295, M_w = 6864, PD = 2.09 (from ^{1}H-NMR, MW = 8,710, n = 112, m = 1.63, calculated for 2.5% NH_2).

Acetamidopropyl-AMS-152 [AMS-152-ACE].

(Assignments as for (3-acetamidopropyl)-DMS-A11) ^{1}H-NMR ($CDCl_3$, 200.13 MHz) δ 3.20, 1.94, 1.53, 0.49, 0.05; ^{13}C-NMR ($CDCl_3$, 50.32 MHz) δ 169.9, 42.3, 23.2 (2 x C), 14.6, 1.7, 1.0, 0.3, -0.6; FT-IR (neat): ν (cm^{-1}) 3293, 2965, 1654, 1561, 1261, 1099, 814; GPC: M_n = 3583, M_w = 7774, PD = 2.17 (from ^{1}H-NMR, MW = 7,960, n = 96, m = 4.35, calculated for 4.5% NH_2).

Acetamidopropyl-AMS-162 [AMS-162-ACE].

(Assignments as for (3-acetamidopropyl)-DMS-A11) ^{1}H-NMR ($CDCl_3$, 200.13 MHz) δ 3.19, 1.93, 1.52, 0.48, 0.04; ^{13}C-NMR ($CDCl_3$, 50.32 MHz) δ 169.8, 42.3, 23.2 (2 x C), 14.7, 1.7, 1.0, 0.3, -0.6; FT-IR (neat): ν (cm^{-1}) 3293, 2965, 1654, 1561, 1261, 1094, 1022, 801; GPC: M_n = 1583, M_w = 2801, PD = 1.77 (from ^{1}H-NMR, MW = 4,302, n = 48, m = 3.7, calculated for 6.5% NH_2).

***N*$^{\varepsilon}$-(Benzyloxycarbonyl)-*N*$^{\alpha}$,*N*$^{\alpha}$-bis(carboxymethyl)-L-lysine tri(4-nitro-benzyl) ester.**

p-Nitrobenzylchloride (15.450 g, 0.010 mol) and triethylamine (12.6 mL) were added to a will stirred suspension of *N*$^{\varepsilon}$-(benzyloxycarbonyl)-*N*$^{\alpha}$,*N*$^{\alpha}$-bis(carboxymethyl)-L-lysine (Z-NTA) (7.920 g, 0.020 mol) in ethyl acetate (150 mL) and heated to reflux overnight. Precipitated triethylammonium hydrochloride was removed by hot filtration and a small amount of methanol (6 mL) was added to the cooled filtrate. The organic phase was washed with cold water (150 mL), 1M HCl (130 mL), water (100 mL), 1M $NaHCO_3$ (130

mL), and brine (2 x 100 mL). After drying over anhydrous sodium sulfate, the solvent was removed *in vacuo*. Silica gel chromatography using hexanes / ethyl acetate (1:1) yielded the product as a clear orange oil (13.650 g, 0.017 mol, 85.2%). TLC in hexanes/ ethyl acetate (1:1), UV-det.: $R_{f\,(product)} = 0.27$, $R_{f\,(p\text{-nitrobenzylchloride})} = 0.76$, $R_{f\,(Z\text{-NTA})} = 0.00$. ^{1}H-NMR ($CDCl_3$, 200.13 MHz) δ 8.16 (m, 6H, C*H*CNO_2), 7.47 (m, 6H, 6 x C*H*CHCNO_2), 7.30 (m, 5H, Ph), 5.14 (s, 6H, 3 x C*H*$_2C_6H_4NO_2$), 5.06 (s, 2H, C*H*$_2$Ph), 3.73 (s, 4H, 2 x C*H*$_2CO_2CH_2C_6H_4NO_2$), 3.49 (t, 1H, *J* = 7.1 Hz, C*H*$CO_2CH_2C_6H_4NO_2$), 3.13 (m, 2H, NHC*H*$_2$), 1.71 (m, 2H, NCH_2CH_2), 1.47 (m, 4H, C*H*$_2$C*H*$_2$CH); ^{13}C-NMR ($CDCl_3$, 50.32 MHz) δ 172.0 (CH*C*O_2Bn), 170.7 (2 x CH_2CO_2Bn), 156.4 (NH*C*=O), 147.8 (*C*-NO_2), 142.6 (*C*CHCHCNO_2), 136.6 (Ph), 128.6 (Ph), 128.5 (Ph), 128.4 (*C*HCHCNO_2), 128.1 (Ph), 123.7 (*C*HCNO2), 66.6 (NCHCO_2), 64.9 (3 x *C*H_2Ph), 64.6 (*C*H_2Ph), 52.5 (N*C*H_2), 40.7 (NH*C*H), 29.9 (*C*H_2), 29.4 (*C*H_2), 22.9 (*C*H_2); FT-IR (neat): ν (cm^{-1}) 3405 (NH), 3083 (arom. CH), 2945 (aliph. CH), 1732 (C=O), 1607 (N-C=O), 1522 (NO_2), 1348 (NO_2); ES-MS (+ve mode in MeOH): m/z (% intensity), 802.5 (43) [M^+].

N^{α},N^{α}-Bis(carboxymethyl)-L-lysine tri(4-nitrobenzyl) ester, hydrobromide.

N^{ε}-(Benzyloxycarbonyl)-N^{α},N^{α}-bis(carboxymethyl)-L-lysine tri(4-nitrobenzyl) ester (2.000 g, 2.5 mmol) was dissolved in glacial acetic acid (5 mL). A solution of HBr in acetic acid (30 %, 2.5 mL, 12.5 mmol) was added and the reaction was continued for 25 min at room temperature. Diethyl ether (100 mL) was added and the reaction mixture was stirred vigorously for 10 min at 0°C. The precipitate obtained was separated by filtration, dissolved in acetone (5 mL), diethyl ether (100 mL) was added and vigorous stirring was

continued for 15 min at 0°C. The product separated as a white precipitate, which was filtered and dried *in vacuo* (0.971 g, 1.500 mmol, 59 %).

^{1}H NMR (CD_3OD, 200.13 MHz) δ 8.17 (d, 6H, J = 8.1 Hz, 6 x C*H*CNO_2), 7.58 (m, 6H, 6 x C*H*$CHCNO_2$), 5.22 (s, 6H, 3 x C*H*$_2$$PhNO_2$), 3.87 (s, 4H, 2 x C*H*$_2$$CO_2Bn$), 3.69 (t, 1H, *J* = 7.3 Hz, C*H*CO_2Bn), 2.88 (m, 2H, NHC*H*$_2$), 1.85 – 1.40 (m, 6H, $NCH_2CH_2CH_2CH_2$); ^{13}C NMR (CD_3OD, 50.32 MHz) δ 172.8 ($CHCO_2Bn$), 172.0 (CH_2CO_2Bn), 149.0 (*C*-NO_2), 144.7 (*C*$CHCHCNO_2$), 144.6 (*C*$CHCHCNO_2$), 129.9 (*C*$HCHCNO_2$), 129.6 (*C*$HCHCNO_2$), 124.6 (*C*HCNO2), 66.4 (NCHCO$_2$), 66.2 (2 x *C*H$_2$Ph), 65.9 (*C*H$_2$Ph), 54.0 (N*C*H$_2$), 40.5 (H_2NCH), 30.2 (*C*H$_2$), 28.0 (*C*H$_2$), 23.8 (*C*H$_2$); FT-IR (neat): ν (cm^{-1}) 2963, 1747, 1607, 1522, 1349; ES-MS (+ve mode in MeOH): m/z (% intensity), 668 (100) [M^+].

N^{α},N^{α}-Bis(carboxymethyl)-L-lysine tri(4-nitrobenzyl) ester-terminated poly dimethylsiloxane-DMS-A11.

N^{α},N^{α}-Bis(carboxymethyl)-L-lysine tri(4-nitrobenzyl) ester hydrobromide (0.829 g, 1.0 mmol) in absolute ethanol (15 mL) was added to a stirred solution of succinimidylsuccinyl terminated polydimethylsiloxane DMS-A11 (0.648 g, 0.5 mmol) and triethylamine (0.3 mL) in dry methylene chloride (20 mL) under nitrogen atmosphere. The reaction was allowed to continue at room temperature for 24 h. The solvents were removed *in vacuo* and the solid obtained was redissolved in methylene chloride (40 mL). The organic phase was washed with 1M HCl (25 mL), water (10 mL), sat. $NaHCO_3$ (25 mL), and brine (3x 25 mL). After drying over anhydrous sodium sulfate

and solvent removal *in vacuo*, the product was obtained as a clear orange solid (1.040 g, 0.4 mmol, 72%).

^{1}H-NMR ($CDCl_3$, 200.13 MHz) δ 8.17 (d, 12H, J = 8.3 Hz, 12 x C*H*CNO_2), 7.46 (d, 12H, J = 8.3 Hz, 12 x C*H*$CHCNO_2$), 5.17 (s, 12H, 6 x C*H*$_2C_6H_4NO_2$), 3.74 (s, 8H, 4 x C*H*$_2CO_2$), 3.48 (m, 2H, 2 x NC*H*CO_2Bn), 3.15 (m, 8H, 4 x NHC*H*$_2$), 2.47 (s, 8H, 2 x O=CC*H*$_2$C*H*$_2$C=O), 1.69 (m, 4H, 2 x NCH_2CH_2), 1.43 (m, 12H, 2 x $NCH_2CH_2CH_2CH_2$ + 2 x $SiCH_2CH_2$), 0.48 (m, 4H, 2 x SiC*H*$_2$), 0.04 (m, SiC*H*$_3$).

Attempt to synthesize N^{α},N^{α}-bis(carboxymethyl)-L-lysine-terminated polydimethylsiloxane-DMS-A11 by 4-nitrobenzyl ester cleavage.

N^{α},N^{α}-Bis(carboxymethyl)-L-lysine tri(4-nitrobenzyl) ester-terminated polydimethylsiloxane-DMS-A11 (1.040 g, 0.4 mmol) was dissolved in ethyl acetate (40 mL). A spatula tip of 10% palladium on charcoal was added and the hydrogenation was allowed to proceed at room temperature and normal pressure for 24 h with vigorous stirring. The catalyst was removed by filtration through a Celite pad and the solvent was removed *in vacuo*. TLC showed the presence of some *p*-nitrotoluene and some partly deprotected product. Separation by gel filtration chromatography through Toyopearl gel filtration resin using water/ ethanol (85:15) yielded a multitude of decomposition products.

6.4.2 Synthesis of Vinylsilanes and Preparation of Wood-PE Composites (Chapter 4)

Chlorodimethyl(2-phenylethyl)silane (and Chlorodimethyl(1-phenylethyl)silane). Styrene (4.6 mL, 4.166 g, 0.040 mol) was added drop-wise to a stirred mixture of

chlorodimethylsilane (5.677 g, 0.060 mol) and Karstedt's catalyst (3-4 drops) via a syringe. The mixture was stirred under a nitrogen atmosphere at room temperature for 24 h and then at 50 °C for 24 h. Distillation under reduced pressure yielded the desired product as a clear oil (9.910 g, 0.050 moles, 90%, mixture of isomers with a ratio chlorodimethyl(2-phenylethyl)silane : chlorodimethyl(1-phenylethyl)silane = 4.3 : 1). *Chlorodimethyl(2-phenylethyl)silane*: b.p. 192 °C/60 mm Hg; ^{1}H-NMR ($CDCl_3$, 200 MHz): δ 7.02-7.26 (m, 5H), 2.68 (m, 2H), 1.12 (m, 2H), 0.33 (s, 6H); ^{13}C-NMR ($CDCl_3$, 50.3 MHz): δ 143.74, 128.42, 127.85, 125.85, 29.06, 20.85, 1.65; ^{29}Si-NMR ($CDCl_3$, 59.6 MHz): δ 31.12; FT-IR (neat): ν (cm^{-1}) 3063, 3027.4, 2961.5, 2929.4, 2877.1, 1602.8, 1495.5, 1453.6, 1407.9, 1255.8, 1177.8, 1068.4, 1031.7, 846.7, 807.1, 782.8, 754.8, 698, 466.9; MS (DEI, m/z (%)): 200 (13, M^++2), 198 (32, M^+), 185(10, M^+-CH_3), 183 (22, M^+-CH_3), 155 (41), 105 (34), 104 (48), 95 (35), 93 (100), 91 (42), 77 (11); (high resolution, DEI): calculated mass for $^{12}C_{10}H_{15}SiCl$: 198.0627 amu, observed, 198.0628 amu. *Chlorodimethyl(1-phenylethyl)silane*: ^{1}H-NMR ($CDCl_3$, 200 MHz): δ 7.02-7.26 (m, 5H), 2.35 (q, 1H, J = 7.5 Hz), 1.39 (d, 3H, J = 7.5 Hz), 0.26, 0.27 (2 x s, 6H); ^{13}C-NMR ($CDCl_3$, 50.32 MHz): δ 142.70, 128.30, 127.47, 125.31, 31.62, 14.38, 0.29, -0.77; ^{29}Si-NMR ($CDCl_3$, 59.60 MHz): δ 29.89.

Dimethyl(2-phenylethyl)vinylsilane and Dimethyl(1-phenylethyl)vinylsilane). Vinylmagnesium bromide (160 mL, 1 M in hexanes, 0.160 mol) was added dropwise to a solution of dimethyl(2-phenylethyl)vinylsilane (23.760 g, 0.120 mol) in anhydrous THF (100 mL) at 0 °C via a syringe over 30 min. The reaction mixture was stirred at 0 °C for 2 h under a nitrogen atmosphere and then heated under reflux for 2 hours. The desired

product was extracted with water. The organic phase was washed with brine, filtered through a silica gel pad, and dried over anhydrous $MgSO_4$. Removal of volatile organic solvents by rotary evaporation yielded the desired products as a clear oil (13.250 g, 0.070 mol, 58%). This product was a mixture of two isomers: dimethyl(2-phenylethyl)vinylsilane : dimethyl(1-phenylethyl)vinylsilane = 4.3:1.

Dimethyl(2-phenylethyl)vinylsilane: b.p.: 231 °C; ^{1}H-NMR ($CDCl_3$, 200 MHz): δ 7.05-7.34 (m, 5H), 6.20 (dd, 1H, J = 14.7, 19.5 Hz), 6.00 (dd, 1H, J = 4.6 , 14.7 Hz), 5.73 (dd, 1H, J = 4.6, 19.5 Hz), 2.66 (m, 2H), 0.97 (m, 2H), 0.12 (s, 6H); ^{13}C-NMR ($CDCl_3$, 50.3 MHz): δ 144.99, 138.59, 131.7, 128.18, 127.72, 125.43, 29.89, 17.39,-3.57; ^{29}Si-NMR ($CDCl_3$, 59.6): δ -5.995; IR (neat): ν 3104.8, 3026.8, 2956.5, 2905.1, 2857.2, 2796.6, 1939.9, 1602.2, 1495.3, 1453.2, 1405.1, 1250.5, 1172.6, 1123.8, 1009.0, 951.2, 900.9, 837.6, 772.0, 698.7 cm^{-1}; MS(DEI, m/z(%)): 190 (3, M^+), 175 (15, M^+-$_{CH3}$), 162 (33, M^+-$CH{=}CH_2$), 147 (23), 105 (14), 91 (8), 85 (100, $^+Si(CH_3)_2CH{=}CH_2$), 71 (29), 59 (75); (high resolution, DEI): calculated mass for $^{12}C_{12}H_{18}Si$: 190.1173 amu, observed: 190.1168 amu.

Dimethyl(1-phenylethyl)vinylsilane: ^{1}H-NMR ($CDCl_3$, 200): δ 7.05-7.34 (m, 6.2H), 5.32-6.28 (3H), 2.23 (q, 1H, J= 7.5 Hz), 1.39 (d, 3H, J= 7.5 Hz), 0.03 (2 x s, 6H), 0.01; GPC: $\overline{M}_n$ 285, $\overline{M}_w$ 288, $\overline{M}_w/\overline{M}_n$ 1.009 (PS standard).

1-(Dimethylvinylsilyl)naphthalene.

n-Butyllithium (39 mL, 1.6 M in hexanes, 0.062 mol) was added dropwise to a stirred solution of 1-bromonaphthalene (10.350 g, 0.050 mol) in diethyl ether (200 mL) at 0 °C via a syringe over a 30 min period under a N_2 atmosphere. The solution was then allowed

to warm to room temperature and heated under reflux for 20 min. The solution was cooled at room temperature and chlorodimethylvinylsilane (10 mL, 8.300 g, 0.060 mol) was added drop-wise over a 30 min period. The solution was stirred for 2 h and chilled hexanes were added. LiCl was removed by vacuum filtration through sintered glass and a Celite pad. The solvents and by-products were removed by rotary evaporation. Distillation under reduced pressure yielded the desired product as a pale yellow liquid (8.050 g, 0.038 mol, 76%).

b.p. 105-108°C (0.4 mm Hg); ^{1}H-NMR ($CDCl_3$, 200 MHz): δ 8.19 (m, 1H), 7.94 (dd, 2H, J = 2.8, 9.5 Hz), 7.81 (dd, 1H, J = 1.3, 6.8 Hz), 7.54 (m, 3H), 6.58 (dd, 1H, J = 14.6, 20.1 Hz), 6.18 (dd, 1H, J = 3.7, 14.6 Hz), 5.92 (dd, 1H, J = 3.7, 20.1 Hz), 0.62 (s, 6H); ^{13}C-NMR ($CDCl_3$, 50.32 MHz): δ 138.80, 136.94, 136.16, 133.88, 133.36, 132.74, 129.97, 128.98, 128.35, 125.56, 125.32, 125.07, -1.66; MS (DEI, m/z(%)): 212(42, M^+), 197 (100, M^+-CH_3), 185 (63, M^+-$CH{=}CH_2$), 171 (35), 155 (48), 128 (18, $^+C_{10}H_8$), 85 (21, $^+Si(CH_3)_2CH{=}CH_2$), 59 (24); (high resolution, DEI): calculated mass for $^{12}C_{14}H_{16}Si$: 212.1021 amu, observed: 212.1023 amu.

4-Bromo-1-[*N*,*N*-bis(trimethylsilyl)amino]naphthalene.

n-Butyllithium (82.5 mL, 1.6 M in hexane, 0.132 mol) was added dropwise to a stirred solution of 4-bromo-1-aminonaphthalene (13.330 g, 0.060 mol) in freshly distilled THF (140 mL) at 0°C via a syringe over a period of 30 min, under a nitrogen atmosphere. The reaction was allowed to proceed for 10 min when chlorotrimethylsilane (14.340 g, 0.132 mol) was added drop-wise via a syringe over a 45 min period. The reaction mixture was heated at 50°C for 16 h. LiCl was removed by filtration through a sintered glass frit and

the solvents were removed by rotary evaporation. Distillation under reduced pressure yielded the desired product as a clear, slightly yellow oil (15.810 g, 0.043 mol, 72%). b.p.: 137-139°C/3 mm Hg; ^{1}H-NMR ($CDCl_3$, 200.1 MHz): δ 8.22-8.29 (m, 2H), 7.71 (d, 1H, J = 7.9 Hz), 7.56-7.66 (m, 2H), 6.98 (d, 1H, J = 7.9 Hz), 0.12 (s, 18H); ^{13}C-NMR ($CDCl_3$, 50.3 MHz): δ 135.49, 132.70, 129.50, 127.35, 127.03, 126.81, 125.96, 125.60 , 118.05, 1.89; ^{29}Si-NMR ($CDCl_3$, 59.60 MHz): δ 5.45; FT-IR (neat): ν 3068.4, 3045.3, 2955.5, 2897.4, 1580.0, 1513.4, 1453.9, 1373.2, 1252.7, 1225.7, 1050.1, 958.5, 870.8, 842.0, 762.5, 684.1 cm^{-1}; MS (DEI, m/z(%)): 370 (3), 369 (5), 368 (14), 367 (32), 366 (13), 365 (28, M^+), 352 (12), 350 (14, M^+-CH_3), 272 (47), 271 (100, M^+-CH_3-Br), 256 (36, M^+-2xCH_3-Br), 223 (11), 221 (13), 184 (7), 143 (8), 73 (36); (high-resolution, DEI): calculated mass for $^{12}C_{16}H_{24}N^{79}BrSi_2$, 365.0630 amu, observed, 365.0630.

1-(Dimethylvinylsilyl)-4-[*N*,*N*-bis(trimethylsilyl)amino]naphthalene.

n-Butyllithium (31.1 mL, 1.6 M in hexane, 0.050 mol) was added dropwise to a stirred solution of 4-bromo-1-[*N*,*N*-bis(trimethylsilyl)amino]naphthalene (14.000 g, 0.038 mol) in dry diethyl ether (100 mL) at 0°C via a syringe over a 30 min period, under a nitrogen atmosphere. The reaction was allowed to proceed for 1 h at 0 °C, and for 1 h at room temperature. Chlorodimethylvinylsilane (6.000 g, 0.050 mol) was added drop-wise at room temperature via a syringe over 15 min. The reaction mixture was heated under reflux for 16 h. LiCl was removed by filtration through sintered glass and the solvents were removed by rotary evaporation. Distillation under reduced pressure yielded the desired product as a viscous clear pale yellow oil (7.340 g, 0.020 mol, 50%).

b.p.: 132-134°C/0.13 mmHg; ^{1}H-NMR ($CDCl_3$, 500 MHz): δ 8.25 (m, 1H), 8.07 (m, 1 H), 7.57 (d, 1H, J = 7.2 Hz), 7.44 (m, 2H), 7.04 (d, 1H, J = 7.2 Hz), 6.49 (dd, 1H, J = 20.3, 14.6 Hz), 6.08 (dd, 1H, J = 14.6, 3.6 Hz), 5.81 (dd, 1H, J = 20.3, 3.6 Hz), 0.52 (s, 6H), 0.06 (s, 18H); ^{13}C-NMR ($CDCl_3$, 125.7 MHz): δ 146.66, 139.34, 138.33, 134.41, 133.90, 132.40, 131.69, 128.54, 125.87, 125.20, 124.57, 1.97, -1.46; ^{29}Si-NMR ($CDCl_3$, 59.6 MHz): δ -11.82, 5.52; FT-IR (neat): ν 3072.7, 3048.3, 2955.9, 2899.2, 1592.0, 1574.1, 1504.1, 1450.3, 1405.4, 1251.5, 960.9, 934.5, 878.2, 838.0, 817.9, 774.8, 759.7, 686.0, 640.8 cm^{-1}; MS (DEI, m/z(%)): 372 (26, M^++H), 371 (68, M^+), 356 (20, M^+-CH_3), 344 (17, M^+-2xCH_3), 328 (24, M^+-$CH{=}CH_2$), 298 (10, M^+-$Si(CH_3)_3$), 268 (13), 256 (100, M^+-2xCH_3-Me_2SiVi), 85 (41, $(CH_3)_2Si^+CH{=}CH_2$), 73 (40, $(CH_3)_3Si^+$), 59 (26); (high-resolution, DEI): calculated mass for $^{12}C_{20}H_{33}NSi_3$, 371.19208 amu, observed, 371.19064 amu.

General Procedure for Peroxide-Initiated Reactions (homopolymerization, grafting and crosslinking).

In a typical experiment, the reagents (for homopolymerization: vinylsilanes; for grafting reactions: squalane and vinylsilanes, for crosslinking: squalane) and the appropriate peroxide initiator (L101, L130, DCP, BOOB, or BPO) were mixed in a 5 mL reaction vial and flushed with nitrogen for 45 min. The reaction vial was immersed in a preheated oil bath (160°C for Lupersols, DCP, and BOOB, 100°C for BPO). The reaction times were chosen to be > 10 × $t_{1/2}$. The reaction mixtures were kept under a nitrogen atmosphere throughout the experiments. All reactions were done on a 0.5 → 2 g scale. The product mixtures were analysed using gel permeation chromatography, ^{1}H-, ^{13}C-

(proton decoupled and DEPT), and two-dimensional NMR techniques without separation or purification.

Similar reaction conditions were used to establish the optimal conditions for hydrogen abstraction with different alcoxide initiators in the squalane crosslinking reaction. The thermally initiated polymerization of dimethyl(2-phenylethyl)vinylsilane was also attempted in the absence of the peroxide. No polymerization was observed, based on ^{1}H-NMR and GPC analysis.

BOOB-Initiated Grafting of 1-Dimethylvinylsilyl-4-[*N*,*N*-bis(trimethylsilyl)-amino]naphthalene onto PE in 1,3,5-Trichlorobenzene.

1-Dimethylvinylsilyl-4-[*N*,*N*-bis(trimethylsilyl)amino]naphthalene was mixed with initiator (except for the case of the thermal initiation experiment, sample 1) and a small amount of 1,2,4-trichlorobenzene. This solution was added to a mixture of PE in 1,2,4-trichlorobenzene (1,3,5-TCB) at 165°C under an inert atmosphere. The reaction mixture was stirred at 165°C for 10.5 h. PE was precipitated from the mixture with acetone and then filtered. The precipitate was washed with acetone and the traces of unreacted grafting agent were removed by Soxhlet extraction with acetone for 48 h. The PE was dried under vacuum and films were cast onto glass microscope slides previously cleaned with distilled water. Acetone extracts obtained from precipitation and Soxhlet extraction were analyzed by UV spectroscopy. The PE films (after peeling from the glass) were analyzed by fluorescence spectroscopy.

The reactant ratios used in the experiments are presented in **Table 6-1**.

Table 6-1: Reactant ratios used in PE grafting experiments.

Sample	PE (g)	Vinylsilane (g)	BOOB (g)	1,3,5-TCB (mL)
1	1.000	0.100	-	10
2	1.000	0.200	0.020	75
3	2.000	0.400	0.030	25

γ-Trimethylsilyloxy-1-propene.

1,1,1,3,3,3-Hexamethyldisilazane (85.000 g, 0.530 mol) was added dropwise to a stirred mixture of allyl alcohol (58.000 g, 1.000 mol) and chlorotrimethylsilane (0.260 g, 0.002 mol) via a syringe. The mixture was stirred under a nitrogen atmosphere at room temperature for 16 h. Ammonium chloride precipitate was removed by filtration. Distillation under an inert atmosphere (N_2) yielded the desired product as a colourless liquid (102.000 g, 0.790 moles, 79%, contains 3.8% mol hexamethyldisiloxane).

b.p. 98-102 °C/760 mm Hg; ^{1}H-NMR ($CDCl_3$, 200 MHz, $CHCl_3$ std): δ 5.93 (m, 1H), 5.23 (dq, 1H, J = 17.1, 3.6, 1.8 Hz), 5.08 (dq, 1H, J = 10.3, 3.6, 1.6 Hz), 4.13 (t, 1H, J = 1.6 Hz), 4.10 (t, 1H, J = 1.6 Hz), 0.11 (s, 9H), 0.03 (s, 0.7H); ^{13}C-NMR ($CDCl_3$, 50.3 MHz, $CHCl_3$ std): δ 137.30, 114.57, 63.69, -0.42.

Chlorodimethyl-(γ-trimethylsilyloxypropyl)silane.

Chlorodimethylsilane (10.400 g, 0.110 mol) was added dropwise to a stirred solution of 3-trimethylsilyloxy-1-propene (13.000 g, 0.100 moles) and Karstedt's catalyst (5-6 drops) via a syringe. The mixture was stirred under a nitrogen atmosphere at 0°C for 2 h and at room temperature for 12 h. The chlorotrimethylsilane present after the reaction

completion was removed by vigorous bubbling of nitrogen through the reaction mixture for 2 h. The crude product was used in the synthesis of dimethyl-(3-trimethylsilyloxy-propyl)vinylsilane.

^{1}H-NMR ($CDCl_3$, 200 MHz, $CHCl_3$ std): δ 3.54 (t, 2H, J = 6.6 Hz), 1.61 (m, 2H), 0.80 (m, 2H), 0.39 (s, 6H), 0.09 (s, 9H); ^{13}C-NMR ($CDCl_3$, 50.32 MHz, $CHCl_3$ std): δ 64.64, 26.21, 14.98, 1.61, -0.49.

Dimethyl-(γ-trimethylsilyloxypropyl)vinylsilane.

Vinylmagnesium bromide (85 mL, 1M in hexanes, 0.085 mol) was added dropwise to a solution of chlorodimethyl-(3-trimethylsilyloxypropyl)silane (10.780 g, 0.048 mol) in anhydrous THF (50 mL) at 0°C over a 1 h period. The reaction mixture was stirred at room temperature for 1 h under nitrogen atmosphere, and then heated under reflux for 2 h. The reaction mixture was carefully poured over ice and extracted with THF (2×100 mL). The organic phase was washed with saturated ammonium chloride, filtered through a silica gel pad, and dried over anhydrous $MgSO_4$. Removal of the organic solvents by rotary evaporation and distillation under reduced pressure yielded the desired product as a pale yellow oil (3.300 g, 47%, contains 10% mol TMS protected product).

b.p. 80 °C/30 mm Hg). ^{1}H-NMR (DMSO-d_6, 200 MHz, DMSO int. std.) δ 6.14 (dd, 1H, J = 19.7, 4.6 Hz), 5.93 (dd, 1H, J = 14.7, 4.6 Hz), 5.66 (dd, 1H, J = 19.7, 14.7 Hz), 4.38 (t, 1H, J = 5.3 Hz), 3.30 (m, 2H), 1.39 (m, 2H), 0.48 (m, 2H), 0.03 (s, 6H); ^{13}C-NMR (Acetone-d_6, 50.32 MHz, acetone int. std.): δ 139.51, 131.57, 64.98, 27.60, 11.30, -3.74; ^{29}Si-NMR (DMSO-d_6, 59.6MHz, TMS ext. std.): δ -4.93; MS DEI, m/z, (%): 129 (4.8,

M^+-CH_3), 117 (9.6, M^+-CH_2=CH), 99 (4.8), 87 (48.8), 85 (100, $[CH_2=CHSi(CH_3)_2]^+$), 75 (47.2), 59 (31.2), 45 (12).

Wood-PE composites.

The components were mixed in a K-mixer (E5=3300 rpm), discharged at 170°C, cooled at room temperature, and ground. The composites were injection moulded in dog-bone-shaped tensile specimens using an Engel 28/82 press using the moulding conditions shown in Table 6-2.

Table 6-2: Injection moulding conditions.

Variable	Value
Injection time	9 sec
Cooling time	25 sec
Mould open time	2 sec
Ejector counter	2 sec
Nozzle temperature	65 F
Zone 1 temperature	390 F
Zone 2 temperature	390 F
Zone 3 temperature	390 F

7 References

1 M.J. Owen, in *Siloxane Polymers*, S.J. Clarson and J.A. Semlyen (eds.), PTR Prentice Hall, Englewood Cliffs, New Jersey, 1993, pp. 309 – 372.

2 M.J. Owen, *Ind. Eng. Chem. Prod. Res. Dev., 19* (1980) 97.

3 B. Gruening, G. Koerner, *Tenside Surf. Det., 26* (1989) 312.

4 J.W. Adams, in *Surface Phenomena and Additives in Water-Based Coatings and Printing Technologies*, M.K. Sharma (ed.), Plenum Press, New York, 1991, pp. 73 – 82.

5 H.F. Fink, *Tenside Surf. Det., 28* (1991) 306.

6 D. Schaefer, *Tenside Surf. Det., 27* (1990) 154.

7 S.A. Snow, L.M. Madore, *U.S.Patent 5,026,489* (1991).

8 S.A. Snow, *Langmuir, 9* (1993) 424.

9 E.R. Martin, *U.S.Patent 4,384,130* (1983).

10 W.G. Reid, *U.S.Patent 3,389,160* (1968).

11 H.-J. Kollmeier, R.-D. Langenhagen, K. Hoffmann, *U.S.Patent 4,609,750* (1986).

12 H.-J. Kollmeier, R.-D. Langenhagen, K. Hoffmann, *U.S.Patent 4,654,161* (1987).

13 B. Kanner, R.H. Pike, *U.S.Patent 3,507,897* (1970).

14 E.L. Morehouse, *U.S.Patent 3,531,417* (1970).

15 E.L. Morehouse, *U.S.Patent 3,513,183* (1970).

16 W.J. Raleigh, J.A. Campagna, M.A. Lucarelli, *U.S.Patent 5,447,997* (1995).

17 G.L. Gaines, Jr., in *Insoluble Monolayers at Liquid-Gas Interfaces*, Interscience, New York, 1966.

18 D.J. Crisp, in *Surface Phenomena in Chemistry and Biology*, J.F. Danielli, K.G.A. Pankhurst, A.C. Riddiford (eds.), Pergamon Press, New York, 1959, p. 23.

19 A.W. Adamson, A.P. Gast, *Physical Chemistry of Surfaces*, 6th edition, Wiley-Interscience, New York 1997.

20 H.W. Fox, P.W. Taylor, A. Zisman, *Ind. Eng. Chem., 39* (1947) 1401.

21 H.W. Fox, E.M. Solomon, A. Zisman, *J. Phys. Colloid Chem., 54* (1950) 723.

22 S. Granick, S.J. Clarson, T.R. Formoy, J.A. Semlyen, *Polymer, 26* (1985) 925.

23 M.J. Newing, *Trans. Faraday Soc., 46* (1950) 755.

24 T.J. Lenk, D.H.T. Lee, J.T. Koberstein, *Langmuir, 10* (1994) 1857.

25 J. Porath, B. Olin, *Biochemistry, 22* (1983) 203.

26 E. Hochuli, H. Doebeli, and A. Schacher, *J. Chromatogr., 411* (1987) 177.

27 T. Yokoyama, M. Kanesato, T. Kimura, T.M. Suzuki, *Chem. Lett.*, (1990) 693.

28 T. Yokoyama, S. Asami, M. Kanesato, T.M. Suzuki, *Chem. Lett.*, (1993) 383.

29 Y. Inoue, H. Kumagai, Y. Shimomura, T. Yokoyama, T.M. Suzuki, *Anal. Chem., 68* (1996) 60.

30 L.R. Paborsky, K.E. Dunn, C.S. Gibbs, J.P. Daugherty, *Anal. Biochem., 234* (1996) 60.

31 D.J. O'Shannessy, K.C. O'Donnell, J. Martin, M. Brigham-Burke, *Anal. Biochem., 229* (1995) 119.

32 G.B. Sigal, C. Bombad, A. Barberis, J. Strominger, G.M. Whitesides, *Anal. Chem., 68* (1996) 490.

33 L. Schmitt, C. Dietrich, R. Tampé, *J. Am. Chem. Soc., 116* (1994) 8485.

34 I.T. Dorn, K.R. Neumaier, R. Tampé, *J. Am. Chem. Soc., 120* (1998) 2753.

35 J.J. Balatinecz , R.T. Woodhams, *J. Forestry, 91* (1993) 22.

36 J.A. Youngquist, R.M. Rowell, in *Proceedings, 23rd International Particleboard/Composite Materials Symposium*, T.M. Maloney (ed.), Washington State University, Pullman, 1990, pp. 141 – 157.

37 J.M. Felix, P. Gatenholm, *J. Applied Polym. Sci., 42* (1991) 609.

38 J.M. Kim, S.Y. Park, S.J. Park, *Eur. Polym. J., 27* (1991) 349.

39 D.N.-S. Hon (ed.), *Chemical Modification of Lignocellulosic Materials*, Marcel Dekker, New York, 1996.

40 R.G. Raj, B.V. Kokta, in *Thermomechanical Properties of Polyethylene-Wood Fiber Composites, ACS Symp. Ser. 489 (Visoelasticity Biomater.)* (1992), 99.

41 J.A. Meyer, in *The Chemistry of Solid Wood*, R.M. Rowell (ed.), ACS, Washington, D.C., 1984, p. 257.

42 H. Matsuda, *Wood Sci. Technol., 27* (1993) 23.

43 H. Matsuda, M. Ueda, H. Mori, *Wood Sci. Technol., 22* (1988) 21.

44 B.V. Kokta, D. Maldas, C. Daneault, P. Beland, *J. Vinyl Technol., 12* (1990) 146.

45 T.C. Laver, *U.S.Patent 5,516,472* (1995).

46 N.C. Liu, W.E. Baker, *Adv. Polym. Tech., 11* (1992) 249.

47 M.K. Naqvi, M.S. Choudhary, *J.M.S.-Rev. Macromol. Chem. Phys., C36* (1996) 601.

48 M.Narkis, A. Tzur, A. Vaxman, H. G. Fritz, *Polymer Eng. Sci., 25* (1985) 857.

49 D.Munteanu, in "*Metal Containing Polymeric Systems*", J.E. Sheats, C.E. Carraher, Jr., C.U. Pittman, Jr., (eds.), Plenum Press, New York, 1983, 399.

50 D. Munteanu, in *Reactive Modifiers for Polymer*, S. Al-Malaika, (ed.), Chapman & Hall, London, 1996.

51 S. Ultsch, H.G. Fritz, *Plastics Rubber Proc. Applic., 13* (1990) 81.

52 K.E. Oliphant, K.E. Russell, W.E. Baker, *Polymer, 36* (1995) 1597.

53 C. Beveridge, A. Sabiston, *Materials & Design, 8* (1987) 264.

54 W.K. Wong, D.C. Varrall, *Polymer, 35* (1994) 5447.

55 T.M. Stefanac, M.A. Brook, R. Stan, *Macromolecules, 29* (1996) 4549.

56 G.H. Wagner, D.L. Bailey, A.N. Pines, M.L. Dunham, D.B. McIntire, *Ind. Eng. Chem., 45* (1953) 367.

57 K.L. Berry, J.R. Caddell, *US Patent 2,739,906* (1956).

58 R.Y. Mixer, D.L. Bailey, *US Patent 2,777,868* (1957).

59 R.Y. Mixer, D.L. Bailey, *J. Polym. Sci., 18* (1955) 573.

60 D.L. Bailey, R.Y. Mixer, *US Patent 2,777,869* (1957).

61 A.K. Sen, B. Mukherjee, A.S. Bhattacharyya, P.P. De, A.K. Bhowmick, *J. Appl. Polym. Sci., 44* (1992) 1153.

62 P. Liptak, O. Mlejnik, *Kautschuk und Gummi, Kunststoffe, 45* (1992) 703.

63 J.C. Forsyth, W.E. Baker, K.E. Russell, R.A. Whitney, *J. Polym. Sci.: Part A: Polym. Chem., 35* (1997) 3517.

64 R.K. Freidlina, A.B. Terent'ev, *Acc. Chem Res., 10* (1977) 9.

65 J.M. Felix, *Enhancing Interactions between Cellulose Fibers and Synthetic Polymers*, PhD Thesis, Chalmers University of Technology, Göteborg, Sweden, 1993.

66 R.G. Raj, B.V. Kokta, *Annu. Tech. Conf.-Soc. Plast. Eng.*, 48th (1991) 1883.

67 R.G. Raj, B.V. Kokta, C. Daneault, *J. Mater. Sci., 25* (1990) 1851.

68 R.G. Raj, B.V. Kokta, C. Daneault, *Polym.-Plast. Technol. Eng., 28* (1989) 247.

69 E.W. Colvin, in *Silicon in Organic Synthesis*, Butterworths, London, 1981.

70 W.P. Weber, in *Silicon Reagents for Organic Synthesis*, Springer Verlag, Heidelberg, 1983.

71 M. Bodanszky, Y.S. Klausner, M.A. Ondetti, *Peptide Synthesis*, Springer Verlag, Berlin, 1984.

72 M. Bodanszky, Y.S. Klausner, M.A. Ondetti, in *Peptide Synthesis*, 2nd ed., John Wiley & Sons, New York, 1976.

73 G.T. Hermanson, in *Bioconjugate Techniques*, Academic Press, London, 1996.

74 D.A. Skoog, D.M. West, in *Fundamentals of Analytical Chemistry*, 4th ed., Saunders College Publishing, Philadelphia 1982, p. 293.

75 F.L. Garvan, in *Chelating Agents and Metal Chelators*, F.P. Dwyer, D.P. Mellor (eds.), Academic Press, New York 1964, pp. 283 – 329.

76 F.W. McLafferty, F. Tureček, in *Interpretation of Mass Spectra*, 4th ed., University Science Books, Mill Valley, California 1993, p 339.

77 H. Schwarz, K. Arakawa, *J. Am. Chem. Soc., 81* (1959) 5691.

78 M. Bodanszky, V. du Vigneaud, *J. Am. Chem. Soc., 81* (1959) 5688.

79 L. Salem, *J. Chem. Phys., 37* (1962) 2100.

80 I. Langmuir, *J. Chem. Phys., 1* (1933) 756.

81 D.J. Crisp, *J. Colloid. Sci., 1* (1946) 161.

82 A. Matsubara, R. Matuura, H. Kimizuka, *Bull. Chem. Soc. Japan, 38* (1965) 369.

83 J.A. Spink, J.V. Sanders, *Trans. Faraday Soc., 51* (1955) 1154.

84 J. Marsdden, J.H. Schulman, *Trans. Faraday Soc., 34* (1938) 748.

85 E. Havinga, *Rec. Trav. Chim., 71* (1952) 72.

86 I. Langmuir, V.J. Schaefer, *J. Am. Chem. Soc., 59* (1937) 2400.

87 J. Bagg, M.B. Abramson, M. Fichman, M.D. Haber, H.P. Gregor, *J. Am. Chem. Soc., 86* (1964) 2759.

88 P.M. Jeffers, J. Daen, *J. Chem. Phys., 69* (1965) 2368.

89 (a) J. Goubeau, J. Jimenez-Barberá, *Z. Anorg. Allgem. Chem., 261* (1950) 361. (b) U. Wannagat, *Advan. Inorg. Chem. Radiochem., 6* (1964) 232.

90 (a) J.-P. Picard, S. Grelier, T. Constantieux, J. Dunoguès, J.M. Aizpurua, C. Palomo, M. Pètraud, B. Barbe, L. Lunazzi, J.-M. Lèger, *Organometallics, 12* (1993) 1378. (b) S. Grelier, T. Constantieux, D. Deffieux, M. Bordeau, J. Dunoguès, J.-P. Picard , C. Palomo, J.M. Aizpurua, *Organometallics, 13* (1994) 3711.

91 K.E. Russell, E.C. Kelusky, *J. Polym. Sci., Part A: Polym. Chem.*, *26* (1989) 2273.

92 A. Sipos, J. McCarthy, K.E. Russell, *J. Polym. Sci., Part A: Polym. Chem.*, *27* (1989) 3353.

93 Elf-Atochem, *Organic Peroxides*, Philadelphia, PA.

94 (a) Dow Corning (Sioplast, *US Patent 3646155* to Midland Silicones, 1968) and other companies including Neste OŸ have sold this material. (b) D. Munteanu., *Moisture Crosslinkabled Silane-modified Polyolefins*, in *Reactive Modifiers for Polymers*, S. Al-Malaika, (ed.), Chapter 5, 196, Chapman & Hall, London, 1997. (c) W.K. Wong, D.C. Varrall, *Polymer, 35* (1994) 5447.

95 V.V. Korshak, A.M. Polyakova, V.F. Mironov, A.D. Petrov. *Izvest. Akad. Nauk S.S.S.R., Otdel. Khim. Nauk* (1959) 178.

96 D.R. Thomas. In *Siloxane Polymers*, S.J. Clarson, and J.A. Semlyen (eds.). Prentice Hall, Englewood Cliffs, NJ, 1993.